

IMPERIAL COLLEGE LONDON

DEPARTMENT OF MECHANICAL ENGINEERING

ADVANCED MECHANICAL ENGINEERING COURSE

**Modelling of an actively controlled blisk: Optimal
piezo placement and their impact on the dynamic
response**

By

Matías Lasen Andrade

Professional Degree in Mechanical Engineering

University of Chile

A thesis submitted in partial fulfilment of the requirements for the Master of Science
Degree of Imperial College London and the Diploma of Membership of Imperial College
September 2018

ABSTRACT

The fan of a modern aircraft engine is crucial for the industry in terms of profits and safety. Vibrations in fans are detrimental for the lifetime of blades. Control strategies can be implemented in order to diminish the harmful effects of vibrations. These strategies can be carried out by means of piezoelectric patches attached to the fan blades.

The problem is finding the optimal location for these piezoelectric patches in a complex structure such as a real aircraft fan.

The work presented in this report aims to address the problem from a semi-analytic perspective. This work explores 2 different numerical models of the aircraft fan and 2 different models for the forces representing the piezoelectric patches. The first fan model consider 1 Degree of Freedom per blade and the second considers 2 Degrees of Freedom per blade. As for the force model, the first is a simple model acting in 1 Degree of Freedom, the second is a useful model acting in 2 Degrees of Freedom, accounting for the actual capability of a patch to tense and extend. Different number of patches, excitation forces and mistuning are also examined.

The numerical models present reliable results and in accordance with the literature. The optimal locations are successfully found for various combinations of the previously mentioned variables. A practical case where the piezos are fixed in a certain position is successfully studied to analyse the effect on other modes as well. The results show a good suppression is achievable in these other modes, however, care must be taken in the displacement of each Degree of Freedom.

ACKNOWLEDGEMENTS

I am grateful to my supervisor Dr. Christoph Schwingshackl and my co-supervisor Dr. Daniele Dini for their extremely good guidance. They recommended paths to follow that otherwise would have taken me a long time to find. I believe the best form of recognition of their help is to recall them explicitly. Hence, among the best advises I received are: to keep things simple enough for my objectives, to find always a practical approach to the results and to always look into the physical representation of the results.

I am also grateful to Conicyt-Chile (code: 73180611) for funding my master at Imperial College London.

Nomenclature

ν_{us}	Unsuppressed displacement
ω'_r	r^{th} damped resonant frequency
$\bar{\omega}_r$	r^{th} undamped resonant frequency
β	Stiffness proportional constant
\ddot{x}	Acceleration
\dot{x}	Velocity
ϵ	Electric Field
η_r	Damping loss factor of the r^{th} mode
γ	Mass porportional constant
ν_s	Suppressed displacement
Ω	Rotational speed of the blades structure
ϕ_r	r^{th} mass normalised eigenvector
σ	Stress field
θ_j	Phase difference between blade jth and its neighbours
ξ	Absolute dielectric permittivity
ξ_r	Damping ratio

$_r A$	r^{th} modal constant
C	Proportional Damping Matrix
D	Dielectric Displacement
d	Piezoelectric charge constant
f	Forcing
$f_{l,m_{t/m}}^*$	Optimal force for minimum MSF with one piezoelectric patch (*) for suppression of mode m in location l , for a tuned or mistuned system (t/m)
$f_{l,m_{t/m}}^{**}$	Optimal force for minimum MSF with two piezoelectric patches (**) for suppression of mode m in location l , for a tuned or mistuned system (t/m)
f_k	Force in blade k.
F_n	Amplitude of the nEOE force.
$f_{l,m_{t/m}}$	Minimum force capable to suppress mode m in a location l , for a tuned or mistuned system (t/m)
H	Hysteretic Damping Matrix
K	Stiffness Matrix
M	Mass Matrix
$max_{x,y}$	Maximum ratio of suppress to unsuppressed displacement in a DOF of mode y with optimal piezoelectric patches fixed at the optimal position for mode x
max_x	Maximum ratio of suppress to unsuppressed displacement in a DOF of mode x
$min_{x,y}$	Minimum ratio of suppress to unsuppressed displacement in a DOF of mode y with optimal piezoelectric patches fixed at the optimal position for mode x
min_x	Minimum ratio of suppress to unsuppressed displacement in a DOF of mode x
MSF_x	Optimal Modal Scale Factor for mode x
$MSF_{x,y}$	Optimal Modal Scale Factor for mode y with piezoelectric patches fixed at optimal positions for mode x

N number of blades

n nth order of the EOE.

S Strain field

s Compliance

t time

x Displacement

Contents

1	Introduction	1
1.1	Overview of the problem	1
1.2	Objectives of the study	3
1.3	Overview of the thesis	3
2	Literature review	6
2.1	Models	6
2.1.1	Discrete Models	7
2.1.2	Semi-Discrete Models	7
2.1.3	Finite Element Models	7
2.1.4	Terminology for continuous and discrete representation of fans.	8
2.2	Excitation force	10
2.2.1	Engine Order Excitation	10
2.2.2	Single Blade Excitation	11
2.3	Damping	11
2.4	Mistuning	12
2.4.1	Frequency shift	12
2.4.2	Localised response	14
2.5	Passive and active control	14
2.5.1	Passive control	14
2.5.2	Active Control	15
2.6	Piezoelectric materials	16
2.7	Background of the problem	17

3 Theory of the models	19
3.1 Definition of the models.	19
3.2 Suppression force	21
3.2.1 Forms of modal suppression	23
3.2.2 Measures of the Optimum force for suppression	24
3.2.3 Models of the piezoelectric force in the discrete model	25
3.3 Restrictions on the models.	28
4 Model validation.	30
4.1 Mode shapes and displacement	30
4.1.1 Mode shapes	30
4.1.2 Displacement extraction	33
4.2 Different excitation forces	34
4.2.1 Single Blade Excitation	34
4.2.2 Multiple Blades Excitation	35
4.3 Damping	37
4.4 Mistuning	38
4.4.1 FRF of a mistuned and tuned system	38
4.4.2 Displacement of an increasingly mistuned system	40
5 Active control of 1 DOF per blade model	44
5.1 Analytic approach for suppression	45
5.2 Statistical approach for suppression	53
6 Active control of a 2 DOFs per blade model	60
6.1 Minimum force to total suppression of a mode with one piezoelectric patch.	63
6.2 Minimum MSF for a given force of 1% of the excitation force.	68
6.2.1 Using 1 piezoelectric patch.	69
6.2.2 Using 2 piezoelectric patches.	73
7 Active control: optimal suppressing patterns and their effect on secondary modes.	78
7.1 Study of the different suppressing patterns.	79
7.2 Effect of the optimal location for all the suppressing forces over the rest of the modes.	91

8 Conclusions	101
9 Future work	103
Bibliography	105
Appendix A Constitutive matrices for a model with 1 DOF per blade.	110
Appendix B Constitutive matrices for a model with 2 DOFs per blade.	111
Appendix C Optimum forces $f_{l,m_{t/m}}$ for a suppressing force acting in 2 DOFs for a model with 2 DOFs per blade.	112

List of Figures

1.1	Piezos installed in a couple of fan blades. Duffy et al. (2013)	2
1.2	Fan of a Trent 1000 engine (a)(Rolls-Royce (2016)) and simplified representation: Blisk (b)(Sever (2004))	2
1.3	Model 1: 1 DOF per blade.	4
1.4	Model 2: 2 DOFs per blade.	4
1.5	Scheme of the line of work in chapters 4, 5, 6 and 7.	5
2.1	Families of mode shapes in a single flat blade (Sever (2004)). (a) Bending, (b) Edgewise, (c) Torsional and (d) Extension.	8
2.2	Nodal diameters and circles representation. Left: 2 ND, right: 1 NC and 2 NDs. Sever (2004)	9
2.3	Macro Fiber Composite developed at Nasa (Wilkie et al. (2007))	17
3.1	Terminology for model 1.	20
3.2	Terminology for model 2.	20
3.3	Piezoelectric patch operation represented as 1DOF suppressing force	26
3.4	Piezoelectric patch operation represented as 2DOF suppressing force in three different possible locations.	27
3.5	Restrictions on 2 Piezoelectric patches operation represented as 2DOF suppressing force per patch.(a) Case 1. (b) Case 2. (c) Case 3. (d) Case 4.	28
4.1	Mode shapes of a perfectly tuned system with 2 DOFs per blade.	31
4.2	Mode shapes of a perfectly tuned system with 2 DOFs per blade.	32
4.3	Magnitude and phase picking.	33

4.4	Three different excitation forces patterns.(a) 12th DOF excited. (b) All 12 DOFs excited. (c) DOFs 9 and 11 are excited.	34
4.5	Effect of 4 excitation forces, each in a tip blade.	35
4.6	FRF of the 12th DOF after with excitation force. (a) FRF with an excitation force in the 12th DOF. (b) FRF with an excitation force applied in all 12 DOFs. (c) FRF with an excitation force exciting the 9th and 11th DOFs.	36
4.7	Three different levels of proportional damping and their impact in the FRF.(a) $\gamma=0.005$.(b) $\gamma=0.05$.(c) $\gamma=0.5$. $\beta=0.08$ for all cases.	37
4.8	FRF of a k -mistuning for every DOF in the model. Top: Tuned systems, bottom: Mistuned system.	39
4.9	FRF of a m -mistuning for every DOF in the model. Top: Tuned systems, bottom: Mistuned system.	39
4.10	Stiffness mistuning. Ratio of the Mistuned to the Tuned displacements for all the modes and elements (left). MAC (right). k -mistuning factor: (a) 0%, (b) 10%, (c) 50% and (d) 200%.	41
4.11	Mass mistuning. Ratio of the Mistuned to the Tuned diplacements for all the modes and elements (left). MAC (right). m -mistuning factor: (a) 0%, (b) 10%, (c) 50% and (d) 200%.	42
5.1	Alternating mistuning pattern in a 1 DOF per blade model.	45
5.2	(a) Model of 1 DOF per blade. (b) Excitation force pattern.	45
5.3	Forces needed to suppress all the modes with a force acting in 1 DOF in a model with 1 DOF per blade. (a) Tuned system. (b) Mistuned system.	46
5.4	Forces, within a comparable range with respect to the excitation force, needed to suppress all modes with a force acting in 1 DOF in a model with 1 DOF per blade. (a) Tuned system. (b) Mistuned system.	47
5.5	Effect of a suppressing force $f_{6,7_t} = 1$ in a tuned system. (a) Unsuppressed displacement. (b) Suppressed displacement. With a suppressing force acting in 1 DOF.	49
5.6	Effect of a suppressing force $f_{6,7_t} = 1$ in a mistuned system. (a) Unsuppressed displacement. (b) Suppressed displacement. With a suppressing force acting in 1 DOF.	50

5.7	Effect of a suppressing force $f_{5,8_t} = 1.3$ in a tuned system. (a) Unsuppressed displacement. (b) Suppressed displacement. With a suppressing force acting in 1 DOF.	51
5.8	Effect of a suppressing force $f_{6,8_m} = -1.2$ in a mistuned system. (a) Unsuppressed displacement. (b) Suppressed displacement. With a suppressing force acting in 1 DOF.	52
5.9	Distribution of 75 MSFs from randomly generated forces aiming to suppress mode 2F-1ND (7) and 2F-2ND (8). (a.1) 2F-1ND (7)/tuned. (a.2) 2F-1ND (7)/mistuned. (b.1) 2F-2ND (8)/tuned. (b.2) 2F-2ND (8)/mistuned.	55
5.10	FRFs for a randomly generated force capable of delivering a lower MSF than an optimal single DOF suppressing force targeting mode 2F-1ND , for a tuned and a mistuned systems.(a.1) Tuned-unsuppressed. (a.2) Tuned-suppressed. (b.1) Mistuned-unsuppressed. (b.2) Mistuned-suppressed.(a) Displacement of each DOF for a tuned suppresses/unsuppressed system. (b) Displacement of each DOF for a mistuned suppresses/unsuppressed system. (a-b) Optimal single DOF suppressing force and randomly generated forces to suppress a tuned and mistuned system.	57
5.11	FRFS for a randomly generated force capable of delivering a lower MSF than an optimal single DOF suppressing force targeting mode 2F-2ND , for a tuned and a mistuned systems.(a.1) Tuned-unsuppressed. (a.2) Tuned-suppressed. (b.1) Mistuned-unsuppressed. (b.2) Mistuned-suppressed.(a) Displacement of each DOF for a tuned suppresses/unsuppressed system. (b) Displacement of each DOF for a mistuned suppresses/unsuppressed system. (a-b) Optimal single DOF suppressing force and randomly generated forces to suppress a tuned and mistuned system.	58
6.1	(a) Nomenclature for the possible positions of a single piezo acting in 2 DOFs.(b) Force $f_{1,2_t} > 0$	61
6.2	Alternating mistuning pattern in a 2 DOFs per blade model. 1 Piezo electric patch acting in 2 DOFs.	62
6.3	(a) Model of 2 DOFs per blade. (b) Excitation force pattern.	62
6.4	Forces needed to suppress all modes with a force acting in 2 DOFs in a model with 2 DOFs per blade. (a) Tuned system. (b) Mistuned system. . .	63

6.5	Forces, within a comparable range with respect to the excitation force, needed to suppress all modes with a force acting in 2 DOFs in a model with 2 DOFs per blade. (a) Tuned system. (b) Mistuned system.	64
6.6	Effect of a suppressing force $f_{15,8_t} = -0.4108$ in a tuned system. (a) Unsuppressed displacement. (b) Suppressed displacement. With a suppressing force acting in 2 DOFs.	66
6.7	Effect of a suppressing force $f_{13,8_m} = -0.4207$ in a mistuned system. (a) Unsuppressed displacement. (b) Suppressed displacement. With a suppressing force acting in 2 DOFs.	67
6.8	Scheme of force $f_{13,8_{t/m}}^*$	69
6.9	Effect of a suppressing force $f_{13,8_{t/m}}^* = -0.01$ in a tuned and mistuned systems. (a.1) Tuned-unsuppressed. (a.2) Tuned-suppressed.(a.3) Tuned Displacements suppressed/unsuppressed. (b.1) Mistuned-unsuppressed. (b.2) Mistuned-suppressed. (b.3) Mistuned Displacements suppressed/unsuppressed.	70
6.10	Ratio suppressed/unsuppressed displacement for every DOF at the frequency of mode 2F-2ND.	71
6.11	MSF for every mode under optimal suppressing force f^*	72
6.12	Scheme of force $f_{13-14,8_{t/m}}^{**}$	73
6.13	Effect of a suppressing force $f_{13-14,8_{t/m}}^{**} = -0.01$ in a tuned and mistuned systems. (a.1) Tuned-unsuppressed. (a.2) Tuned-suppressed.(a.3) Tuned Displacements suppressed/unsuppressed. (b.1) Mistuned-unsuppressed. (b.2) Mistuned-suppressed. (b.3) Mistuned Displacements suppressed/unsuppressed.	74
6.14	Comparison of ratios suppressed/unsuppressed displacement for every DOF at frequency of mode 2F-2ND, with 1 and 2 piezos.	75
6.15	Comparison of MSFs for every mode under optimal suppressing forces type: f^* and f^{**}	76
7.1	Alternating mistuning pattern in a 2 DOF per blade model.	79
7.2	Comparison of the optimal forces found for k -mistuning and m -mistuning for a MSF considering disks and blades elements.	80
7.3	Comparison of the optimal forces found for k -mistuning and m -mistuning for a MSF considering blades elements only.	80

7.4	<i>k</i> -mistuning. Optimal positions of both piezos for various level of mistuning.	83
7.5	<i>m</i> -mistuning. Optimal positions of both piezos for various level of mistuning.	84
7.6	<i>k</i> -mistuning. Optimal force for each mode for the tuned and mistuned cases.	85
7.7	<i>m</i> -mistuning. Optimal force for each mode for the tuned and mistuned cases.	86
7.8	<i>m</i> -mistuning. Optimal force for each mode for the tuned and mistuned cases with an excitation force in the tip-blade element of the 1st sector.	88
7.9	Suppressing force patterns for a tuned, symmetrically excited and low damped system.	89
7.10	Displacement difference and optimal piezo locations for 4 modes.	90
7.11	Optimal MSF for each mode and the effect on the rest of the modes in a perfectly tuned system.	93
7.12	Optimal MSF for each mode and the effect on the rest of the modes in a mistuned system.	94
7.13	Single maximums and minimums suppress/unsuppressed ratios for each optimal MSF and its effect on the rest of the modes in a perfectly tuned system.	98
7.14	Single maximums and minimums suppress/unsuppressed ratios for each optimal MSF and its effect on the rest of the modes in a mistuned system.	99

List of Tables

3.1	Structural properties of the models.	21
4.1	Eigenvalues of a perfectly tuned system.	32
5.1	Force needed to suppress a certain mode placing the piezo in difference DOFs for a tuned (t) and mistuned (m) system.	47
5.2	MSF for modes 2F-1ND (7) and 2F-2ND (8) for a tuned and mistuned system	56
6.1	Positions of optimal forces f^*	72
6.2	MSF for a tuned and mistuned mode 2F-2ND with 1 and 2 piezos.	75
6.3	Comparison of optimal locations of the piezos for f^* and f^{**} for every mode.	76
6.4	Percentage error between the linear projection of the MSF with 1 piezo-electric piezo to 2 piezoelectric piezos for all tuned and mistuned modes. .	77
C.1	$f_{l,1-4_{t/m}}$ for a force acting in 2 DOFs in a tuned model of 2 DOFs per blade.	113
C.2	$f_{l,5-8_{t/m}}$ for a force acting in 2 DOFs in a tuned model of 2 DOFs per blade.	114
C.3	$f_{l,9-12_{t/m}}$ for a force acting in 2 DOFs in a tuned model of 2 DOFs per blade.	115

Chapter 1

Introduction

1.1 Overview of the problem

Turbofan engines are extensively used in civil aerospace industry due to their high overall efficiency. The fan of the engine delivers around 70% of the thrust of the entire engine, therefore it is crucial for the industry in terms of the service to its clients. Therefore, a failure in these components may be dangerous and potentially fatal for the passengers.

A usual cause of failure is High Cycle Fatigue (HCF) due to the vibrations in the fan blades. At resonance, the amplitude of the displacement of the fan blades increases. This is even magnified by *mistuning* in the structure. Mistuning is defined as a change from blade to blade (or within one blade) of its structural properties due to the tolerances in the manufacturing process. These high amplitude responses will produce high stresses in the blade which will fatigue the material, culminating in a decrease in the lifetime of the component. Thus, it is important to understand the behaviour of the blades, which causes and how to control the amplitude at resonance, to be able to increase their operational lifetime for economic and safety purposes.

A good form to increase the lifetime of these structures is to control them when they vibrate in a harmful manner. In the last couple of decades piezoelectric patches (*piezos*) have been used due to their good properties, these properties allow them to be used as sensors and actuators. They have demonstrated to be effective in suppression of certain modes in blades. Where a suppressed mode is such that, its collaboration in the

displacement is eliminated. However, the challenge to find where the optimal locations to place these piezos are remains open. Figure 1.1 shows the installation of 3 piezos in a real blade.



Figure 1.1: Piezos installed in a couple of fan blades. Duffy et al. (2013)

A Multiple Degrees of Freedom (MDOF) system such as a rotating fan presents several physical phenomena. A logical step to understand these phenomena is to produce a trustful model that permits a confident control of the component.

Three different theses have been developed in previous years to understand and control the vibration of a simplified fan: Agulhon (2015), Poon (2016) and Glasstone (2016). This simplified fan is represented as a continuous component where the disk and blades are considered one single element called blisk. Figure 1.2 shows a real engine fan and a blisk.

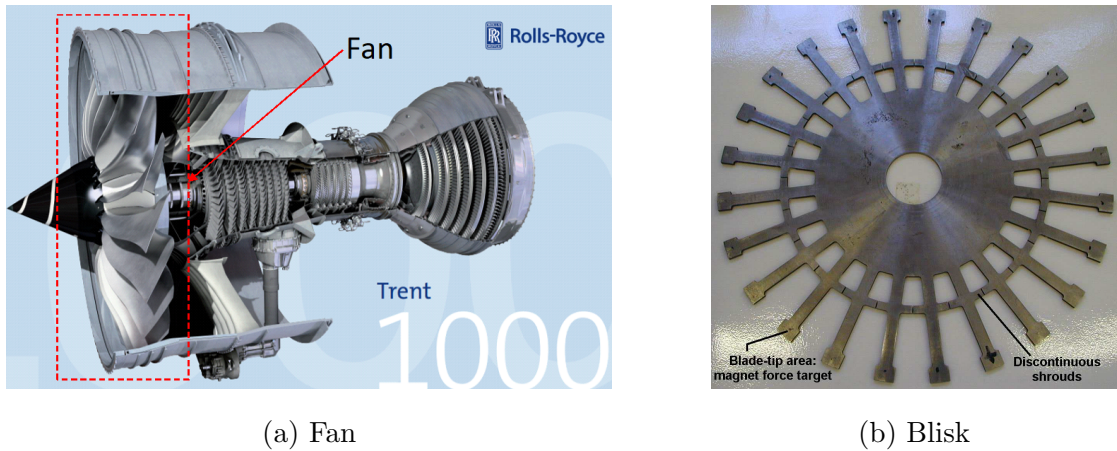


Figure 1.2: Fan of a Trent 1000 engine (a)(Rolls-Royce (2016)) and simplified representation: Blisk (b)(Sever (2004))

First, Agulhon (2015) and Poon (2016), started with an experimental approach. On the one hand, Agulhon experimented with the effects of using 1 piezoelectric patch in order to reduce the displacement in one blade, finding that it is possible to reduce the amplitude locally and in the rest of the blades. On the other hand, Poon worked with a Laser Doppler Vibrometer (LDV) Scanning Technique in order to track the amplitude reduction on a rotating blade. Secondly, Glasstone (2016) worked on improving the Finite Element (FE) model of the blisk and piezoelectric patch used by his predecessors. In these three experiences a FE model is used as a reference.

In this thesis a more fundamental approach is followed. The system is represented as a discrete model where blades and the disk are depicted as masses and springs.

Once the discrete model responds accurately to the physical variations in their properties, as will be discussed in the Literature Review, it reaches a good level of confidence. After this, the suppression techniques are applied and the optimal locations are searched for.

1.2 Objectives of the study

The main objectives of this study are:

1. To find the optimal locations for the representation of piezoelectric patches forces in a semi-analytic model.
2. To determine and quantify the secondary effects of an optimal force in the rest of the system.

The general route followed to fulfil these objectives is described in the next section.

1.3 Overview of the thesis

A semi-analytic approach is explored in this report. A set of computational studies have been carried out starting from a very simple model and considerations and moving into a more complex representation of the forces and model of the system.

Two discrete models are used in this study. First, a model with one mass representing each blade is created and studied, see figure 1.3. After experimenting with it and obtaining some partial conclusions a more complex model is implemented. A more complex model is then tested. This model has two masses per blade as depicted in figure 1.4.

These models are explored to determine which is the optimal force to suppress a mode. This searching process involves the determination of the magnitude, location, form, amount of these suppressing forces and their performance in suppressing the *Operating Deflection Shape* (ODS) of the structure.

The fundamentals of this exploration are related in the pertinent literature review in chap:lr. This exploration starts in chap:theory where the models, mathematical formulation of the system, definition of suppressing forces and how to measure their performance are explained.

In chap:verifications the model is deeply studied and analysed in order to check if its behaviour is as expected according to the literature review.

Once the model is reliable enough, the suppression effect is explored. This is initially carried out in a model as depicted in figure 1.3 in chap:1DOF. Then, the model is upgraded in chap:2DOF, where the model illustrated in figure 1.4 is studied.

The research in chap:1DOF and chap:2DOF aims to suppress one mode. On the other hand, in chap:general the study covers the effect of the optimal force for one mode over the rest of the modes. These four chapters: 4, 5, 6 and 7, are summarised schematically in figure 1.5.

Finally, some overall conclusions are summarised in chap:conclusions. note that the discussion pertinent to each chapter is delivered at the end of each of them. Future work is recommended in chap:fut.

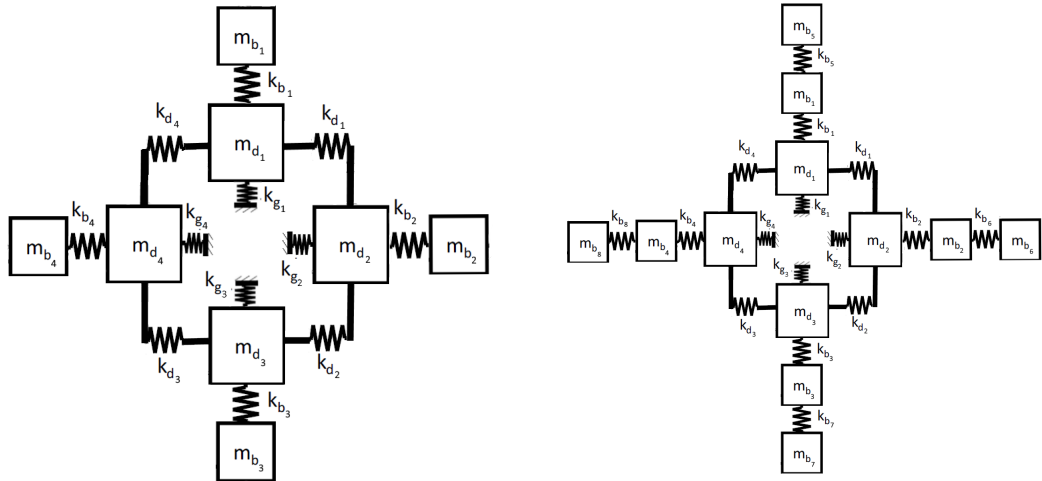


Figure 1.3: Model 1: 1 DOF per blade. Figure 1.4: Model 2: 2 DOFs per blade.

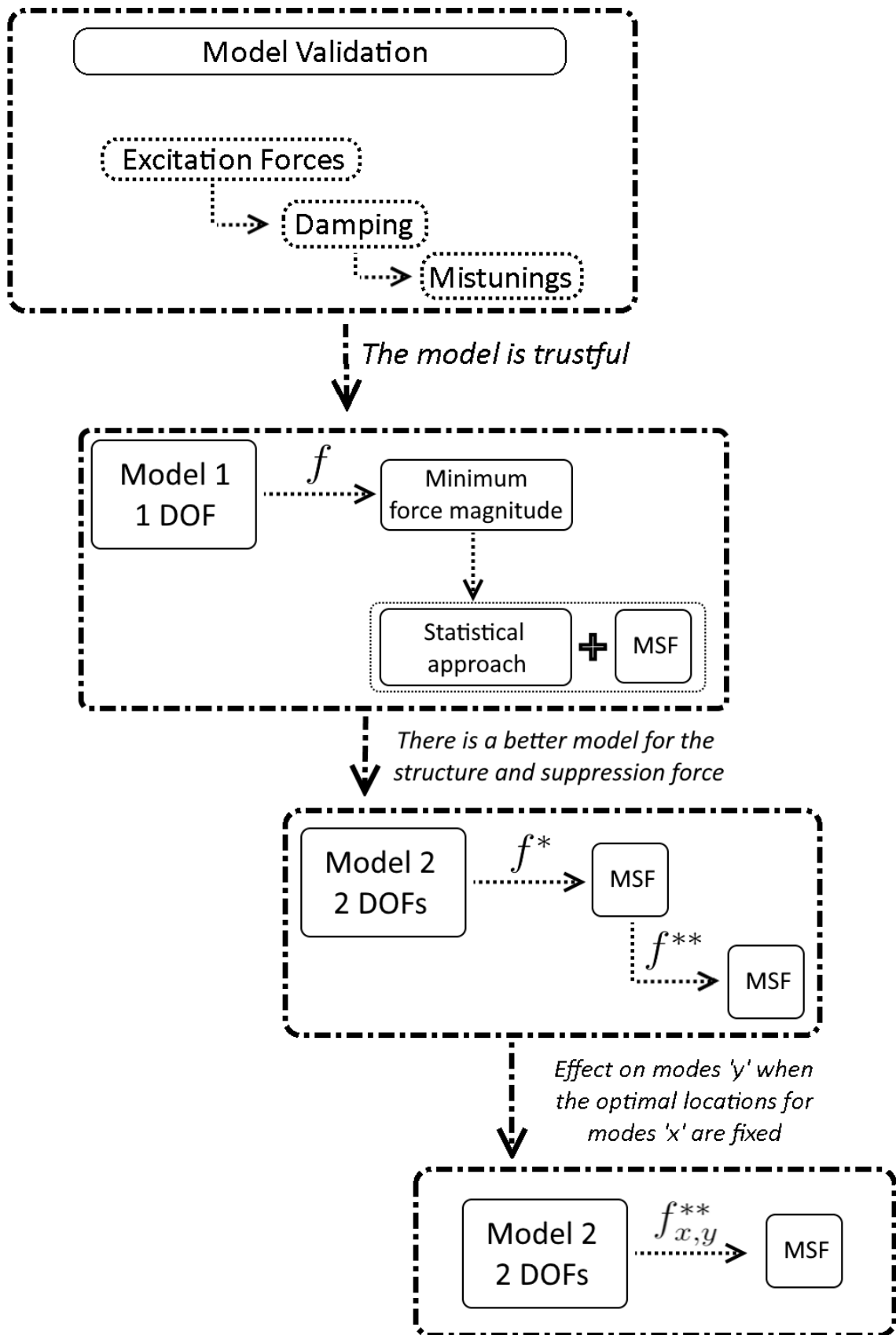


Figure 1.5: Scheme of the line of work in chapters 4, 5, 6 and 7.

Chapter 2

Literature review

This chapter aims to deliver a general overview of the available topics in the literature which are more relevant to this work. Among these are: the possible models to represent an aircraft fan, the excitation forces acting in a fan, structural properties such as damping and mistuning and finally forms of passive and active control.

2.1 Models

Several models for blisks have been used in the literature in the last 20 years. They cover a wide range of complexity depending on the numbers of Degrees of Freedom (DOFs) per blade considered by different authors. The models also vary depending on the research purpose covering: free/forced responses of the structure, detection of structural properties, control of vibrations, among others. Thus, simpler models are used when the focus is in suppression of vibration, a relatively new topic, in contrast with the increasingly more complex models that are employed when the aim is the exploration of vibration patterns only. These models are hereby classified as Discrete, Semi-discrete, and Finite Element (FE) models.

Discrete models represent the blades with masses and springs as well as dampers. More masses are added as the complexity of the model is increased. Finite Element models consider the blisk or blade as a whole. It is worth noting that there are authors who explored a blade representation by means of cantilever beams or plates, these models

are tabulated here as semi-discrete models since they are more complex than a simple discrete model, but still not as elaborated as a FE geometry. Note than the following selection is just a group of all the available models available in the literature.

2.1.1 Discrete Models

Ewins and Han (1984), explored the response of a mistuned system with an emphasis in the most excited blade, he employed a model with 2 DOF per blade. Wei and Pierre (1988) study the localisation effect due to mistuning in a shrouded fan modelled as a series of single masses per blade connected with a spring. Rotea and D'Amato (2002), used a discrete model with 2 masses per blade in a mistuned rotor to indicate which is the optimal position to introduce an intentional mistuning to reduce the maximum displacement in the response.

2.1.2 Semi-Discrete Models

Crawley and Mokadam (1984), aiming to study the effect of the stagger angle of the blade on the vibration behaviour, modelled a fan with blades as cantilever beams attached to a solid disk capable of moving as a cylindrical membrane. Griffin (1988), looked for the response of the fan considering aeroelastic effects modelled as dampers and springs in parallel connecting one of the two masses designed to represent a blade. Yu and Wang (2007), aiming to determine the suppression effect of a network of piezoelectric patches, explored the bending modes of a fan with 10 blades represented as clamped cantilever beams coupled by springs.

2.1.3 Finite Element Models

Bladh et al. (2001), used reduced order models of a fan to determine its response, he also introduced a novel algorithm for the reduction of the model. Sever et al. (2008), used a finite element model to determine the effect of under-platform friction dampers on the response of mistuned blisks. Jung et al. (2012), made use of a 3-D finite element model of blades to be able to detect cracks in mistuned blades. Mokrani et al. (2012), used a full 3-D model, this time of a compressor drum, to study the effect of piezoelectric patches located underneath the blades in the vibration suppression. Chandrashaker et al. (2016), proposed a quantitative index to quantify the mode localisation due to mistuning, he used a rather simple finite element model to support his findings. Deng et al. (2017), used a

simple finite element of a flat mistuned blisk to demonstrate the suppression capacity of a bi-periodic network of piezoelectric patches.

2.1.4 Terminology for continuous and discrete representation of fans.

As research in aircraft fans vibrations grew in the last 30 years, specific terminology has been established to express concisely the phenomena occurring in these structures. In this subsection it is aimed to deliver a brief summary of the terminology used in this analysis, further definitions regarding topics not examined in this report can be obtained from Sever (2004) and the contributions of professor D.J. Ewins at the technical report elaborated by the Advisory Group for Aerospace and Research Development (AGARD, NATO, Platzer and Carta (1988)).

Before going into the fan itself it is worth taking a look into the units that conform it: the blades. A single blade can show four different families of mode shapes during vibration:

- Bending: mode shapes displace parallel to the axial direction of the engine.
- Edgewise: mode shapes move parallel to the rotational direction of the engine.
- Torsional: mode shaped rotate around the main axis of the blade.
- Extension: mode shapes vibrate parallel to the main axis of the blade

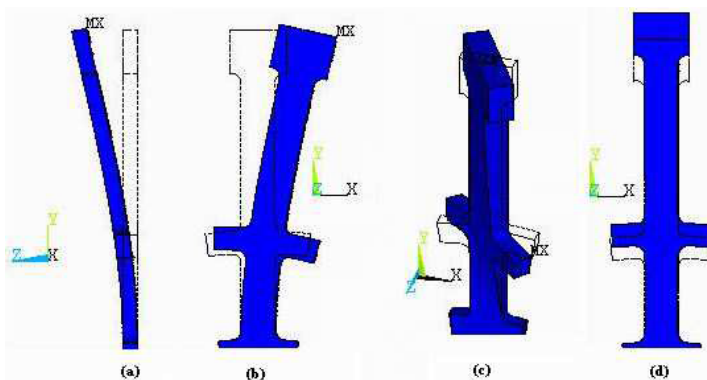


Figure 2.1: Families of mode shapes in a single flat blade (Sever (2004)). (a) Bending, (b) Edgewise, (c)

Torsional and (d) Extension.

Figure 2.1 exemplifies this in a single blade. In a real fan, the blades have complex 3-D shapes, therefore this families no longer apply since each blade contains various axes describing its form. Therefore,

a combination of these families can be observed.

Evidently, each blade has their own mode shapes at their blade-only resonant frequencies. However, when the blades are packed together in a bladed disk they form different patterns at different frequencies, not necessarily the same as the blades. These patterns can be organised by families named identically to the families of a single blade, as described previously. The mode shapes patterns can be classified according to the family they belong, but also the Nodal Diameters (ND) and Nodal Circles (NC) present in the mode shape.

A ND is a line where the displacement is null. Immediately contiguous to the nodal line the displacements in the structure are anti-symmetric with respect to the line. In other words, the displacement pivot from positive to negative across the nodal diameter.

A NC is essentially the same as a ND, the difference consists in that the nodal circle is a line around the structure and the nodal diameter is a line across the structure.

A mode in a family can be classified depending on the number of NCs and NDs in the mode. Figure 2.2 displays in the left hand side a bending (or flexing) mode with 2 NDs and 0 NCs in a flat blisk and on the right hand side the same mode with 1 NC.

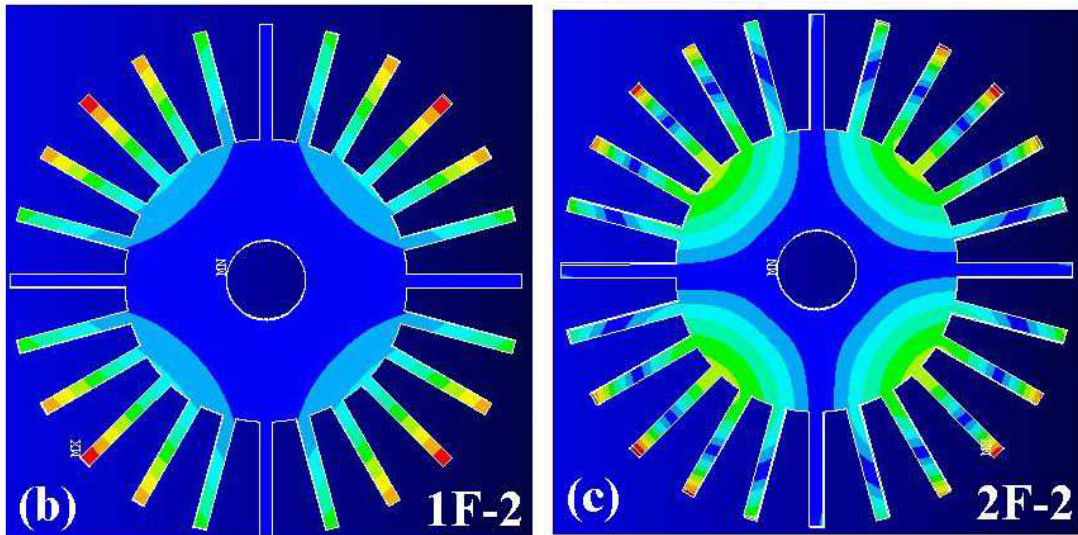


Figure 2.2: Nodal diameters and circles representation. Left: 2 ND, right: 1 NC and 2 NDs. Sever (2004)

The first group of modes do not have any nodal circle, corresponding to each blade performing a first cantilever mode. Also, since each blade is a continuous element, each of them and therefore the collection of them in a blisk, can have virtually an infinite number of NCs. Any group can have up to $N/2$ NDs, where N is an even number of blades ($(N-1)/2$ NDs for an odd N).

Thus, a mode is coded as ‘ $nc + 1$ X- nd ’, where nc is the number of NCs, nd is the number of NDs and X is the family of the mode. With this, the mode depicted on the right in the image above is named: 2F-2 corresponds to the Bending (or flexing) family of modes, with 1 NC and 2 NDs.

It is worth noting that a nodal diameter does not necessarily set down in a pair of opposite blades, the line can be in between of two blades as well. Also, in continuous systems with blades with complex 3-D shapes the nodal line may not be a straight line but a complex 3D curve as well.

2.2 Excitation force

A forced response involves an excitation force. These forces originate in real fans due to structural issues, for example, bearing misalignments. Or aeroelastic forces, for example due to vortexes originated in the ground surface and impacting the lower part of the aircraft fan when the aircraft is taking off or simply taxiing in the airport. Also, when there is a static pressure field, such as the one caused by the vanes after periodic structures such as bladed disks, all the blades can be excited by this impact behind them.

2.2.1 Engine Order Excitation

The form of force that excites all the blades in a bladed disk is called *Engine Order Excitation* (EOE). 1 EOE means that each blade is excited once per rotation. 2 EOE, means that the blades are excited twice per rotation and $nEOE$ means n excitation impacts. With this, the formulation of the excitation -per blade- is (Platzer and Carta (1988)):

$$f_k = F_n * \cos(n\Omega t + \frac{2\pi nj}{N}) \quad (2.1)$$

Where:

f_k : Force in blade k.

F_n : Amplitude of the nEOE force.

n : nth order of the EOE.

Ω : rotational speed of the blades structure

t : time

N : number of blades

j : $\sqrt{(-1)}$

Note that the last term: $\theta_j = \frac{2\pi nj}{N}$, is the phase jump between one blade and the next one.

2.2.2 Single Blade Excitation

If the blisk does not rotate the definition of EOE loses meaning. In this case one or various blades can be excited. The simplest form of excitation is forcing a single blade or *Single Blade Excitation* (SBE). In that case, the vector of force over all the DOFs is simply: $\{f_e\} = \{0, \dots, 0, F_k, 0, \dots, 0\}$, where only blade kth is excited.

2.3 Damping

Damping in structural dynamics is itself a field of study and various authors across the world have carried out research to investigate their impact on the response of certain structures.

Damping is basically a dissipation of the energy in the system. Damping is usually classified under two main models. These are: Proportional (or Viscous, or Rayleigh) Damping and Structural (or Hysteretic) Damping. Proportional Damping is proportional to velocity whereas Structural Damping is proportional to the displacement in a structure. Below, the general equations of motion (Ewins (2000)) exemplify these characteristics for Proportional Damping: eq. 2.2 and Structural Damping: eq. 2.3.

$$[M] \{\ddot{x}\} + [C] \{\dot{x}\} + [K] \{x\} = \{f\} \quad (2.2)$$

$$[M] \{\ddot{x}\} + [K] \{x\} + i[D] \{x\} = \{f\} e^{i\omega t} \quad (2.3)$$

$$\text{with : } [C] \text{ or } [H] = \beta [K] + \gamma [M] \quad (2.4)$$

Where:

M : Mass Matrix

C : Proportional Damping Matrix

K : Stiffness Matrix

H : Hysteretic Damping Matrix

\ddot{x} : Acceleration

\dot{x} : Velocity

x : Displacement

f : Forcing

Note that β and γ are not necessarily the same for $[C]$ and $[H]$. Also, simpler forms of damping can be found in the literature where $[C]$ and $[H]$ are only proportional to $[K]$ or $[M]$. In other words, β or γ are zero, in these cases, these forms are called Simple Proportional Damping or Simple Structural Damping.

The effect of damping in general in the FRF is twofold: in amplitude and frequency. In amplitude, damping limits the maximum displacement that an element will describe. In frequency, if damping is low, it can cause that two or more undamped modes merge together. In an extreme case the response can be overdamped and the natural frequencies may not be recognisable anymore.

2.4 Mistuning

Different mechanical properties: stiffness, mass and damping, can be found within real fans due to different outcomes of the manufacturing process. These differences are within the tolerances allowed by the manufacturer, however, it can introduce a higher amplitude response in comparison with a tuned Fan. This phenomena is referred as mistuning, Sever (2004).

Mistuning in the structural properties leads to three main consequences in the frequency response of a MDOF system: frequency shifting, frequency splitting and, more importantly, a localised response.

2.4.1 Frequency shift

A frequency shift can be introduced in a MDOF system by modifying the stiffness and/or mass of one or many of the DOF. A fundamental approach to understand the phenomena

of frequency shifting in a MDOF system such as an aircraft fan is to understand a simple configuration, for instance, a beam. In a simple beam two different effects can occur by the modification of the stiffness only and mass only.

- Stiffness modification: connecting a spring to the free boundary of a cantilever beam to the ground will increase the resonant frequencies. Nevertheless, the antiresonant frequencies are not changed by the attachment of the spring. Therefore, when a resonant frequency is sufficiently increased, by means of the spring's stiffness increase, it will reach and antiresonance and cancel out. In the limit, when the stiffness of the attached spring is high enough, all the resonances are cancelled out, leaving the system as grounded in the previously free boundary. Analogously, the decrease in the stiffness of the spring moves the resonances to the left in the FRF.
- Mass modification: adding a mass in the free boundary has the opposite effect as the previously explained spring. As the mass is increased the resonant frequencies are reduced or displaced to the left in the FRF. As the mass is continuously increased the resonances and antiresonances cancel out leaving a null FRF.

A third effect can also be introduced, now in a slightly more complex model of multiple masses connected in series. The complexity lies in that a ‘spring+mass’ subsystem is attached to any of the existing masses in the system.

- Stiffness and Mass modification: another method of structural modification is suggested by Skingle (1989). This model incorporate both the stiffness and mass effects described above. The natural frequency of the subsystem ‘spring+mass’ ($\sqrt{k/m}$) sets a limit in the FRF from which to the left all the resonances are displaced to the right and to the right of $\sqrt{k/m}$ all the resonant frequencies are moved to the left. In other words, all the resonant frequencies now tend to the artificially incorporated natural frequency of the subsystem.

Maia and e Silva (1997), describe these three effects¹ on their book.

Another consequence of the shift in frequency, due to mistuning, is that double modes separate, Ewins (1976). This means that double tuned modes separate into two different resonant frequencies. This separation is not the same for all double modes, therefore a simple prediction on where the new mistuned natural frequencies will lay, based on a known mistuning pattern, is not direct.

¹They refer to these changes as structural modifications, instead of stiffness or mass mistuning.

2.4.2 Localised response

A localised response means that the amplitude of one or some blades in the row is increased more than its expected level at resonance. A critical issue is to identify which is the upper limit of the amplitude provided a certain mistuning pattern.

Various factors have been proposed to account for this upper limit. The most popular is the Whitehead factor, Whitehead (1996):

$$A_{WH} = \frac{1}{2}(1 + \sqrt{N}) \quad (2.5)$$

A_{WH} implies that the amplitude of a certain DOF will be increased A_{WH} times with respect to its tuned version. It is important to note that this factor derives from several assumptions. Among these assumptions the most important to this work is that it requires an *nEOE*.

A localised response can occur in the FRF not only due to variation in the stiffnesses and masses from blade to blade in an arrangement. They can also happen due to damping mistuning as explored by Lin and Mignolet (1993), where they found that the amplitude of some blades were increased for certain damping mistuning patterns.

2.5 Passive and active control

To alleviate and eventually to compensate the forced response of a structure, due to aeroelastic or structural forces, passive and active control have been explored in the literature. Decreasing the amplitude of the response aims to reduce the stresses in the blades helping to reduce fatigue and improving their lifetime.

2.5.1 Passive control

Passive methods do not feedback the control device with the ongoing behaviour of the structure. Indeed any form of damping introduced by an external source, i.e. not from the material of the structure, is a passive control device when it is designed for this purpose. This external devices dissipate the energy of the structure. This energy dissipation arises from the friction of the material through contact surfaces with these devices.

Theoretical models and experimental research can be found in the literature from the fundamentals of energy dissipation through friction to the design of passive control devices.

For example, Menq et al. (1991), Sanliturk and Ewins (1996) and Yang et al. (1998) worked on mathematical models of a simple punctual and local friction force between 2 surfaces under various conditions of forcing, stiffness and adhesion in the surfaces.

In parallel some researchers worked on discrete models of non-linear friction damping. For instance, Muszyńska and Jones (1983) elaborated a model to analyse the effect of Coulomb forces between blade-blade and between blades and disks in a mistuned blisk.

Some 3-D computational models have been also used to study the effect of external sources of damping such as underplatform dampers. For instance, Petrov and Ewins (2004) studied this and found that the responses in a given blade vary their response, and also their scattering pattern, depending on the load and stiffness of the underplatform dampers. A few years later, Petrov and Ewins (2006) showed that not only the surfaces of external devices, such as underplatform dampers, but also the surfaces generated by the contact of the root of a blade and the disk (root joint) can dissipate energy and modify the FRF.

Experimentally, underplatform dampers devices have been studied in the literature by Sever et al. (2008), Firrone and Zucca (2009), Schwingshakl et al. (2012), Pesaresi et al. (2017), among others. A passive device can also be embedded in the blade, as demonstrated by Bachmann et al. (2012), where a comparison of Shape Memory Alloys (SMA) and piezoelectric was carried out.

Most of the models and experimental validations of these passive devices aim to optimise these components to deliver the best possible design to operate once they are installed in the structure. However, after installation, information is not gathered from these devices.

2.5.2 Active Control

For real time control, feedback from the structure needs to be implemented, therefore active control is needed. This approach demands participation of both sensors and actuators such that the vibration amplitude is measured and controlled in real time.

Promising devices to carry out this challenge are piezoelectric patches. These patches can operate as both sensor and actuator, as a sensor they will deliver an electrical signal from the mechanical stresses and strains that perceived, and as an actuator they will exert a force into the patch-structure interface due to an electrical signal sent to the patch in the first place.

Research on a single blade was carried out at Nasa Glenn Research Centre, where Duffy et al. (2013) successfully reduced the amplitude of vibration of the first bending mode in a real 3-D rotating fan blade. Another approach, now general rather than localised, was explored by Yu and Wang (2007) where a network of piezoelectric patches was attached to all the blades. Once the potential of the technique was demonstrated, research on the optimisation was carried out. This optimisation aimed to find the best position to locate a patch. Botta et al. (2013), Han and Lee (1999) and Biglar et al. (2015) have demonstrated that it is indeed possible to suppress various modes of vibration in beams and plates. Not only that, also Botta et al. (2018), studied an efficient approach to suppress multimodal vibration in a cantilever beam. Interestingly, Han and Lee (1999) and Biglar et al. (2015) have used Genetic Algorithms (GA) to test the best position and angle of rotation of the patches with respect to the blades. The challenge of getting similar achievements in blisks and real fans is still open.

2.6 Piezoelectric materials

A good control and model require full understanding of the physics of the controlling device. The piezoelectric effect is present in these materials, this effect refers to the electromechanical relation between electric polarization (of the grain in a microstructural level) and strain (of the macrostructure). The effect can be direct or converse: the direct piezoelectric effect occurs when a stress field is applied to the material and it produces an electrical field and change in voltage consequently; the converse piezoelectric effect is the opposite, meaning that provided an electrical field polarising the grains they strain (Jalili (2009), Ballas (2007)). Therefore, piezoelectric patches can be used both as sensors (direct effect) or as actuators (converse effect). The general constitutive relations, in 1 dimension, are presented in eqs. in 2.6.

$$\begin{aligned} S &= s^\epsilon \sigma + d\epsilon \\ D &= d\sigma + \xi^\sigma \epsilon \end{aligned} \tag{2.6}$$

Where:

S : Strain []

D : Dielectric Displacement [C/m^2]

s : Compliance [m^2/N]

ϵ : Electric Field [N/C]

σ : Stress [Pa]

d : Piezoelectric charge constant (or piezoelectric coefficient) [m/V]

ξ : Absolute dielectric permittivity (or permittivity) [F/m]

It can be observed that d couples both equations in 2.6, uniting the electrical with the mechanical effects.

A real piezoelectric material is anisotropic and 3D, thus all the values expressed before turn into tensors of higher orders. Therefore, the strains can be different from the computational representation because each grain would displace in a different direction. To overcome this limitation scientists at NASA Langley Research Center have developed a series of actuators aiming to make the stress and strain as isotropic as possible. Wilkie et al. (2007) developed a Macro Fiber Composite (MFC) actuator which attaches a series of unidirectional piezoelectric wires sandwiched by composite layers. This configuration reduces the effect of the stresses in the direction transverse to the wires (see fig. 2.3).



Figure 2.3: Macro Fiber Composite developed at Nasa (Wilkie et al. (2007))

2.7 Background of the problem

This section provides a short background on the equations that account for the changes in different excitation forces, damping, mistuning and suppression forces used in this work.

The advantage of the damping form described in eq. 2.7 is that the eigenvectors are the same as for the undamped case ($[C]=[0]$) and the eigenvalues are really close to the undamped case. Indeed, for a the r^{th} eigen value:

$$\begin{aligned}\omega'_r &= \bar{\omega}_r \sqrt{1 - \xi_r^2} \\ \xi_r &= \beta \bar{\omega}_r^2 / 2 + \gamma / 2\bar{\omega}_r\end{aligned}\tag{2.7}$$

Where:

ω'_r : Damped resonant frequency

$\bar{\omega}_r$: Undamped natural frequency

ξ_r : Damping ratio

β : Stiffness proportional constant

γ : Mass porportional constant

This model leads to the definition of the displacement for a MDOF system ($\{x\}$), under the assumption that the displacement of a DOF can be estimated as the direct sum of the contribution of every mode's amplitude. If the vector $\{f\}$ is zero except for F_k in the k^{th} position, then the transference function, $\alpha_{jk}(\omega)$, is used to express the displacement at position X_j .

$$\begin{aligned}\{x\} &= \sum_{r=1}^N \frac{\{\phi_r^T\} \{f\} \{\phi_r\}}{\omega_r^2 - \omega^2 + i\eta_r \omega_r^2}; \\ \eta_r &= \beta + \gamma / \bar{\omega}_r^2 = 2\xi_r / \omega_r \\ \alpha_{jk}(\omega) &= \left(\frac{X_j}{F_k} \right) = \sum_{r=1}^N \frac{{}_r A_{jk}}{\omega_r^2 - \omega^2 + i\eta_r \omega_r^2} \\ {}_r A_{jk} &= (\phi_{jr})(\phi_{kr})\end{aligned}\tag{2.8}$$

Where:

ϕ_r : Mass normalised eigenvector

α_{jk} : Frequency response function, measured in the j^{th} with an excitation in the k^{th} position.

$_r A_{jk}$: Modal constant

j : Refers to the j^{th} row in the matrix $[\Phi]$

k : Refers to the k^{th} column in the matrix $[\Phi^T]$

η_r : Damping loss factor

Chapter 3

Theory of the models

3.1 Definition of the models.

A more specific definition of the models is explained in this section. In this thesis two models are explored. First, a model with 1 DOF¹ per blade and a simple suppression force is studied. Then, a second DOF² per blade is added in order to allow a more complex and realistic form for the suppressing force and also the blades themselves.

First, some general terminology is defined in figures 3.1 and 3.2 which will be helpful to easily understand the rest of this chapter. Each model consists of 4 different sectors, sectors are counted clockwise. The first sector is labelled in the figures for each model. A sector is comprised of a disk element and a blade element. In the case of the second model, the blade element contains a Tip-blade element and a Base-blade element. Each of these, as for the blade elements in model 1, is formed by a corresponding mass and spring. For simplicity, dampers have not been added in the model, but damping is considered in this exploration. With these configurations any family of modes can be explored: Bending, Edgewise, Torsional or Extension. The most potentially harmful family for actual blades is the bending family due to the aeroelastic and structural forces occurring axially in a real aircraft engine. Therefore, in this piece of research this family will be referred to. Having said this, the number of DOFs in the first model is 8 and the second is 12. Finally,

¹See constitutive matrices in cons1

²See constitutive matrices in cons2

the form of damping used in these models is Proportional, i.e. $: [C] = \beta[K] + \gamma[M]$.

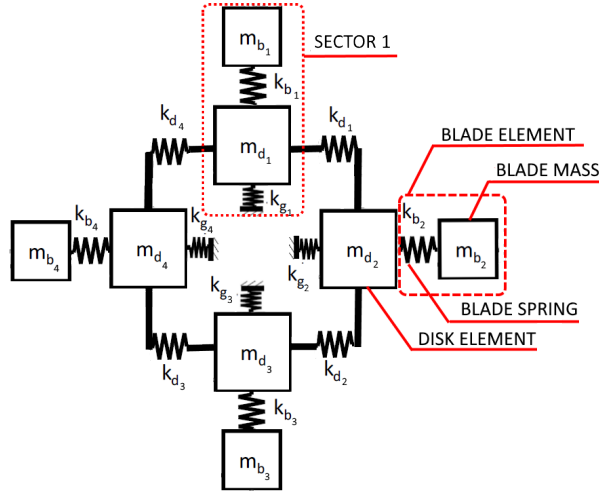


Figure 3.1: Terminology for model 1.

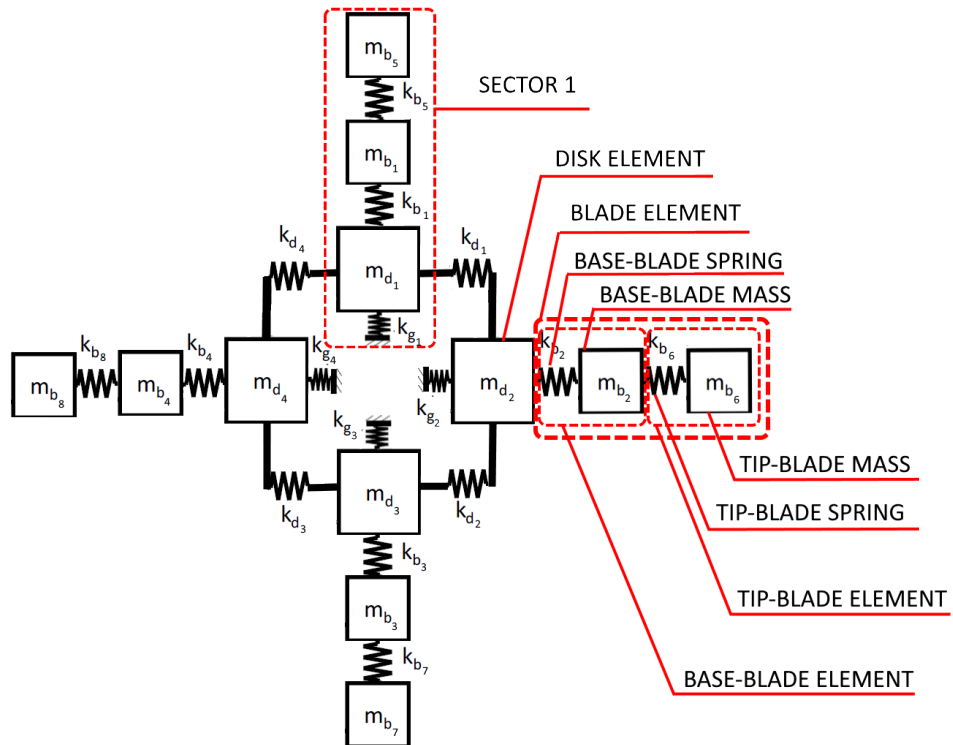


Figure 3.2: Terminology for model 2.

Finally, the structural properties are summarised in table 3.1

Definition	Name	Value
Ground stiffness	k_g	10000 [N/m]
Disk stiffness	k_d	10000 [N/m]
Blade stiffness	k_b	1000 [N/m]
Disk mass	m_d	30 [kg]
Blade mass	m_b	1 [kg]
stiffness Matrix proportional damping constant	β	0.005
Mass Matric proportional damping constant	γ	0.08

Table 3.1: Structural properties of the models.

3.2 Suppression force

The force for suppression aims to reduce the amplitude of the ODS for a certain mode shape. From eq. 2.8 this can be achieved by imposing: $\{f\} \{\phi_r\} = 0$. Consider force $\{f\}$ to be formed by two different forces: an excitation force and a suppression force. More complex models will consider 1 excitation + 2 suppression forces (1+2), 1+3, 1+4,..., 1+N. Hence, the process to obtain, algebraically, the force needed to suppress the r^{th} mode is:

$$\{f\} = \{f_e\} + \{f_s\} \quad (3.1)$$

$$\Rightarrow \text{Imposing} : \{f\} \{\phi_r\} = 0 \quad (3.2)$$

$$\Leftrightarrow \sum_{i=1}^N \{f_e\}_i \phi_{ir} = - \sum_{i=1}^N \{f_s\}_i \phi_{ir} \quad (3.3)$$

If the simplest model for the suppression mode is considered then:

$\{f_s\} = \{0, \dots, 0, F_k, 0, \dots, 0\}$, where F_k is the magnitude of the single DOF suppression force acting in the k^{th} DOF. Note that for this case, with the suppression and excitation forces acting in one DOF only, something interesting occurs. The minus sign at the right hand side of equation 3.3 implies directly that the suppressing force has an opposite direction with respect to the excitation force, or equivalently, that there is a lag phase of 180° (note that the sum disappears and only ϕ_{ir} remains on each side for this case). This does not necessarily take place for a more complex pair of excitation-suppression forces, because the eigenvectors interact in a different form.

Thus, for the case proposed before, equation 3.3 is simplified to (where $\{f_e\}_i$ is the only non zero value of the excitation force):

$$F_k = \frac{-\sum_{i=1}^N \{f_e\}_i \phi_{ir}}{\phi_{kr}} \quad (3.4)$$

If the suppression force was applied to two DOF, say k th and j th, then:

$$F_k \phi_{kr} + F_l \phi_{lr} = - \sum_{i=1}^N \{f_e\}_i \phi_{ir} \quad (3.5)$$

By adding more DOFs into $\{f_s\}$, the model will return to equation 3.3 with:

$$\{f_s\} = \{f_1, \dots, f_N\}$$

This last force: $\{f_s\} = \{f_1, \dots, f_N\}$, can be modelled as a group of forces proportional to each other, such that: $F_i = \alpha_{i,j} * F_j$, with F_i the magnitude of the suppressing force in the i th DOF. Then if the location of one of the forces is fixed, say for $j = k$, the magnitude F_k could be obtained if the set of constants $\alpha_{k,j}$ are known (note that $\alpha_{k,k} = 1$). With these two conditions: F_k fixed and $\alpha_{k,j}$ known, equation 3.5 transforms into:

$$F_1 \phi_{1r} + \dots + F_k \phi_{kr} + \dots + F_N \phi_{Nr} = - \sum_{i=1}^N \{f_e\}_i \phi_{ir} \quad (3.6)$$

$$\Rightarrow \alpha_{1,k} * F_k * \phi_{1r} + \dots + F_k \phi_{kr} + \dots + \alpha_{N,k} * F_k * \phi_{Nr} = - \sum_{i=1}^N \{f_e\}_i \phi_{ir} \quad (3.7)$$

$$\Rightarrow F_k = \frac{-\sum_{i=1}^N \{f_e\}_i \phi_{ir}}{\alpha_{1,k} \phi_{1r} + \dots + \phi_{kr} + \dots + \alpha_{N,k} \phi_{Nr}} \quad (3.8)$$

$$\Leftrightarrow F_k = \frac{-\sum_{i=1}^N \{f_e\}_i \phi_{ir}}{< \alpha, \phi_r >} \quad (3.9)$$

A particular case of equation 3.5 is: $F_k = -F_l$, such that: $\{f_s\} = \{0, \dots, \pm F, \dots, \mp F, \dots, 0\}$. In that case, if the location of both F s are known, say i and j , then the magnitude F can be derived. For simplicity, consider: $\{f_s\} = \{0, \dots, F, \dots, -F, \dots, 0\}$. Then the magnitude of the force at both locations i and j : $F_{i,j}$, is obtained by means of:

$$F_{i,j} = \frac{-\sum_{i=1}^N \{f_e\}_i \phi_{ir}}{\phi_{ir} - \phi_{jr}} \quad (3.10)$$

A similar case, this time slightly more complex, is when this pair of locations (i, j) is repeated somewhere else, say (k, l) , in such case the suppressing force would look like: $\{f_s\} = \{0, \dots, F, \dots, -F, \dots, F, \dots, -F, \dots, 0\}$. Thus, analogously to the previous case, if F is the same for the four positions, and the locations are known, the force can be derived using:

$$F_{i,j,k,l} = \frac{-\sum_{i=1}^N \{f_e\}_i \phi_{ir}}{\phi_{ir} - \phi_{jr} + \phi_{kr} - \phi_{lr}} \quad (3.11)$$

3.2.1 Forms of modal suppression

As mentioned in the previous section, a suppressing force can be applied in various forms depending on how many modes and piezoelectric forces are used, these suppressing forms can be divided into 4 groups:

- Single Force - Single Mode (SFSM): A single DOF suppressing force is used to target one mode only.
- Single Force - Multiple Modes (SFMM): A single DOF suppressing force is used to target multiple modes.
- Multiple Forces - Single Mode (MFSM): A force in multiple DOFs is used to suppress a single mode.
- Multiple Forces - Multiple Modes (MFMM): A force in multiple DOFs is used to suppress multiple modes.

As will be discussed later in this report, each of them differs in their degree of effectiveness and real applicability. For example, a single force necessary to suppress a mode can be easily found in a discrete system, as shown in equation 3.4. It can be very effective in reducing the displacement of various or all the DOFs in the system, but it may not be realistic because, it could have a very high value not reachable by a commercial piezo. This is also not realistic since during normal operation various modes in the structure will occur.

A SFMM method of suppression, can be seen in three different ways: (a) One piezo could be installed initially in each blade and the single optimum piezo is activated in the optimum location obtained to suppress a desired mode when it is detected. Alternatively, (b) all the possible optimum locations to suppress all the desired modes can be obtained and only these piezos are installed in the system. Finally, (c) a single piezo can be used to target a single mode, for example the most dangerous for the system, and also be used in all the other modes if it is beneficial in reducing the vibration.

A MFSM approach would apply a force in various DOFs to target one mode only, in

practice it is equivalent to attach various piezos in the structure. This would be more expensive than SFSM because it needs more piezos and control, but it can reach realistic forces with less magnitude up to a point where there may exist commercial patches available. As for SFSM, this is not realistic either because in a real flight several modes would appear.

Finally, a MFMM approach is the more complex approach. As explained for the SFMM approach MFMM possess the same three possible interpretations. (a) Initially one piezo is installed per blade in the structure and the n-optimum piezos activated when needed. (b) The n-optimum piezos for all the modes are localised and installed and activated as required during operation. Or, (c) n-optimum piezos used to target a single mode are attached to the structure and also activated for other modes when their use is not detrimental. Note that multi forcing approaches are always more expensive, from the point of view of the turbomachines manufacturer, because they require to install one piezo per blade in advance. Therefore, the optimisation process suggested in this thesis can be used accordingly, in order to find which are the appropriate positions to locate those critical patches.

In addition, it is worth noting that so far a clear explanation of what is ‘optimum’ has not been provided. This is defined in the following section

3.2.2 Measures of the Optimum force for suppression

Two different paths have been followed for suppression in this work, for each of them an optimum has been defined considering the magnitude and location of the suppressing forces.

On the one hand, the force required for the total suppression of a mode is searched among all the possible locations. The optimum is defined as the minimum of these forces, thus the force magnitude and its location are defined. Since the minimum force found with this method may be too high, and therefore impossible to achieve, another method is proposed.

This second method assumes a force equal to 1% of the excitation force. This is a value more realistic for the stresses exerted by the commercial piezoelectric patches when compared with the aeroelastic and structural forces in the engine.

Thus, the force is chosen and the location is to be found. The optimum location is defined for this method as the location capable of delivering the minimum Modal Scale

Factor (MSF) in a mode. The MSF is defined as follows:

$$MSF = \frac{\sum_{j=1}^n (\nu_s)_j * (\nu_{us})_j}{\sum_{j=1}^n (\nu_{us})_j * (\nu_{us})_j} \quad (3.12)$$

Where:

ν_{us} : vector of unsuppressed displacement.

ν_s : vector of suppressed displacement.

j : DOFs in the mode.

Thus, an MSF equal to one means no change between the suppressed and the unsuppressed displacement. Oppositely, an MSF equal to zero means a total suppression of the displacement, this means that every single DOF in the suppressed state is null. Note that this parameter is an overall indicator of the ratio between the suppressed response and the unsuppressed response at each point. This means, for example, that the MSF can be less than one, however, one or more of the elements in the displacement vector ν_{sj} , say the j th DOF, could present a ratio ν_{sj}/ν_{usj} bigger than 1.

Another MSF that only considers blades is also used. Model 1 defines 1 DOF per blades while model 2, 2 DOFs per blade. Each model has four sectors, therefore the first blade for any model is DOF number 5. With this, their corresponding MSF_1 , for model 1, and MSF_2 , for model 2 are defined as follows:

$$MSF_1 = \frac{\sum_{j=5}^8 (\nu_s)_j * (\nu_{us})_j}{\sum_{j=5}^8 (\nu_{us})_j * (\nu_{us})_j} \quad (3.13)$$

$$MSF_2 = \frac{\sum_{j=5}^{12} (\nu_s)_j * (\nu_{us})_j}{\sum_{j=5}^{12} (\nu_{us})_j * (\nu_{us})_j} \quad (3.14)$$

3.2.3 Models of the piezoelectric force in the discrete model

In this thesis the representation of the piezoelectric force considers the mechanical effects only, which means that the electromagnetic effects are not yet coupled with the mechanical stresses applied by the piezoelectric patch.

In this work the force exerted by a piezoelectric patch is explored with three different approaches: a single DOF force, a force acting in two DOFs, and 2 forces acting in 2 DOFs.

1 DOF per piezoelectric patch.

A single DOF force means that the piezoelectric patch is acting in any of the DOFs in the models. This force can be in-phase or out-of-phase with respect to the excitation force. Figure 3.3 shows an example of a force in-phase (in red) an out of phase (blue) in different DOFs.

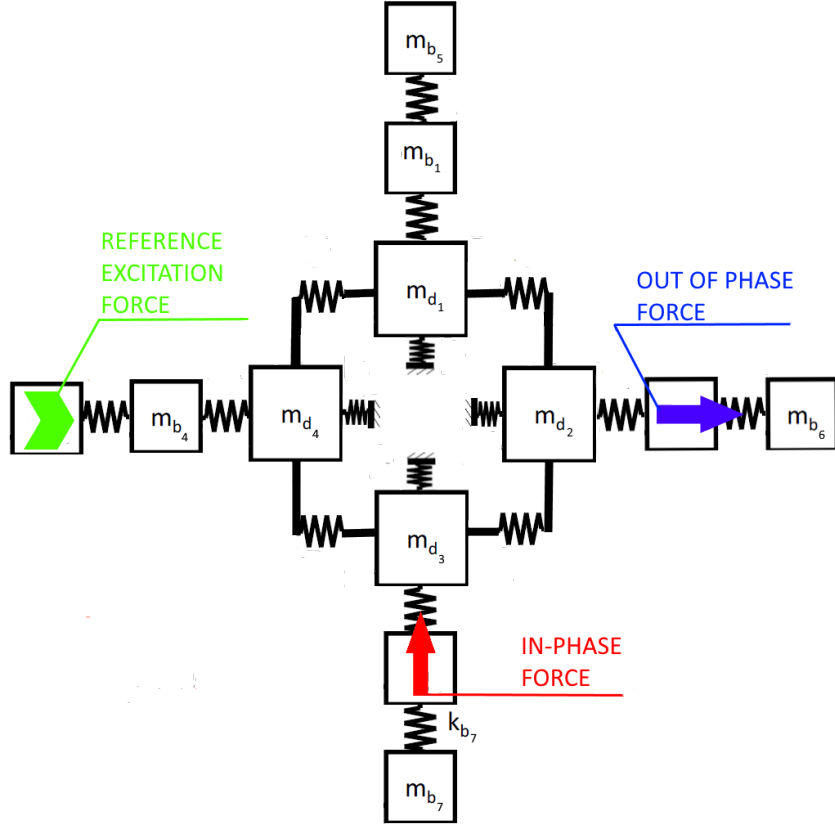


Figure 3.3: Piezoelectric patch operation represented as 1DOF suppressing force

2 DOFs per piezoelectric patch.

A more realistic model of a contracting/expanding piezoelectric patch is a suppressing force acting in 2 DOFs, in compression or tension. Three different forms of links are explored (in a model with 2 DOF per blade) in this research. These forms are: disk-disk link, disk to base of the blade link and a link between base and tip of a blade. Figure 3.4 illustrates an example for each of the three different links. Clearly, in this case the terms in-phase and out of phase loose meaning because always one of the two forces representing the piezoelectric patch is in-phase and the other out of phase with respect to the excitation force.

The colours in the picture are used to differentiate between contraction (red) and tension (blue) for a certain direction of the reference excitation force (green). Also, the reader may have noticed that a fourth type of link is ignored between the tip of the blade and the disk. This is due to the unrealistic consequences of having the DOF in the middle, the base of the blade mass, unaltered when a piezoelectric patch is passing over it.

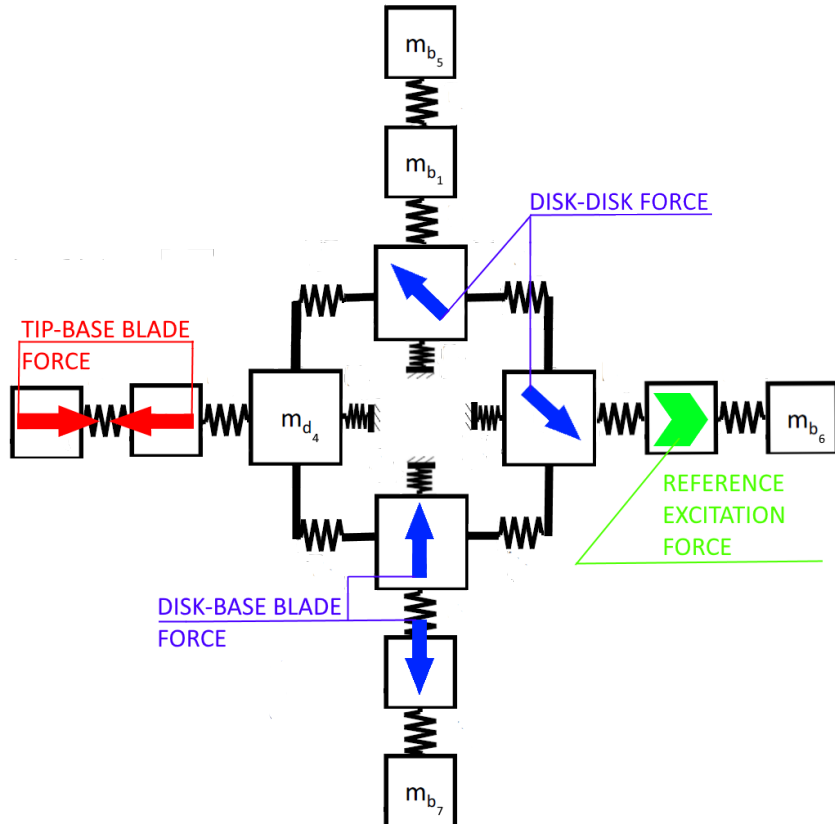


Figure 3.4: Piezoelectric patch operation represented as 2DOF suppressing force in three different possible locations.

2 piezoelectric patches and 2 DOFs per patch.

A third approach for suppression is the implementation of 2 piezoelectric patches, each acting in two DOFs as showed in figure 3.4 for a single patch.

For this approach 2 considerations have been taken into account to make the force more realistic. First, since it is unpractical to pose one piezoelectric on top of another, the two forces cannot superpose in this model. Note that this would represent the trivial case of a piezo with a force of 2% of the excitation force, instead of 1%. Second, it is plausible to conceive a configuration where a piezo is installed in a structure immediately next to other patch, therefore 2 of the 4 punctual forces representing both piezos can

superpose in this model. Note that these 2 superposed forces can be in phase or out of phase, meaning that they will double or cancel out respectively. Figure 3.5 illustrates these restrictions, no excitation force is added for simplification.

Note that the possible positions have been already defined above for one piezo in figure 3.4. In the diagram below, each of the four branches represent one sector, each sector contains a disk and 2 blade elements. The 4 disks are represented here by the 4 intercepts to the horizontal and vertical lines that are closest to the center. From that intercept outwards, the 2 intercepts represents the 2 blade elements.

Four cases are represented in figure 3.5: (1) Two piezos in a disk-blade location. (2) One piezo in disk-blade location and one in a tip-base blade location. Both forces at the base of the blade are superposed because they are in-phase. (3) Same locations as in case (2), now the forces at the base blade are out of phase, which mean they cancel each other. (4) Two patches in a disk-disk configuration. One force is in-phase at one disk.

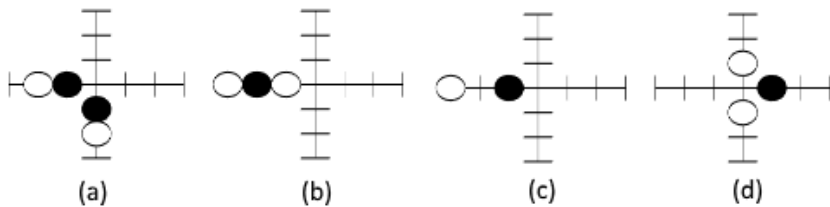


Figure 3.5: Restrictions on 2 Piezoelectric patches operation represented as 2DOF suppressing force per patch.(a) Case 1. (b) Case 2. (c) Case 3. (d) Case 4.

3.3 Restrictions on the models.

Some restrictions on the model are implemented to keep it as simple as possible while keeping the necessary features to achieve the objectives of the research.

1. These models involve a linear representation of the structure. This means two key characteristics. Firstly, the response, at a certain DOF, is directly proportional to the total force in that DOF. Secondly, the response at one DOF is produced by the contributions of each of the mode shapes in the system (principle of superposition).
2. There is no phase between the suppressing force and the displacement. Also, no phase is considered between the excitation force and the suppressing force.
3. The suppressing force is designed to target one mode. This means that it would act

only in a small range of frequency around the resonance of the targeted mode and not in the entire frequency domain. This range is 0.04 [Hz].

4. The piezoelectric effect is not incorporated in this model. In other words, the electromagnetic effects are not coupled with the mechanical effects in the model of the patches in this thesis.
5. These models are static. This means that no rotation is incorporated in the structure. In other words, the centrifugal forces are disregarded in these models.
6. As briefly explained before, for practical and more realistic reasons the family of mode shapes under study in this thesis is the Bending family.
7. There are not links between blade elements of different sectors. This means that the fan blades are not shrouded.
8. The excitation force implemented in this report is a simple SBE in the last element of each model, unless stated otherwise.
9. The range of mistuning explored in this report is from 0-10% for stiffness and mass mistuning, unless something else is specified. Anything bigger than 10% appears to be unrealistic.

Chapter 4

Model validation.

A set of preliminary explorations must be carried out in order to confirm that the model behaves accurately and as expected according to the literature. These studies seek to check whether the changes in the excitation force, damping and mistuning modify the response of the system as described in chap:lr.

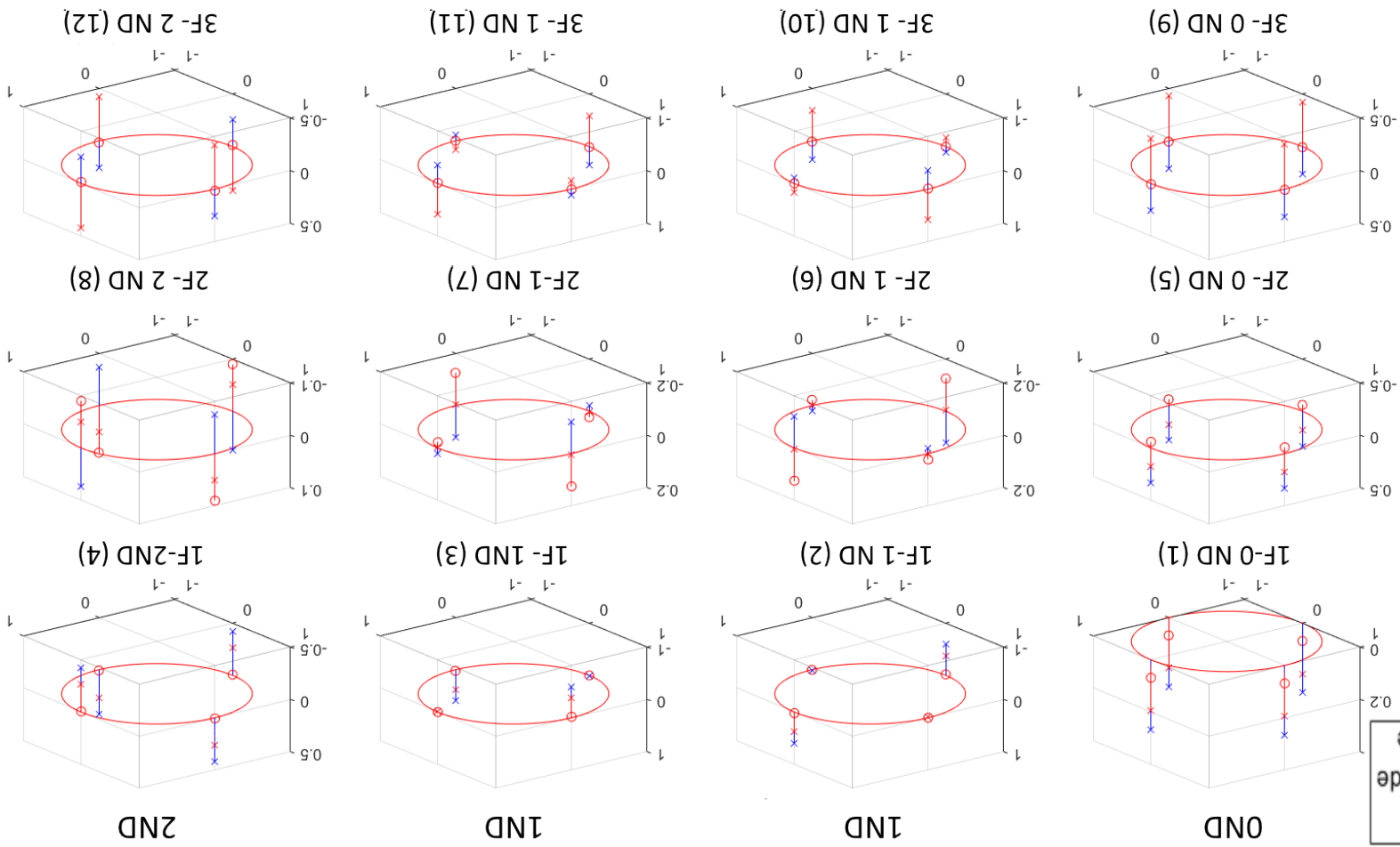
4.1 Mode shapes and displacement

4.1.1 Mode shapes

Initially, this analysis considers a perfectly tuned system only. Figure 4.1 shows the 12 mode shapes for the perfectly tuned model with 2 DOFs per blade. Note that these are the eigen vectors and not the displacement at each DOF. In each column of images the NDs are displayed as well as the NCs in the rows, both of them, NDs and NCs, are ranged from 0 to 2. Below each mode shape the corresponding name is expressed, next to it, in parenthesis, a general index is provided which will be helpful in understanding the rest of this thesis.

Note that the values of the elements lying at the nodal line for the XF-1ND mode shapes are not exactly 0. This is caused by the internal error of the solver in MatLab. The error is almost negligible, therefore no further efforts are made to reduce this even more. However, there are available packages and toolboxes that allow to decrease this error (see:<https://www.advanpix.com/>).

Figure A.1: Mode shapes of a perfectly tuned system with 2 DOFs per blade.



A NC is more complex to be noticed from the mode shapes than a ND. A single sector is composed by 3 different elements: disk, base-blade and tip-blade. There can be up to 2 NCs. The first case is for a 0 NC meaning that all the elements (disks, base-blades and tip-blades) are positive or negative ((+++) or (---)). A second case implies one change in contiguous elements, for example: (+--) or (++-). A third case of 2 NCs, requires 2 changes in sign along a sector, for example: (+-+) or (-+-).

Now that the eigenvectors are fully understood the eigenvalues can be shown to complete the modal information. Table 4.1 displays all the natural frequencies corresponding to every mode shape.

Mode code	Mode name	Frequency [Hz]
1	1F-0ND	16,50
2	1F-1ND	19,18
3	1F-1ND	19,18
4	1F-2ND	19,36
5	2F-0ND	21,58
6	2F-1ND	32,13
7	2F-1ND	32,13
8	2F-2ND	41,00
9	3F-0ND	51,27
10	3F-1ND	51,31
11	3F-1ND	51,31
12	3F-2ND	51,42

Table 4.1: Eigenvalues of a perfectly tuned system.

Each of these modes contributes in the displacement of a DOF. For example, figure 4.2 shows $\alpha_{12,12}$ for a damped and tuned system. The FRF at this drive point shows that, as expected, the total FRF is above all the rest, because it is the summation of all of them. Note that some resonances are very close together, around 20 [Hz] and 50 [Hz], this effect is referred as mode coupling. Mode coupling imply that it is hard to allocate the mayor responsibility of a mode in the total DOF's displacement.

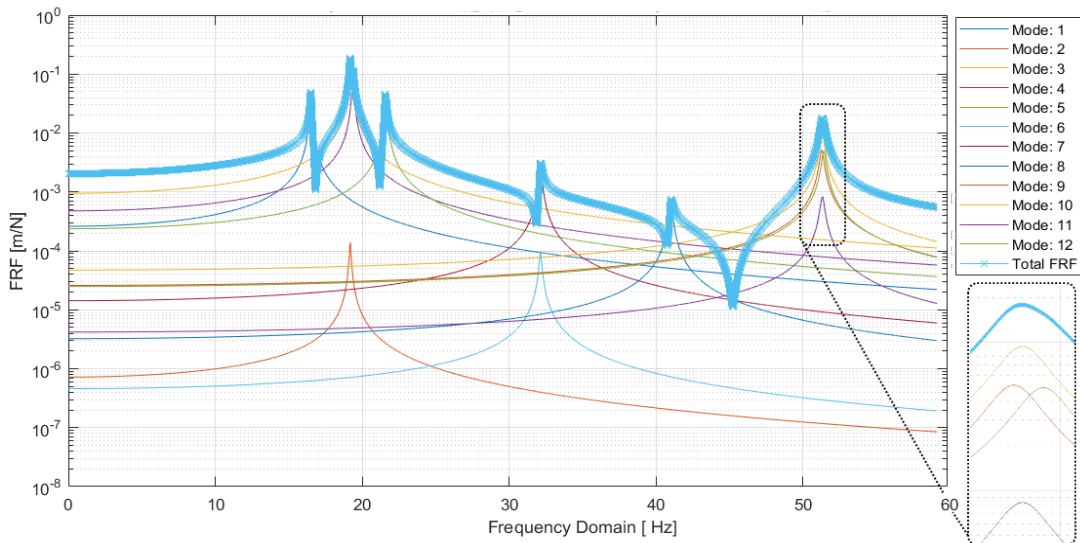


Figure 4.2: Mode shapes of a perfectly tuned system with 2 DOFs per blade.

4.1.2 Displacement extraction

Displacement does not only involve the configuration described by the eigen vectors but also the magnitude and phase corresponding to the resonances derived from each eigen value.

Needless to say, this system is discrete in frequency. Therefore, the corresponding information of magnitude and phase is extracted for each DOF at the closest frequency to resonance. A subtle but relevant problem here arises. The closest frequency found by the software may not be exactly the same as the resonant frequency delivered in the eigen values. This is solved by decreasing the frequency steps until the difference in magnitude for a certain DOF and frequency is negligible. The frequency step used in all these tests is 0.001 [Hz].

After this refinement, the magnitude of the displacement is extracted and the sign is incorporated from the phase information. Figure 4.3 illustrates this procedure schematically. This is carried out for mode 1F-2ND(4) with 10% of m -mistuning increase in the mass corresponding to the tip of the blade of the first sector: m_{b_5} .

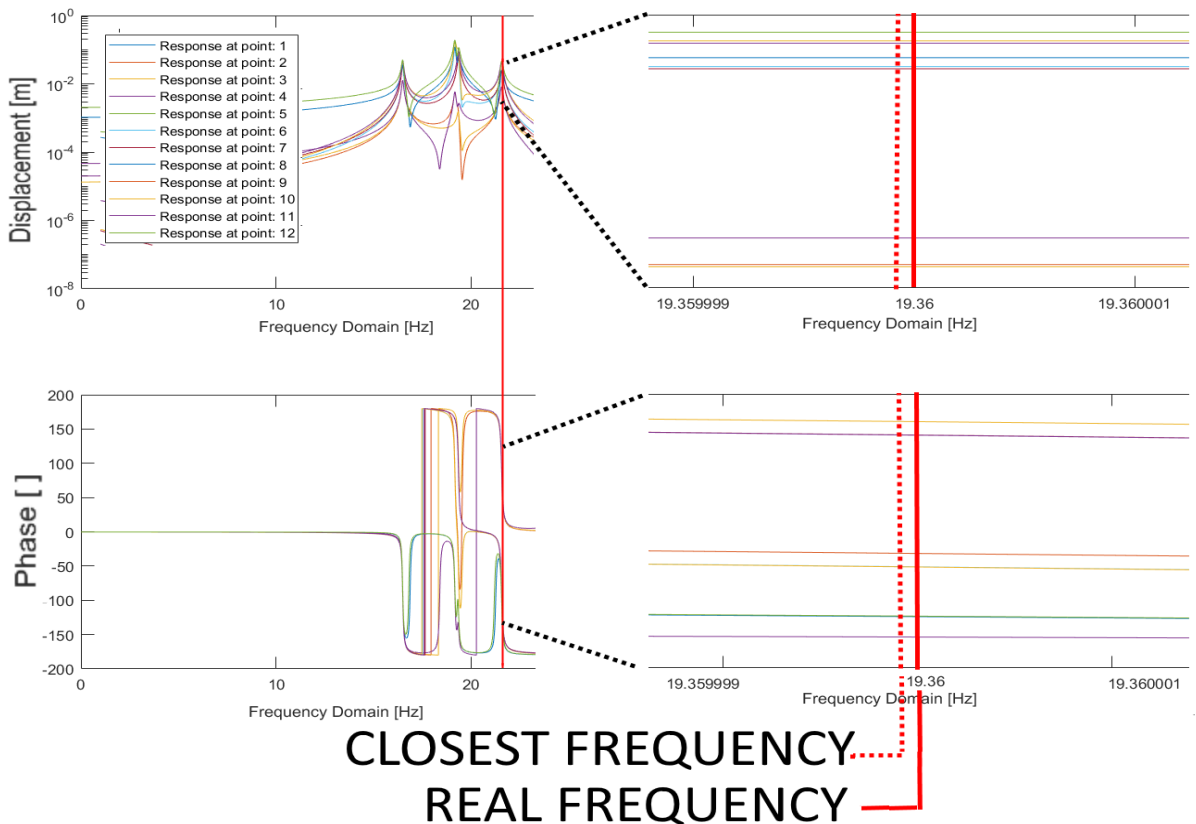


Figure 4.3: Magnitude and phase picking.

4.2 Different excitation forces

Different forcing patterns will excite different modes and DOFs. Also, some forces will completely cancel the activity of some modes. Before thinking in a 12 MDOFs system, a simpler approach can be taken to reason about the activation and cancellation of modes. For example, for a SDOF system, if the excitation goes in the opposite direction of the displacement of the natural mode, the mode is cancelled, on the other hand, if the excitation goes in phase with the natural displacement, the mode is activated or excited. Analogously, for a 2 DOFs system, if the excitation tends to compress when the mode natural movement is to expand, then the mode is cancelled. In this section 3 different excitation forces are displayed. First, a SBE in the last tip-blade element (12th DOF), the second force is acting in all DOFs (1-12 DOFs), finally, a force acting in the tip-blade of the 1st and 3rd sector is used. Figure 4.4 illustrates these forces.

First, the results are explored in terms of the displacement at each DOF and then the FRF is explored.

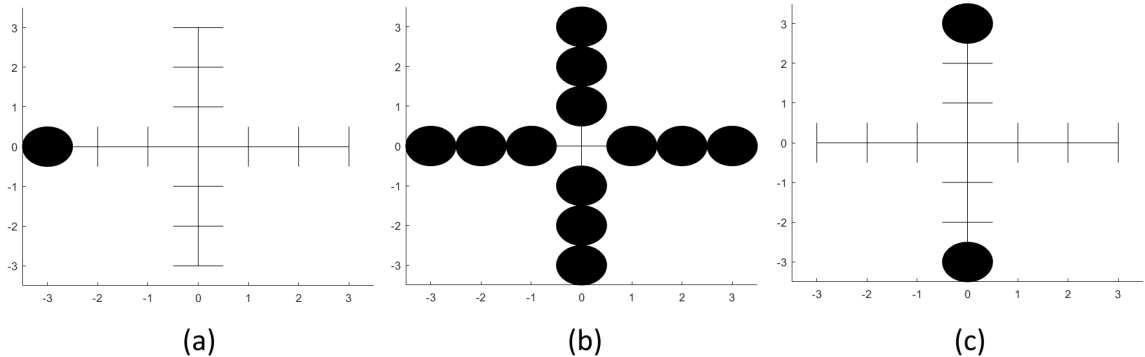


Figure 4.4: Three different excitation forces patterns.(a) 12th DOF excited. (b) All 12 DOFs excited. (c) DOFs 9 and 11 are excited.

4.2.1 Single Blade Excitation

In this section the effect of a force acting in the tip of a blade is implemented. The force is equivalent to the image displayed in 4.4(a). This type of force will tend to push the elements in the blade and disk corresponding to that sector. For example, the force depicted in 4.4(a) would excite masses m_{b_8} , m_{b_4} and m_{d_4} , all of them aligned in the same sector. Equivalently, if the force is applied in mass m_{b_5} , the most displaced DOFs would be m_{b_5} , m_{b_1} and m_{d_1} . This is demonstrated for all four possible excitation of the type

displayed in 4.4(a) in all DOFs in figure 4.5. (The DOFs have been labelled here 1-4 for disks, 5-8 for the base of the blade and 9-12 for the tips.)

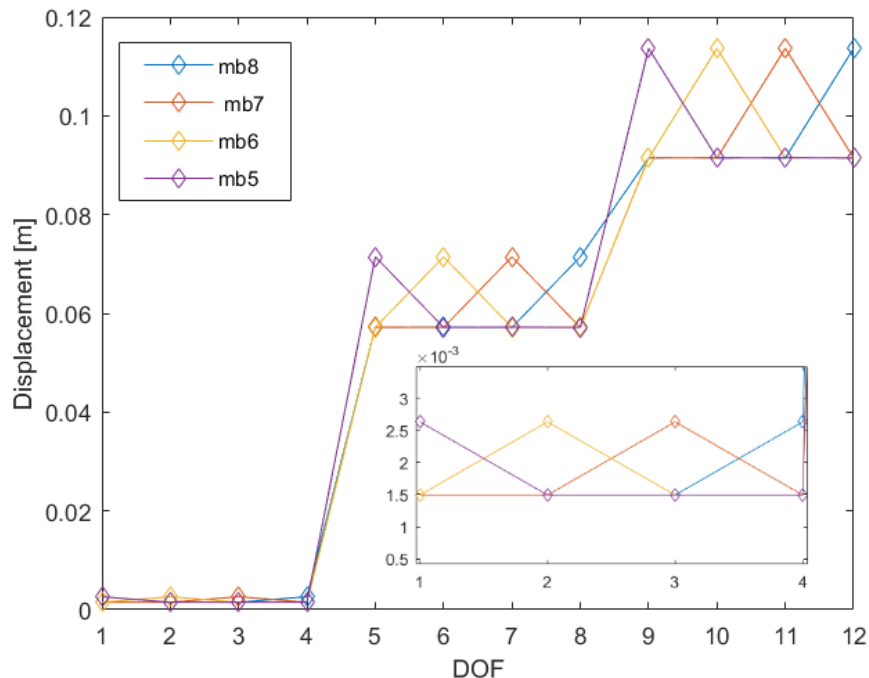


Figure 4.5: Effect of 4 excitation forces, each in a tip blade.

From the image it can be seen how each excitation moves its corresponding blade. Thus, m_{b_8} acts more in DOF: 12, 8 and 4; m_{b_7} in 11, 7 and 3; m_{b_6} in 10, 6 and 2; and m_{b_5} in 9, 5, 1.

Now that it is clear that a single localised force in 1 DOF does push certain DOFs more than the rest, it follows that some excitation patterns acting in several DOFs would excite some natural modes more than others. This is explored in the next section in terms of the FRF.

4.2.2 Multiple Blades Excitation

A useful approach to analyse the effect of these forces into the system is to observe the mode contribution in the FRF. Figure 4.6 illustrates the FRFs for each forcing pattern displayed above in figure 4.5 measured in the 12th DOF. No damping or mistuning is yet applied into the model.

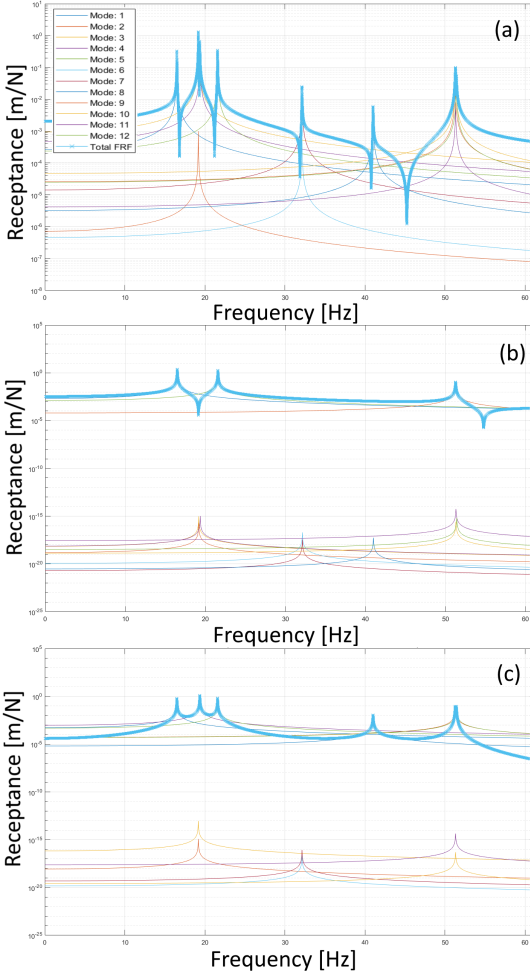


Figure 4.6: FRF of the 12th DOF after with excitation force. (a) FRF with an excitation force in the 12th DOF. (b)

FRF with an excitation force applied in all 12 DOFs. (c) FRF with an excitation force exciting the 9th and 11th DOFs.

First, all the modes are excited in figure 4.6(b). Some of them slightly more than the rest. This occurs because the excitation force is in a 180° phase with the 12th DOF of that mode. However, the rest of the modes still excited, because

they are in phase with the force in the 12th DOF.

Second, the pattern implemented in 4.6(b) does not posses any angular symmetry, indeed the patter does not have any ND. Therefore, this pattern would excite modes without any ND. The modes correspond to this definition are: 1F-0ND, 2F-0ND and 3F-0ND. As expected, the FRF displays the predominance of these modes in the totar response. The rest of the modes are cancelled because the excitation pattern annul the presence of the ND.

Finally, image 4.6(c) shows how 6 modes have a minor participation in the total FRF. This modes corresponds to the double modes of each group: 1F, 2F and 3F. Since the excitation force is located across the model it cancel one ND. However, when there are

none ND or 2NDs the mode still excited by this force because there are still DOFs prone to the movement.

In order to analyse the effect of damping, mistuning and suppression of the modes in this thesis, an excitation force capable of target every single mode is needed. In particular, for this 2 DOFs per blade system the

excitation force acts in the 12th DOF: tip blade element of the 4th sector, as shown in figure 4.4(a). Note that this consideration makes invalid the Whitehead factor (see eq. 2.5) as the upper limit of the mistuned cases, because this is not an *nEOE*.

4.3 Damping

The purpose of this section is to verify the effect of different levels of damping in the FRF. Three different levels of Proportional Damping are computed and displayed in figure 4.7 below. The response is measured in the 12th element (tip-blade of the 4th sector) after a simple SBE in the same location ($\alpha_{12,12}$) is applied. The proportional damping constants are: (a) $\gamma=0.005$, (b) $\gamma=0.05$ and (c) $\gamma=0.5$. β is equal to 0.08 for all cases.

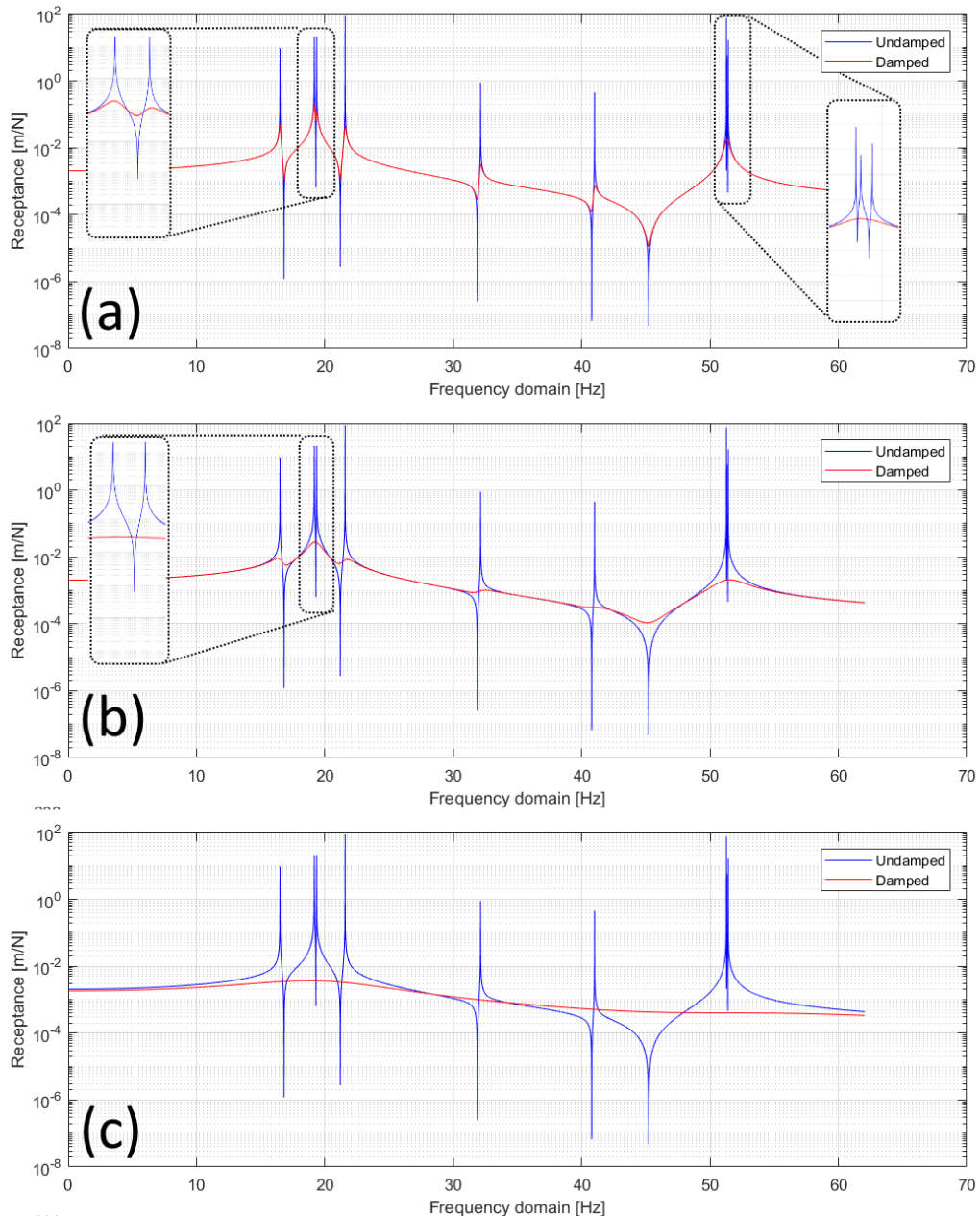


Figure 4.7: Three different levels of proportional damping and their impact in the FRF.(a) $\gamma=0.005$.(b) $\gamma=0.05$.(c) $\gamma=0.5$. $\beta=0.08$ for all cases.

Figures 4.7(a),(b) and (c) display an increasingly flattened curve as effect of the high level of damping. Note also that as the damping increases more modes are coupled together. For example, modes around 50 [Hz] are coupled with $\gamma=0.005$. Also, as γ increases from 0.005 to 0.05 modes around 20 [Hz] are coupled. Finally, when $\gamma=0.5$ all modes are flattened and/or coupled.

The level chosen, based on some references applied to similar models is $\gamma=0.005$ and $\beta=0.08$. These values were kept in order to have some coupled modes as in reality, as for the case of group 3F, but also several decoupled modes to extract the features to be analysed throughout this work (groups 1F and 2F). (Rotea and D'Amato (2002); Wang and Li (2014))

4.4 Mistuning

Initially, this section demonstrates the effects of mistuning in a perfectly tuned system as described in chap:lr, these effects are: frequency shift, frequency split and also localisation of the displacement response.

In this section stiffness and mass mistuning (k -mistuning and m -mistuning respectively) are tested in the model. Damping is also included in all the tests. Each form of mistuning is checked in the model separately, i.e. k -stiffness does not occur simultaneously with m -mistuning. In this chapter, mistuning is only applied in one element, more complex mistuning patterns will be explored in following chapters.

First, mistuning is studied in the FRF, along the entire frequency domain, and then locally in terms of the displacement of each element in the model at resonance.

4.4.1 FRF of a mistuned and tuned system

The mistuned element in the structure is the first blade: k_{b_5} (tip stiffness) and m_{b_5} (tip mass). The mistuned stiffness and mass are both 150% of the tuned properties. Figures 4.8 and 4.9 illustrate the comparison of a mistuned/tuned system for a k -mistuning and m -mistuning respectively.

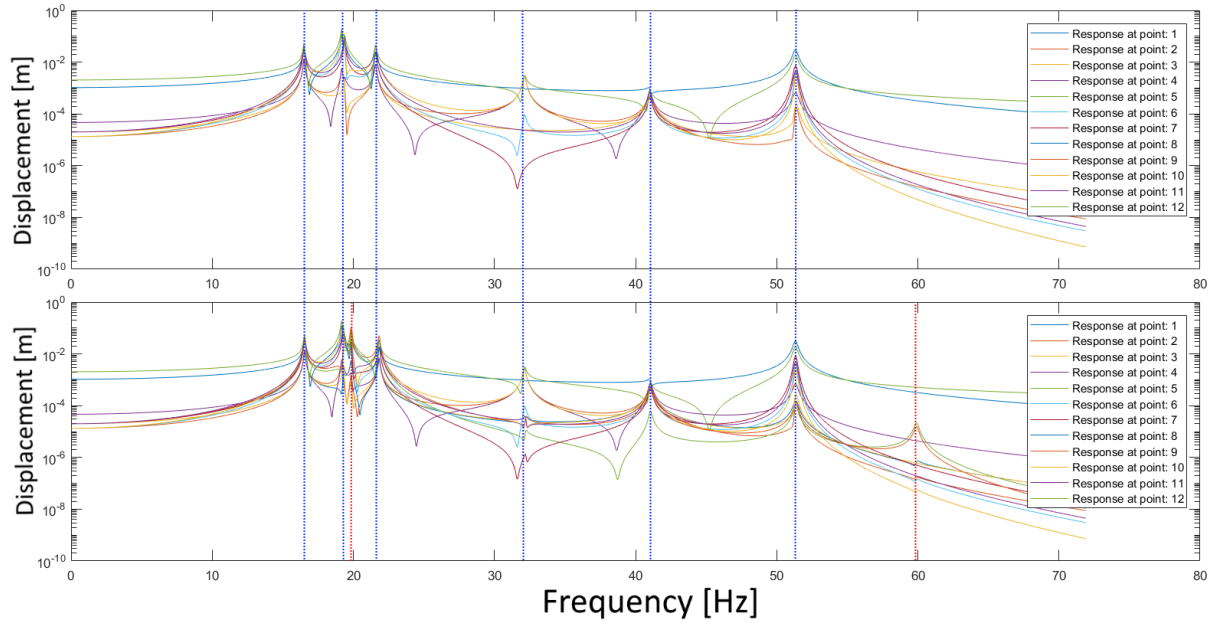


Figure 4.8: FRF of a k -mistuning for every DOF in the model. Top: Tuned systems, bottom: Mistuned system.

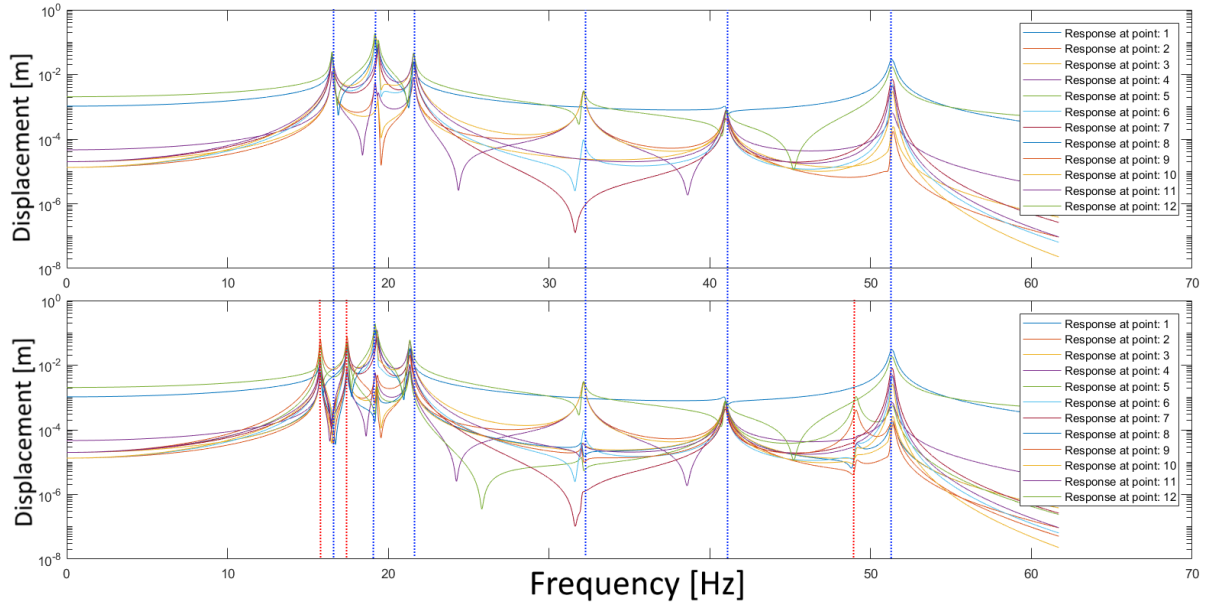


Figure 4.9: FRF of a m -mistuning for every DOF in the model. Top: Tuned systems, bottom: Mistuned system.

Blue lines are added to compare some of the resonant frequencies of the tuned system with mistuned system. Red lines are included to remark the most evident changes in the mistuned system.

As expected, resonances move to the right as the stiffness increases, also the double

modes are splitted into two as it is more evidently showed around 20 Hz in figure 4.8.

4.4.2 Displacement of an increasingly mistuned system

As briefly described at the beginning of this chapter, k -mistuning and m -mistuning are here explored locally for each element in the model. It is worth noting that the aim of this section is rather qualitative. The objective is to show how the displacement tends to localise in certain modes/elements and how the mistuned mode shapes are distorted with respect to the tuned case.

Each case of mistuning is tested for four different magnitudes, where the first case is a perfectly tuned case. For each case, the ratio of the mistuned to the tuned displacement is presented (left hand side in each figure) along with the Modal Assurance Criterion (MAC) (right hand side in each image).

Figure 4.10 shows 4 cases of increasing mistuning: 0%, 10%, 50% and 200%. The mistuned local stiffness is the same as for the analysis in the FRF: k_{b_5} (tip stiffness of the first blade). This corresponds to the spring linking elements 5 and 9.

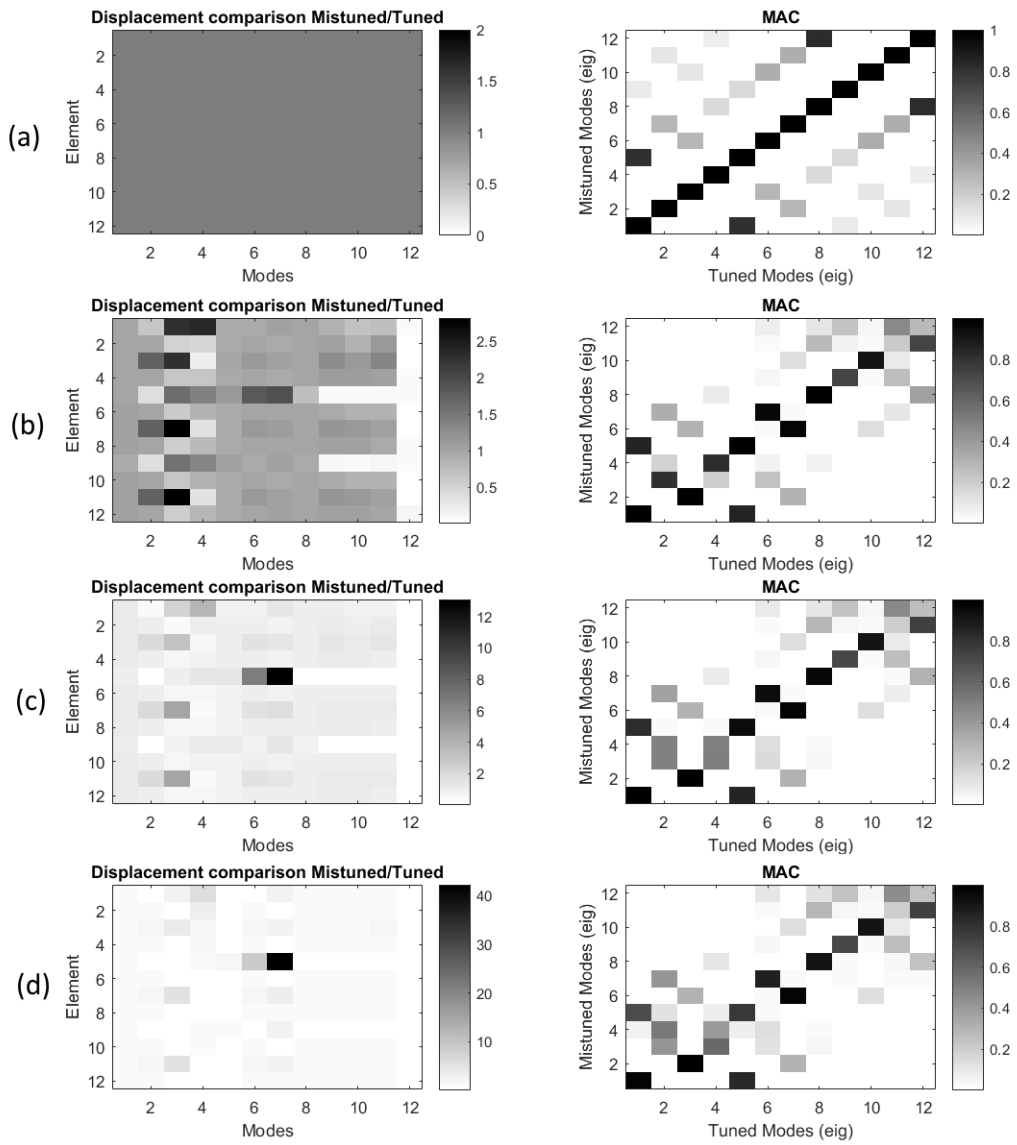


Figure 4.10: Stiffness mistuning. Ratio of the Mistuned to the Tuned displacements for all the modes and elements (left). MAC (right). k -mistuning factor: (a) 0%, (b) 10%, (c) 50% and (d) 200%.

In general, it is observed how the mistuning focuses the responses in some elements, as the left column of images displays. Also, as expected, the modes are distorted in shape and splitted where there are double modes as observed from the MACs. The maximum ratio of the mistuned/tuned displacements increases as the mistuning factor is increased, this ratio ranges from barely more than 4.5 times (in (b)) up to 40 times (in (d)).

Figure 4.11 shows the effect of an increasing mistuning now in a mass element. The mistuned mass is the same as for the FRF study: m_{b_5} (tip mass of the first blade). The mistuning levels in this case are: 0%, 10%, 50% and 200%.

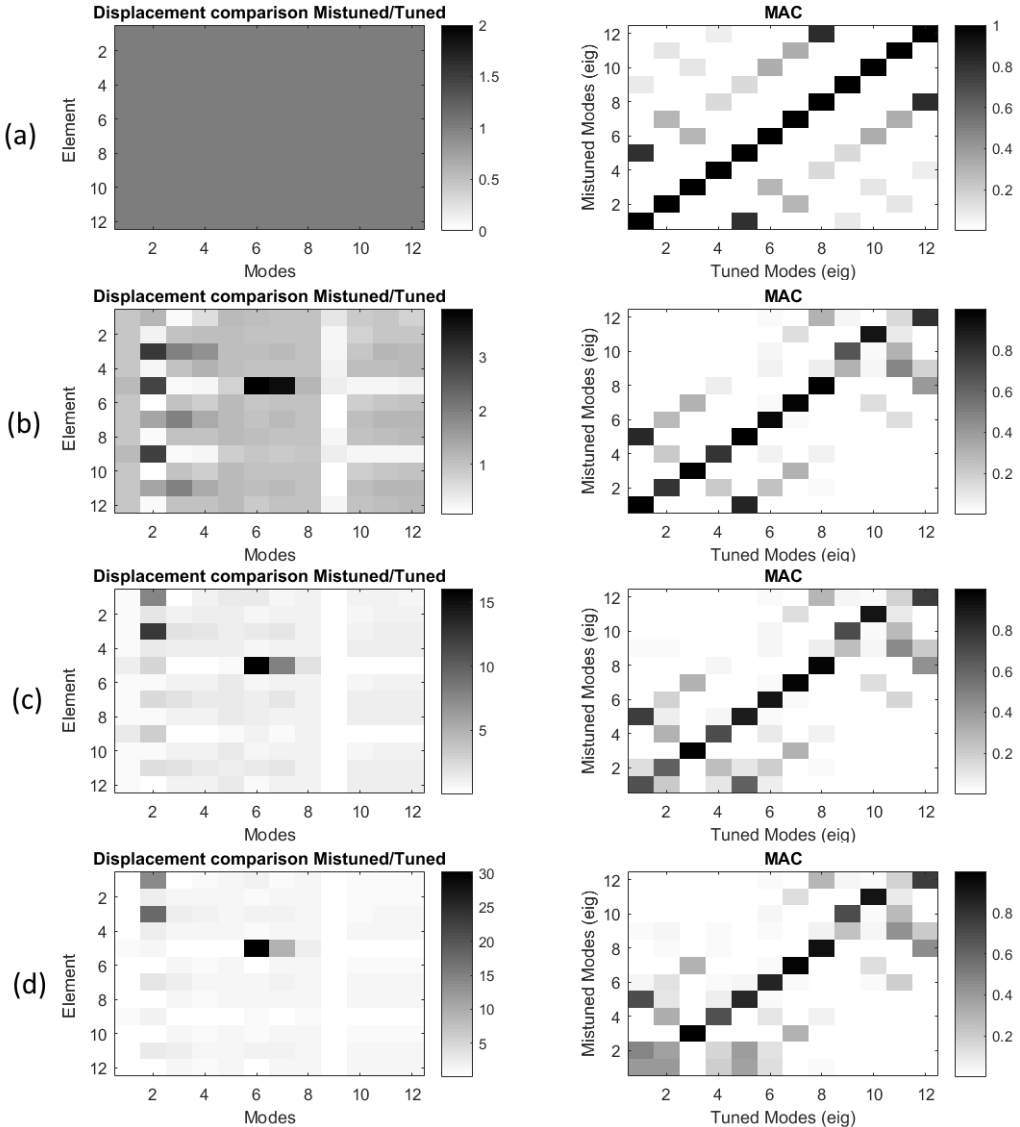


Figure 4.11: Mass mistuning. Ratio of the Mistuned to the Tuned displacements for all the modes and elements (left). MAC (right). m -mistuning factor: (a) 0%, (b) 10%, (c) 50% and (d) 200%.

Modes distortion and mode localisation occur similarly for both k -mistuning and m -mistuning. Mode localisation due to mistuning does not always play a harmful role in the displacement response. Sometimes it can attenuate the response for certain elements in the structure. This is clearly evidenced in the images 4.10(b) and 4.11(b) where the whiter blocks show a ratio mistuned/tuned less than unity. Interestingly, at high frequencies (modes 9-12), the response is most attenuated for elements 5 and 9, exactly the same elements linked by the mistuned stiffness and for the case of m -mistuning: both the mistuned mass element and its closest DOF.

Note that the set of images in the left hand side of figures 4.10 and 4.11 only deliver a ratio between the mistuned and tuned displacement.

Two interesting things can be said from this figure. First, note that both tuned double modes are not here captured. This is for the simple fact that the FRF (magnitude and phase) do not take into account this mathematical result. This is observer in the central two columns where the tuned displacement are identical. Indeed it is impossible for a structure to develop these double modes at the same time.

Second, as explored in the theory of this report, the figures show clearly how a mistuning in a single DOF affects the rest of the elements in the system. This is evident from modes 1F-0ND and 2F-0ND where the element corresponding to m_{b_5} responds in one direction whereas almost all the rest of the elements displace in the opposite direction. More complex relations develop for other modes due to their inherent configurations.

Now that the preliminary analyses provide sufficient confidence in the computer program, further studies are carried out regarding the most important topic covered in this thesis: the optimal localisation and magnitude of the suppressing force in the models.

Chapter 5

Active control of 1 DOF per blade model

A first approach to find the optimal solution for the best suppressing force is to start with a very simple model with 1 DOF per blade as depicted in figure 1.3.

Two different strategies to find the optimal suppression force in this chapter are explored: an analytic approach and a statistical approach.

The analytic strategy consists of two main rules over the location and magnitude of the force. First, the possible locations of the force are as described in figure 3.3. This means that the suppressing force, wherever it is found and regardless of its magnitude, will be a force acting in a single DOF, i.e. not 2 or 3 or N DOFs. Second, the magnitude of the force is extracted analytically from equation 3.4. This means that, theoretically, this force can have any value. Therefore, this optimal suppressing force can be higher or lower than the excitation force, sometimes considerably higher. Note that, from equation 3.4 an in-phase or an out of phase force can be found. No phase in the range of 0° to 180° is covered in this model.

The statistical approach involves trying several forces which are comparable in magnitude to the excitation force. These forces could be applied in many DOFs with different magnitudes for each DOF. For this statistical approach, the MSF was compared to the optimal force found analytically before to check which is the best one.

An alternating type of mistuning is implemented in this model. This means that a

certain level of mass is added in the blade element of the first sector, subtracted from the 2nd, added to the third and subtracted again from the fourth sector. The change in the mass level is 5%. The rest of the structural properties remain as described in table 3.1, i.e. no mistuning is introduced in the stiffness or damping of any element. Figure 5.1 displays the mistuning pattern applied into the structure and figure 5.2 recalls the model and the shape of the excitation force.

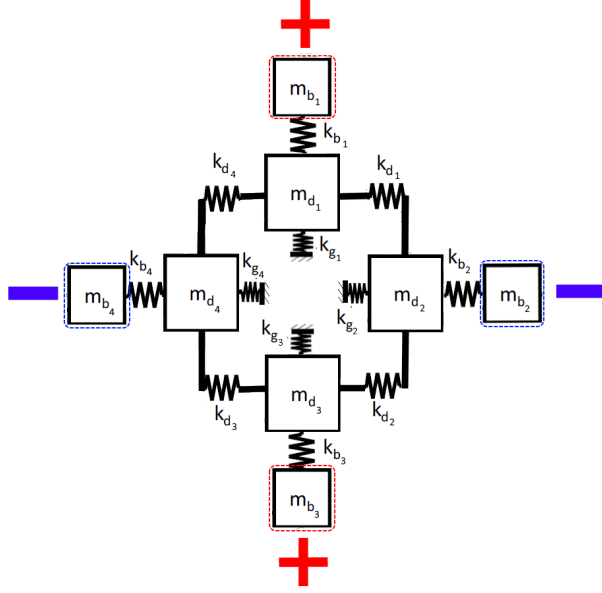


Figure 5.1: Alternating mistuning pattern in a 1 DOF per blade model.

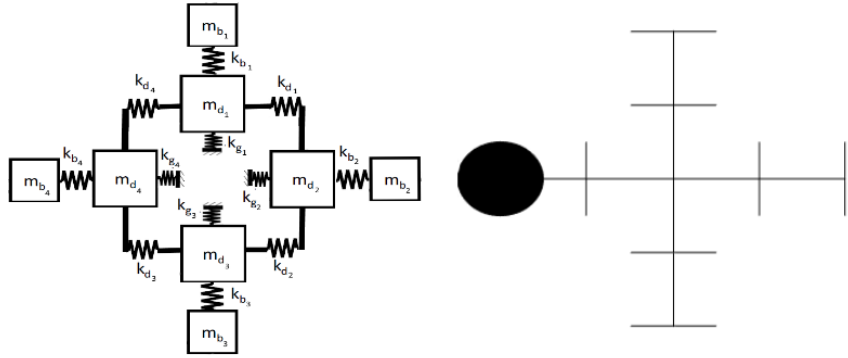


Figure 5.2: (a) Model of 1 DOF per blade. (b) Excitation force pattern.

5.1 Analytic approach for suppression

The searching meta-algorithm to find the best suppressing force in this model is as follows:

1. The model, before any suppression, is checked to behave properly according to the chosen structural properties and excitation force.
2. $\{f\} \{\phi_r\} = 0$ is imposed and from it the necessary force to suppress the r th eigen vector for every position of the single suppressing force is extracted. In other words, for a given mode, equation 3.4 was solved for each of the 8 possible DOFs where the suppressing force can be located.
3. Finally, among the 8 possible location for the forces to suppress the r th mode, the minimum is chosen. This delivers the location and magnitude of the optimum force.

From this procedure the forces to suppress any mode ‘ m ’, in a location ‘ l ’ are obtained: $f_{l,m}$. This is done for a tuned and a mistuned system: f_{l,m_t} , f_{l,m_m} . Figure 5.3 shows f_{l,m_t} and f_{l,m_m} for every l and m in the system. Dotted red lines have been added to show the magnitude of the excitation force. Also, figure 5.4 displays the same results but this time in a range comparable with the magnitude of the excitation force. Table 5.1 accompanies the graph with the corresponding forces.

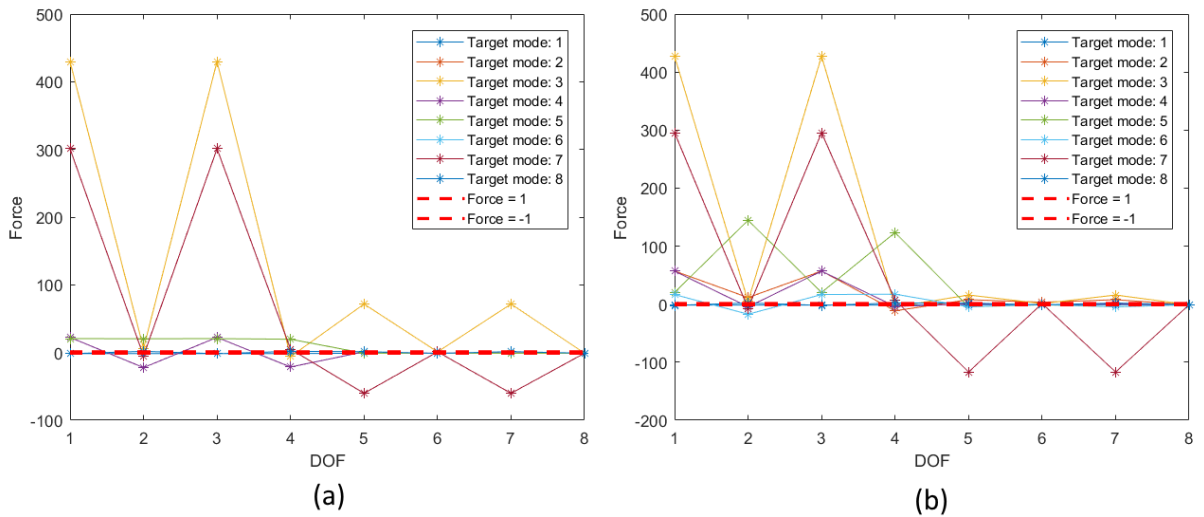


Figure 5.3: Forces needed to suppress all the modes with a force acting in 1 DOF in a model with 1 DOF per blade. (a) Tuned system. (b) Mistuned system.

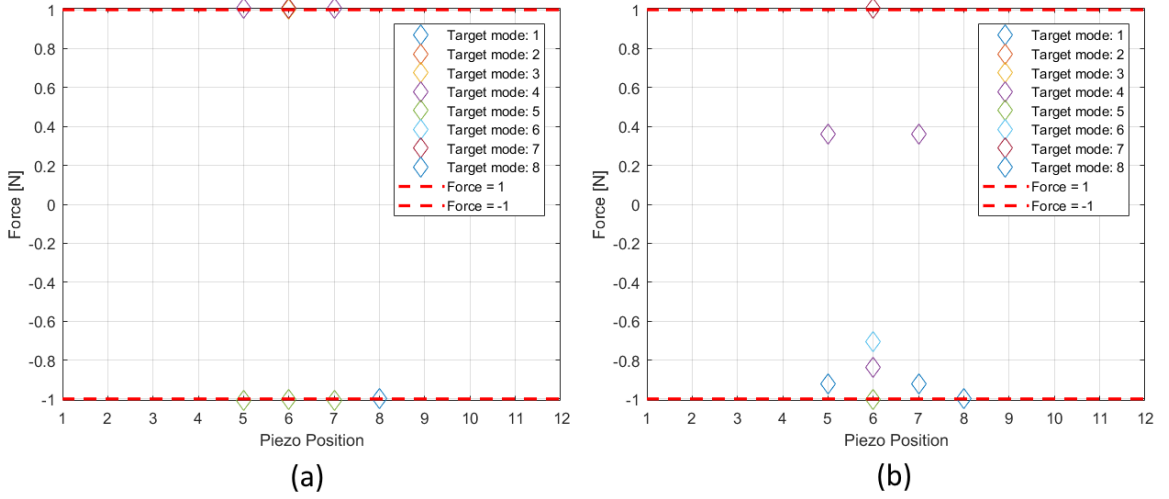


Figure 5.4: Forces, within a comparable range with respect to the excitation force, needed to suppress all modes with a force acting in 1 DOF in a model with 1 DOF per blade. (a) Tuned system. (b) Mistuned system.

		MODES																
		1F-0ND (1)		1F-1ND (2)		1F-1ND (3)		1F-2ND (4)		2F-0ND (5)		2F-1ND (6)		2F-1ND (7)		2F-1ND (8)		
LOC.	t	m	t	m	t	m	t	m	t	m	t	m	t	m	t	m	t	m
1	-1,5	-1,4	429,6	57,1	429,6	427,3	22,4	56,9	20,5	20,3	301,0	16,6	301,0	295,5	-1,8	-2,1		
2	-1,5	-1,4	6,0	11,4	6,0	4,8	-22,2	-4,5	20,4	144,6	-5,0	-17,3	-5,0	-7,1	1,8	2,1		
3	-1,5	-1,4	429,6	57,1	429,6	427,3	22,4	56,9	20,5	20,3	301,0	16,6	301,0	295,5	-1,8	-2,1		
4	-1,5	-1,4	-6,0	-11,4	-6,0	-4,7	-21,3	-3,8	19,7	123,5	5,0	17,2	5,0	7,1	1,8	2,1		
5	-1,0	-0,9	71,6	7,7	71,6	15,8	1,0	0,4	-1,0	-4,6	-60,2	-4,5	-60,2	-116,9	1,3	2,0		
6	-1,0	-1,0	1,0	3,3	1,0	1,0	-1,0	-0,8	-1,0	-1,0	1,0	-0,7	1,0	1,0	-1,3	-1,2		
7	-1,0	-0,9	71,6	7,7	71,6	15,8	1,0	0,4	-1,0	-4,6	-60,2	-4,5	-60,2	-116,9	1,3	2,0		
8	-1,0	-1,0	-1,0	-1,0	-1,0	-1,0	-1,0	-1,0	-1,0	-1,0	-1,0	-1,0	-1,0	-1,0	-1,0	-1,0		

Table 5.1: Force needed to suppress a certain mode placing the piezo in difference DOFs for a tuned (t) and mistuned (m) system.

Various conclusions can be extracted from this figure and its numerical results. First, perhaps the most evident result from this data is that almost all $f_{l,m_t/m}$ in the structure are higher than the excitation force. A relevant location to look at is the 8th DOF, which is the location where the excitation force of magnitude 1 (positive) is being exerted. As expected, the analytic formula reveals that for this location a force equal to -1 is needed to suppress all the modes, which means that a suppression totally in opposite phase and of equal magnitude is required to target a mode for suppression. Clearly, this is hardly achievable with the current technology of piezoelectric patches. Exerting a force

comparable with the aeroelastic and structural forces in the fan is currently impossible. Some forces appear to be less than the excitation force, of the order of 40% to 80% (See $f_{5/7,4_m}$, $f_{6,6_m}$ and $f_{5/7,1_m}$. This is a good result, it means that for some types of mistuning a single force can considerably suppress a mode. Altough these percentages still high, other types or magnitudes of mistuning could reach a lower suppressing force.

Second, note that double modes 1F-1ND and 2F-1ND show that the same tuned forces are required to suppress them. This is because the displacement at each DOF is extracted directly from the FRF, making the pick-peaking blind to this double mode effect. This does not happen for the mistuned modes due to the splitting caused by the change in the blade elements.

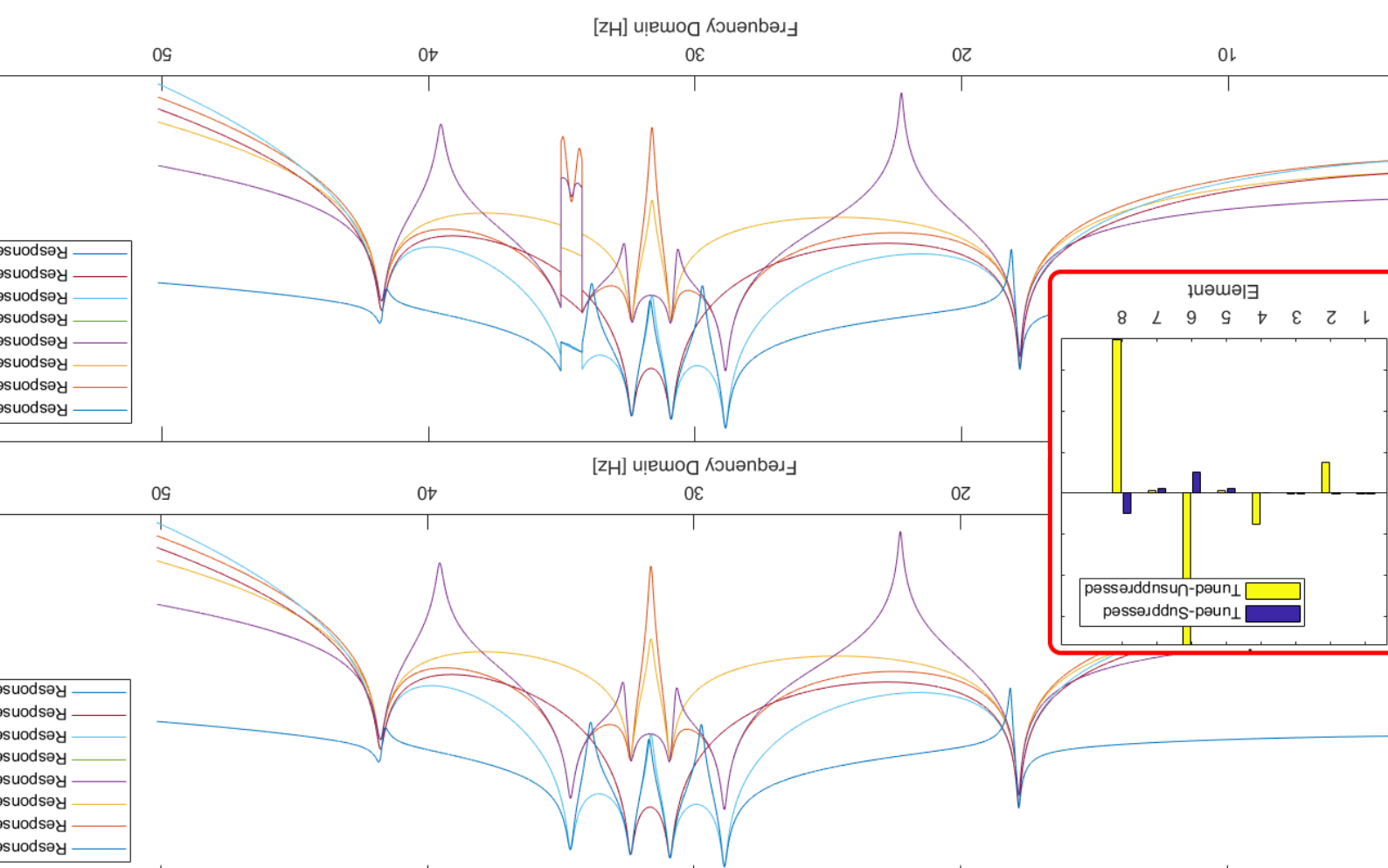
Third, there is a prominent apparently oscillatory pattern in $f_{l,m_{t/m}}$. This behaviour is more evident because the magnitude of the oscillations are bigger for some pairs of (l,m). This is caused by the shape of the 1F/2F-XND modes, which are indeed oscillating due to the presence of a ND in them (see fig. 4.1).

Fourth, $f_{l,m_{t/m}}$ tends to be lower for blades elements. This is due to the lower mass of these elements when compared to the disk elements. This is, however, not always true, because the shape of the mode need to be accounted for as well.

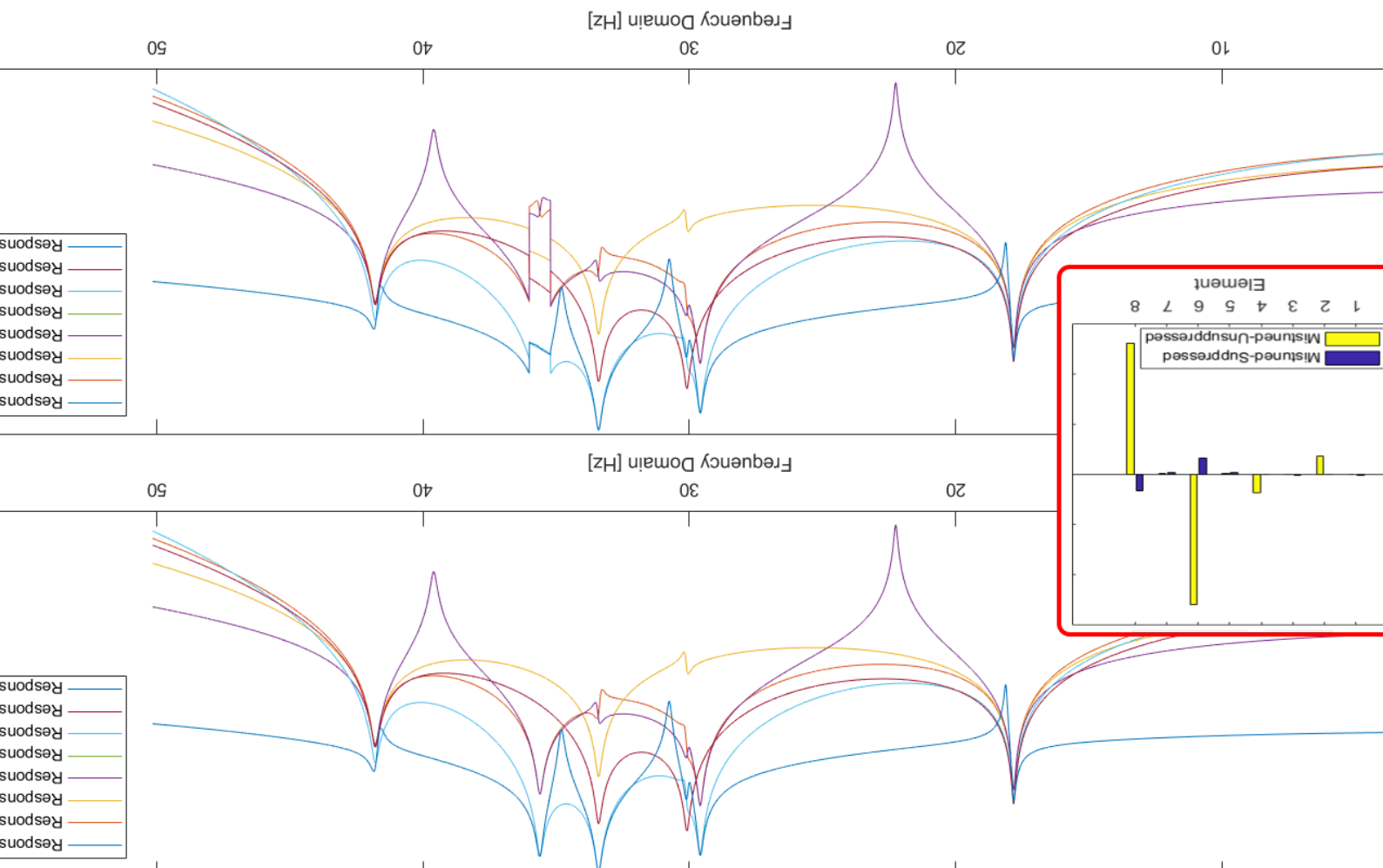
Now that these general appreciations are considered. It is worth looking at the effect of these suppressing forces in the FRF of a tuned and mistuned system. In the following figures the trivial case of a suppressing force equal in magnitude and opposite in phase to the excitation force is disregarded, and in those cases when that force is indeed the minimum $f_{l,m_{t/m}}$, the second minimum force is chosen. Figures 5.5 and 5.6 display the suppression effect in the mode 2F-1ND (7) with the suppressing forces $f_{6,7_t} = f_{6,7_m} = 1$ for the tuned and mistuned systems respectively. This is done for every DOF (or point) in the system. Also, a plot of the comparison between the suppressed and unsuppressed displacement is added in a box within the image. The same is repeated for mode 2F-2ND (8) in figures 5.7 and 5.8. Now, the forces for the mistuned and tuned cases are not located in the same position neither they have the same magnitude, indeed, for the tuned case: $f_{5,8_t} = 1.3$ and for the mistuned case: $f_{6,8_m} = -1.2$.

suppressing force acting in 1 DOF.

Effect of a suppressing force $f_{6,7_i} = 1$ in a tuned system. (a) Unsuppressed displacement. (b) Suppressed displacement

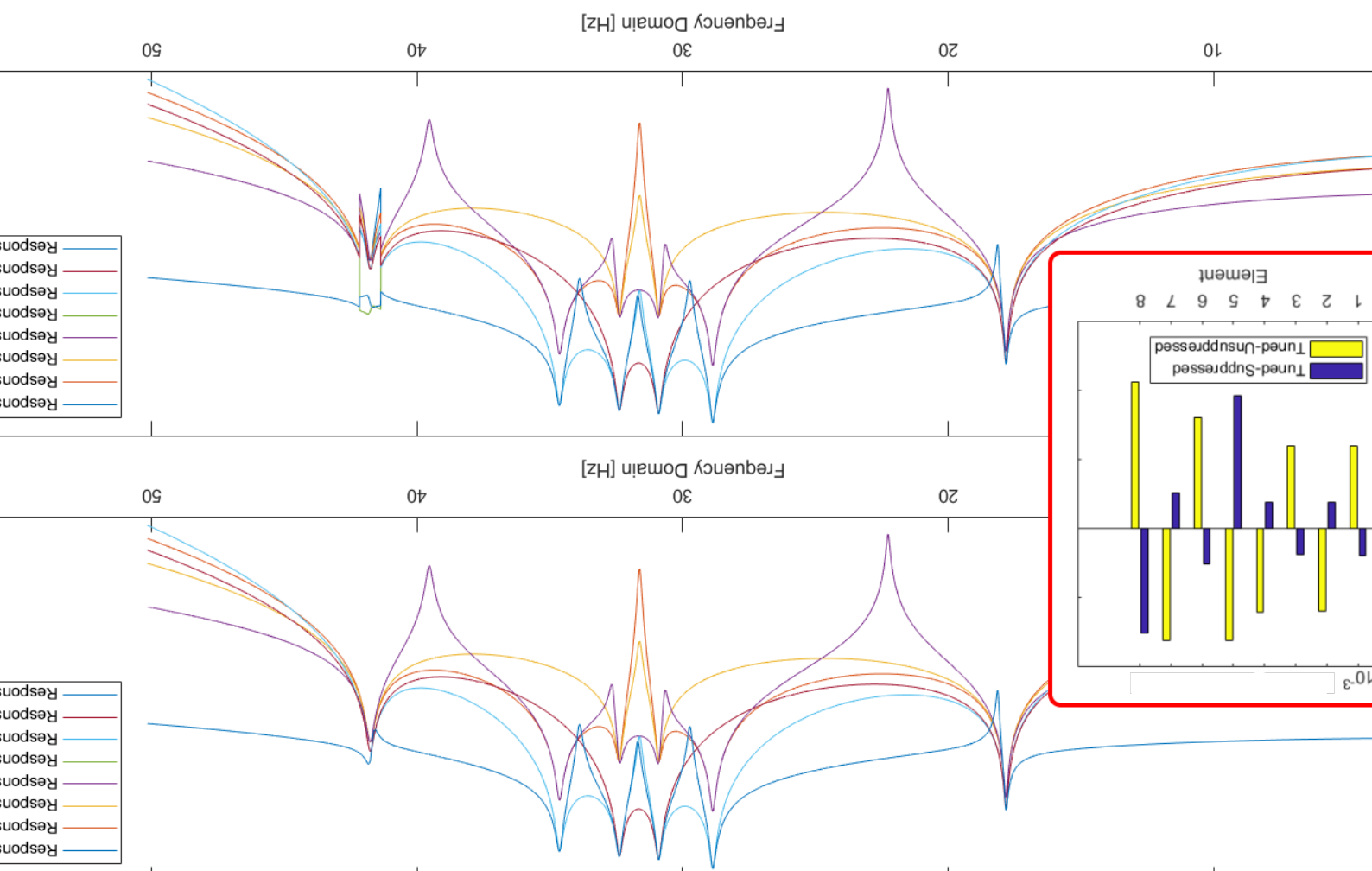


effect of a suppressing force $f_{6,7t} = 1$ in a mistuned system. (a) Unsuppressed displacement. (b) Suppressed displacement supporting force acting in 1 DOF.



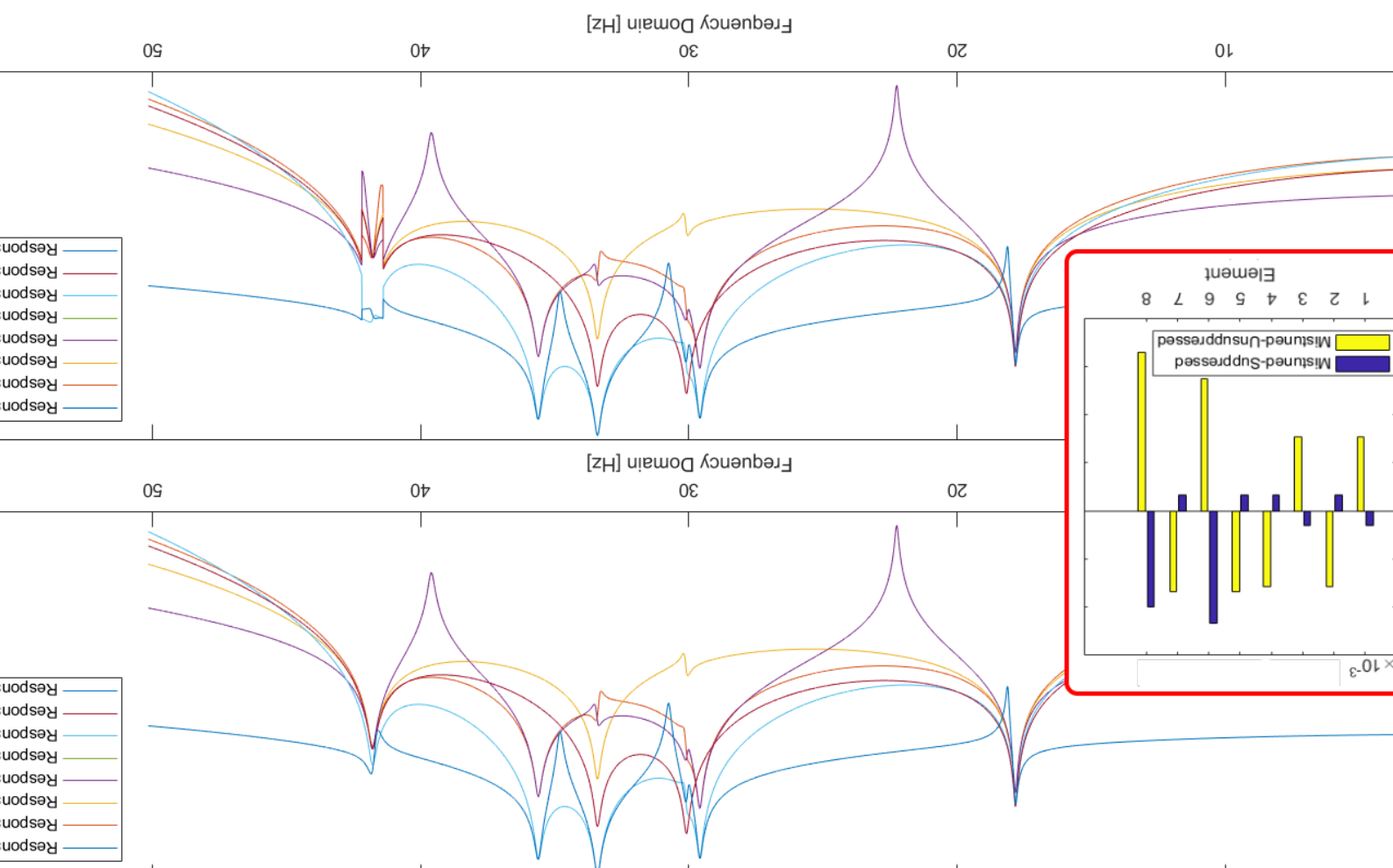
suppressing force acting in 1 DOF.

effect of a suppressing force $f_{5,8} = 1.3$ in a tuned system. (a) Unsuppressed displacement. (b) Suppressed displacement



With a suppressing force acting in 1 DOF.

Effect of a suppressing force $f_{6,8m} = -1.2$ in a mistuned system. (a) Unsuppressed displacement. (b) Suppressed displ-



Two important conclusions can be said from the suppression of modes 2F-1ND (7) and 2F-2ND (8) in tuned and mistuned systems.

First, the optimum single DOF suppressing force does not annul completely the displacement at one DOF. This is due to the principle of superposition in linear models. The mathematical model derived in the background of this thesis only takes into account the suppression of 1 mode at the time, and it does not consider the effect on the rest. Thus, the amplitude at one DOF is not zero because, even though the targeted mode is totally suppressed, the rest of the modes still contributing linearly to the displacement. Even more, in some cases, the suppressing force, which is optimum to suppress a mode may even excite more other modes. This phenomenon can be observed for every plot in the suppressed curves where the values of the amplitude of the FRF is not null.

Second, the behaviour exposed in the previous conclusion varies depending on the DOF. Thus, it can be observed from the comparison of the displacement for a suppressed vs unsuppressed, for each tuned and mistuned mode, that the amplitudes varies considerably when the suppressing force is applied. This is simply because some DOFs are more prone to displace due to certain modes, clearly, if a DOF sits in a ND or NC is will not move as much as the rest of the DOFs.

Finally, the most relevant outcome from this initial analyses is that any $f_{l,m_{t/m}}$ is higher than the excitation force. Since this is impractical in real fans, an alternative, and less deterministic path is followed to seek if there is any force capable of performing better than this single DOF force. With this tentative approach some questions arise. What if a random force is applied in the structure, in any DOF? Would it indeed reduce the amplitude of the ODS? If a random force is capable of achieve that. Will it be better than the analytic forces $f_{l,m}$? These questions are explored in the next section.

5.2 Statistical approach for suppression

In this approach several forces are tried to aim for the lowest MST. These forces obey some simple restrictions regarding the magnitude and location of the forces. First, the magnitude of any suppressing force is totally random in a range of $[-1, 1]$ times the magnitude of the excitation force. In other words, at any DOF, there may be a force in phase or out of phase with respect to the excitation force, but it will be always inferior in magnitude than this. Second, any DOF may be subject to a random force, which means that, except when $\alpha_{i,j} = 0$, every DOF will be suffering some sort of excitation.

The meta algorithm in order to produce a suppressing force that behaves even better than the analytic force is explained as follow:

1. The model is checked to produce accurate responses according to the literature.
2. A target mode is chosen.
3. Any location k is chosen and a vector of constants $\alpha_{i,k}$ is randomly generated. With this, the random suppressing force $\{f_s\}$ is also generated according to equation 3.2.
4. Then, $\{f_s\}$ is applied in the tuned and mistuned systems and the ODSs are obtained.
5. The MSF is computed from this random force ('r') for the tuned ('t') and mistuned ('m') modes 'i': $MSF_{r_{i_t}}$ and $MSF_{r_{i_m}}$.
6. Steps 3-5 are repeated as many times as random forces are tested.
7. The histogram of all the forces $MSF_{r_{i_t/m}}$ is plotted. The optimal single DOF suppressing force ('s') for a mode i is found and its MSF: MSF_{s_i} is computed. Both MSFs are compared.
8. The force capable of delivering the minimum MSF_s is extracted and its FRF is compared with the optimal single DOF suppressing force.

Now, these steps are followed one by one. The model works as expected according to the literature as it can be seen for modes 2F-1ND (7) and 2F-2ND (8) and the exploration in chapter chap:verifications. The modes targeted in this statistical analysis are the same modes as before for comparison purposes.

After steps 3-7 are executed, the histograms extracted from these results are presented in figure 5.9. A dotted red line is added to mark the values of $MSF_{s_{7/8_{t/m}}}$. Note that the modes are named here as (7) and (8) for brevity. The comparison between the random generated forces and the single DOF optimal force is tabulated in table 5.2.

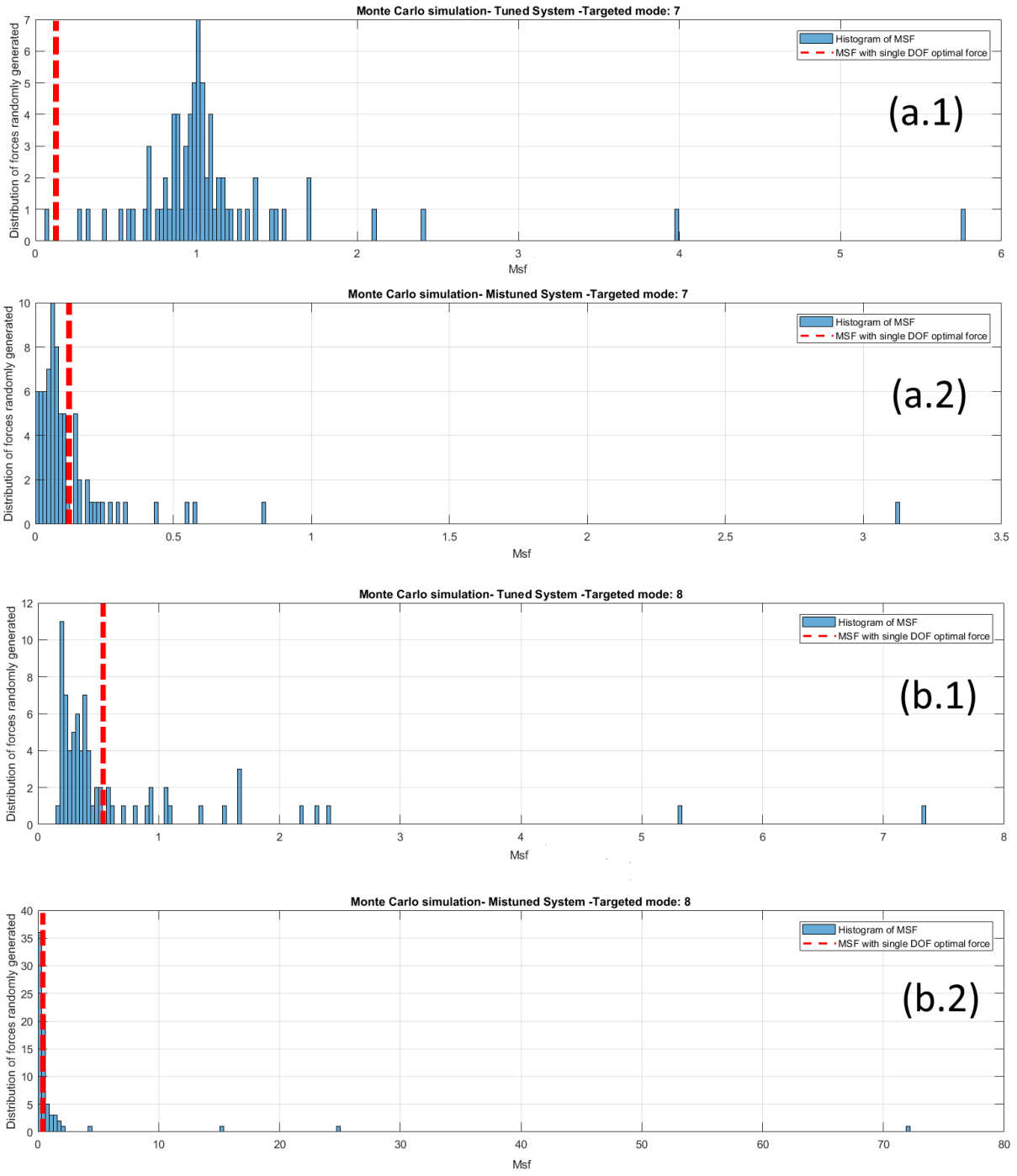


Figure 5.9: Distribution of 75 MSFs from randomly generated forces aiming to suppress mode 2F-1ND (7) and 2F-2ND (8). (a.1) 2F-1ND (7)/tuned. (a.2) 2F-1ND (7)/mistuned. (b.1) 2F-2ND (8)/tuned. (b.2) 2F-2ND (8)/mistuned.

The MSF_{s_7} and MSF_{s_8} are computed and tabulated below.

MODES		
	2F-1ND(7)	2F-2ND (8)
$MSF_{s_{it}} / MSF_{r_{it}}$	0.1296/0.0626	0.5437/0.1537
$MSF_{s_{im}} / MSF_{r_{im}}$	0.1234/0.0041	0.4757/0.0807

Table 5.2: MSF for modes 2F-1ND (7) and 2F-2ND (8) for a tuned and mistuned system

Before proceeding with step 8 some conclusions can be derived from these histograms and table. First, the results cover a wide range of MSF, this means that these forces may or not be actually suppressing the ODSs, indeed they are not designed to suppress but to be simply random. Secondly and more important, there are some of these 75 forces capable of deliver an MSF lower than $MSF_{s_{7/8_{t/m}}}$.

Step 9 is now applied and the forces corresponding to the minimums $MSF_{s_{7/8_{t/m}}}$ are extracted and exerted into the system. Figures 5.10 and 5.11 show the effects of forces $MSF_{s_{7_{t/m}}}$ and $MSF_{s_{8_{t/m}}}$, respectively.

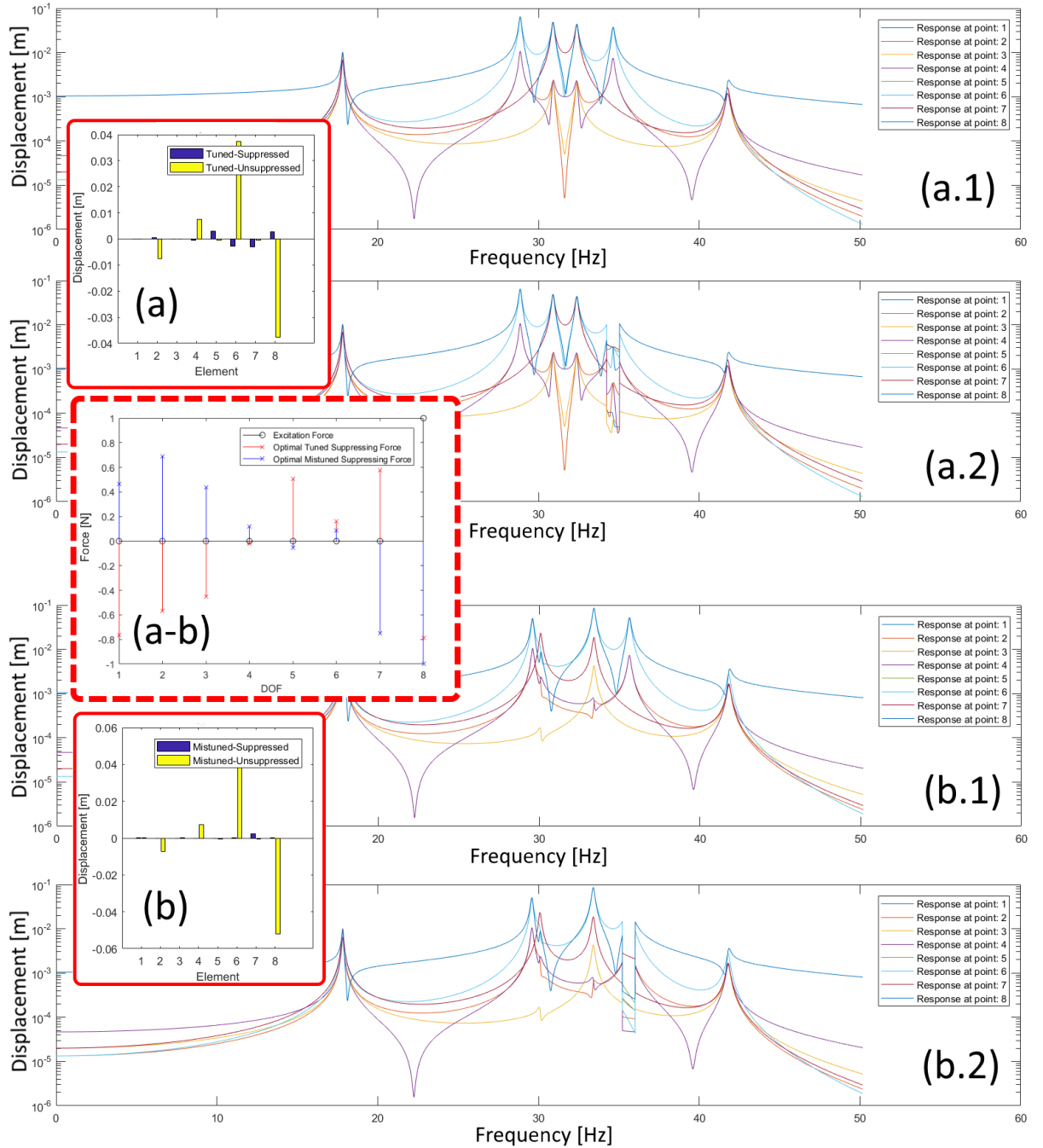


Figure 5.10: FRFs for a randomly generated force capable of delivering a lower MSF than an optimal single DOF suppressing force targeting mode **2F-1ND**, for a tuned and a mistuned systems.(a.1) Tuned-unsuppressed. (a.2) Tuned-suppressed. (b.1) Mistuned-unsuppressed. (b.2) Mistuned-suppressed.(a) Displacement of each DOF for a tuned suppresses/unsuppressed system. (b) Displacement of each DOF for a mistuned suppresses/unsuppressed system. (a-b) Optimal single DOF suppressing force and randomly generated forces to suppress a tuned and mistuned system.

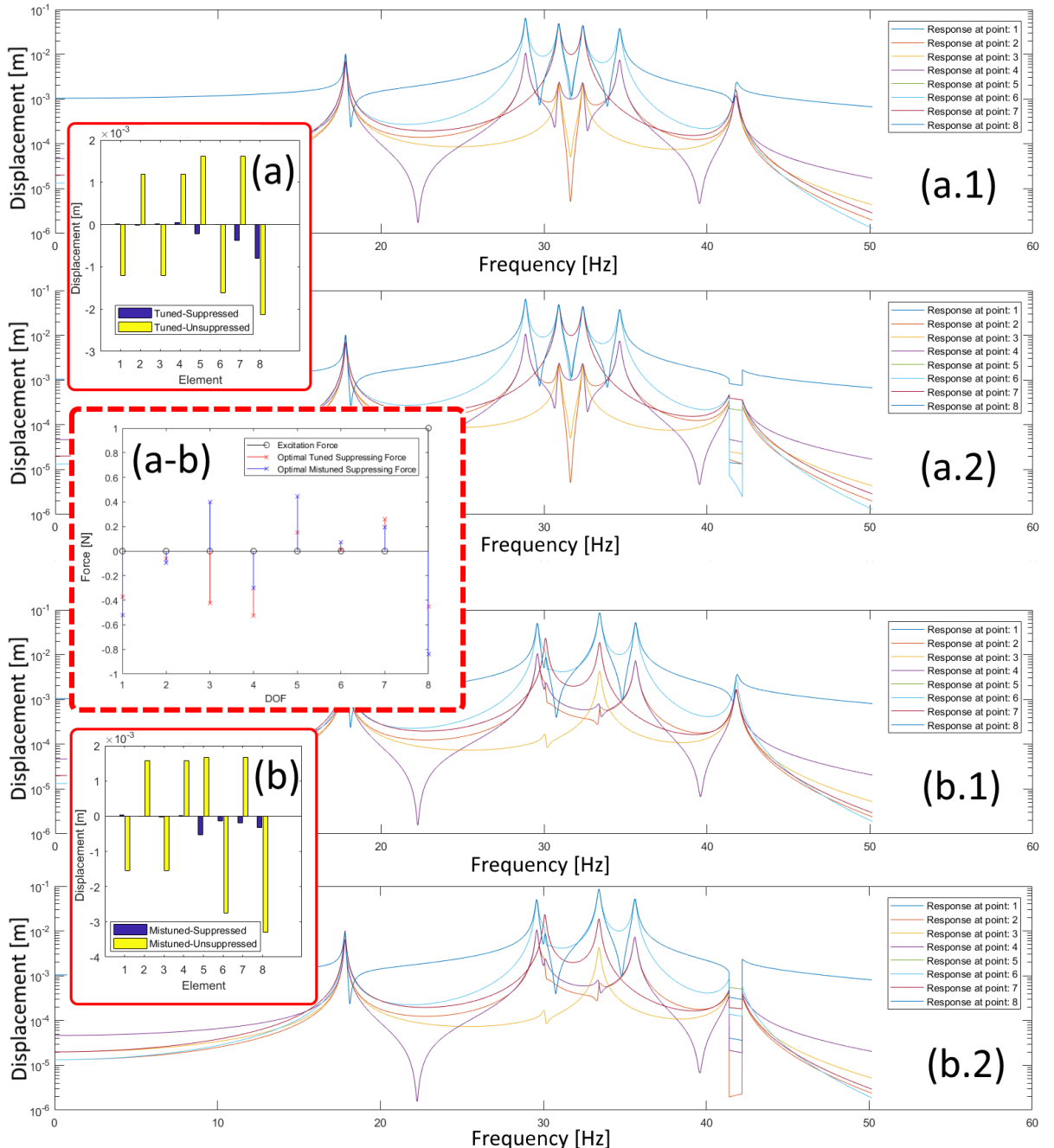


Figure 5.11: FRFS for a randomly generated force capable of delivering a lower MSF than an optimal single DOF suppressing force targeting mode **2F-2ND**, for a tuned and a mistuned systems.(a.1) Tuned-unsuppressed. (a.2) Tuned-suppressed. (b.1) Mistuned-unsuppressed. (b.2) Mistuned-suppressed.(a) Displacement of each DOF for a tuned suppresses/unsuppressed system. (b) Displacement of each DOF for a mistuned suppresses/unsuppressed system. (a-b) Optimal single DOF suppressing force and randomly generated forces to suppress a tuned and mistuned system.

This comparison between an optimal suppressing force acting in 1 DOF and a random force allows some remarks. First, one force may be optimal to target one single mode, however, in linear systems this is not sufficient to reduce totally the displacement of one or various DOFs in the system. As mentioned previously, this is due to the secondary effect of exciting other non-targeted modes. Second, there is indeed an optimal random forces that not only performs better in term of the general factor MSF but also reduce the displacement of every DOF in the system, this can be clearly seen from the comparison of the suppressed and unsuppressed displacements in images (a) and (b) within figures 5.10 and 5.11. Third, as modelled, every single component of the optimal random force generated is less than the excitation force (see images (a-b) in figs. 5.10 and 5.11). More interestingly, some of these forces are really low, below 10% of the excitation force. Also, this random force act, for different DOFs, in phase or out of phase with respect to the excitation force.

The possibility that at the same time a force could be acting in phase and out of phase with respect to the excitation force, as shown by the figures 5.11(a-b) and 5.10(a-b), arises the motivation to define a better model for the suppressing force. This reformulation models the piezoelectric patch as explained in figures 3.4 and 3.5, capable of contract and tense. Now that the first model, with 1 DOF per blade, demonstrated that it is indeed possible to suppress a mode, a more complex model is examined in the following chapter in order to capture more realistically the behaviour of a blade and the fan itself.

Chapter 6

Active control of a 2 DOFs per blade model

As described in the end of the previous chapter, a new model of the force is implemented from now onwards. This model conceives the force exerted by the piezoelectric patches as acting in 2 DOFs in compression or tension, as depicted in figure 3.4. The mathematical formulation of this type of force can be found in chap:theory.

In this chapter, 2 different methods are implemented in order to find the best suppressing force in a model with 2 DOFs per blade. The first method seeks for the minimum force exerted by a piezo such that a certain mode is suppressed totally. The second method assumes a force of the piezoelectric patch equal to 1% of the magnitude of the excitation force and aims to find the minimum MSF in the system. This means that the mode is not necessarily suppressed totally, but the minimum MSF refers to the maximum suppression achievable with that 1% force. No statistical approach is undertaken.

Note that these piezos obey the practical rules established in the Theory of the models (chap:theory): they cannot superpose one over the other, however, one of the two forces of each piezo can indeed be superposed.

Suitable terminology is first defined in order to facilitate the comprehension of this chapter. A simple nomenclature for the position of a piezo acting in 2 DOFs is proposed in figure 6.1(a). Four groups of possible positions are defined in the model: (1) Disk-Base blade, (2)Base-blade to Tip-blade, (3) Tip-blade to Disk and (4) Disk of one sector

to Disk of the following sector. Group (3) has been excluded from the analysis but the software developed allows testing them in any case. Each group contains four possible positions for the piezos. For group one, the first position is defined as the link between disk and base-blade of the first sector. Positions 2, 3 and 4 correspond to sectors 2, 3 and 4 respectively. The second possible position, between the base-blade and the tip-blade is numbered as 5 for the first sector, 6 for the 2nd, 7 for the 3rd and 8 for the 4th sector. Positions 9 to 12 follow an analogous behaviour. Finally, positions 13 to 16 connect the disk elements of the 1st to the 2nd sector, 2nd to 3rd, 3rd to 4th and 4th to 1st sectors, respectively.

For example, force $f_{1,2_t}$ is the force exerted by the piezo in the location 1 of group (1) to suppress the tuned mode 1F-1ND(2). If the force is positive, it means that the first element in the contact with the piezoelectric patch is in phase with the excitation force. The elements are range between 1-12, 1-4 disks, 5-8 base blades and 9-12 tip blades elements. Therefore, $f_{1,2_t} > 0$ means that m_{d_1} is being pushed in the same direction as the excitation force and m_{b_1} is being pushed in the opposite direction. For clarification purposes, this force is displayed in 6.1(b). Note that only the direction of the force is represented in the figure, not the magnitude.

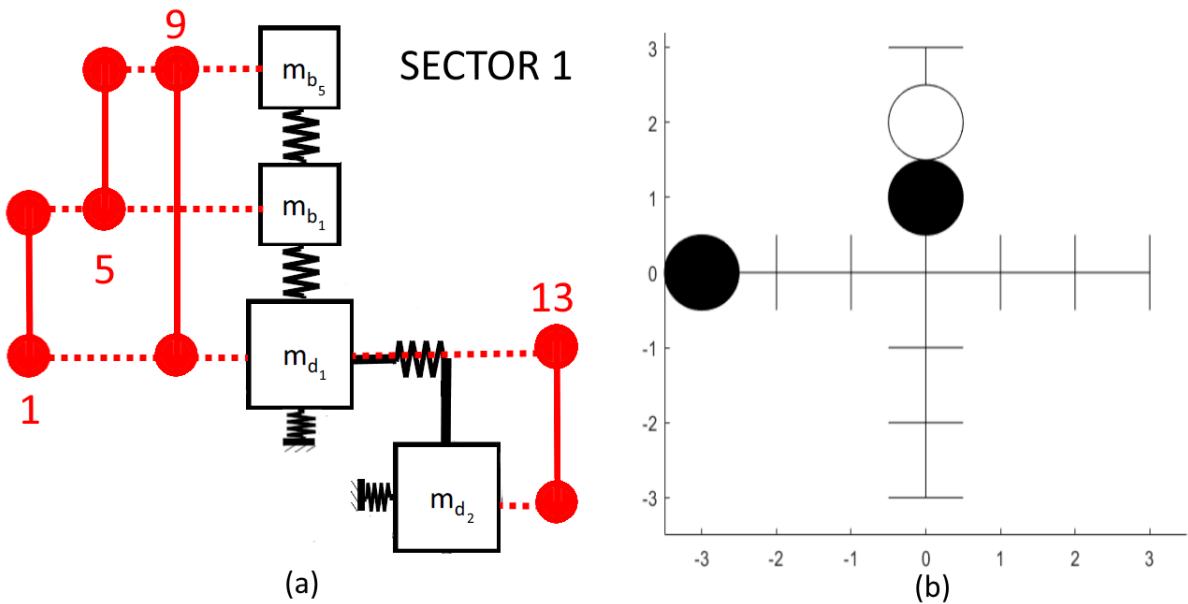


Figure 6.1: (a) Nomenclature for the possible positions of a single piezo acting in 2 DOFs.(b) Force $f_{1,2_t} > 0$.

An alternating 5% m -mistuning configuration on the tip-blade element is adopted. Also, the excitation force is applied in the tip-blade of the 4th sector. Figures 6.2 and 6.3 show this mistuning pattern and the summary of the model and excitation force.

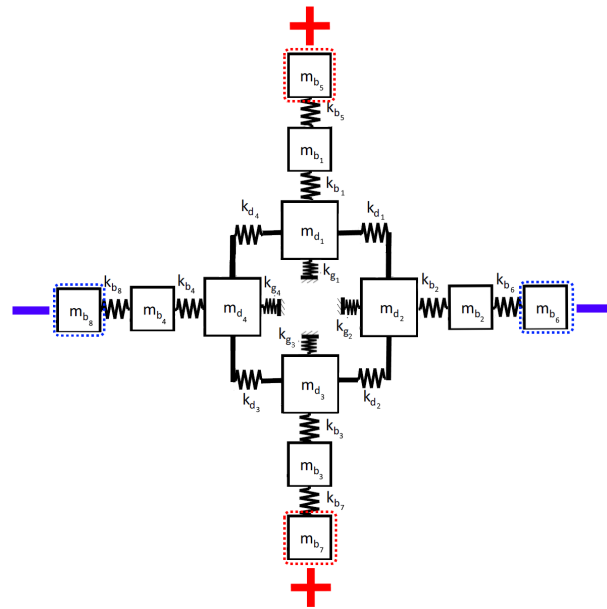


Figure 6.2: Alternating mistuning pattern in a 2 DOFs per blade model. 1 Piezo electric patch acting in 2 DOFs.

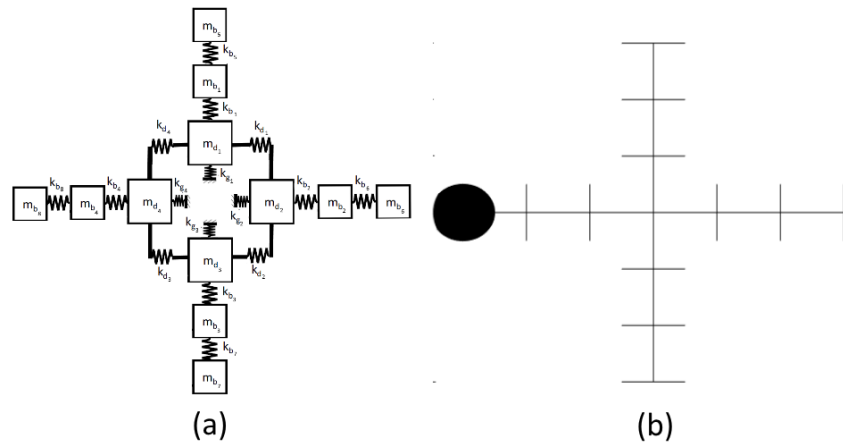


Figure 6.3: (a) Model of 2 DOFs per blade. (b) Excitation force pattern.

6.1 Minimum force to total suppression of a mode with one piezoelectric patch.

The methodology to obtain the minimum force to suppress a mode can be summarised as follows:

1. The model is checked to perform accurately according to the literature review.
2. $\{f\} \{\phi_r\} = 0$ is imposed and equation 3.10 is solved for all 12 modes and 16 possible positions for one piezo only.
3. Unrealistic positions of the piezo: 9 to 13, are neglected in the analysis.
4. The minimum force is found for the targeted mode.
5. The effect of this force on the FRF is tested.

Following these steps the minimum force to suppress a mode m , in a location l is found: $f_{l,m}$. This is performed for a tuned and a mistuned systems, obtaining forces: $f_{l,m_{t/m}}$. Figure 6.4 displays all possible values of $f_{l,m_{t/m}}$. Figure 6.5 shows the same with a restriction in the magnitude of the force equal to 1, which is the magnitude of the excitation force. The numerical results of these figures can be found in ppm1opts.

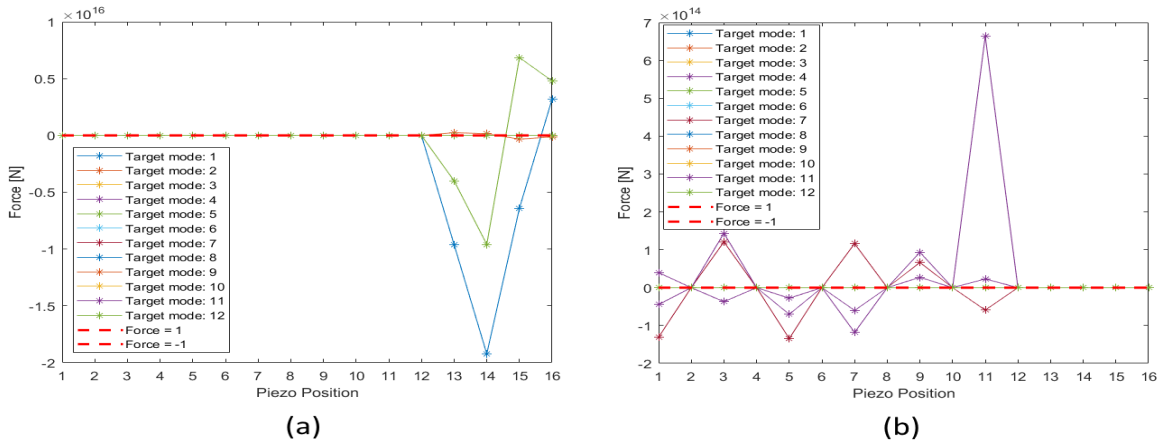


Figure 6.4: Forces needed to suppress all modes with a force acting in 2 DOFs in a model with 2 DOFs per blade. (a) Tuned system. (b) Mistuned system.

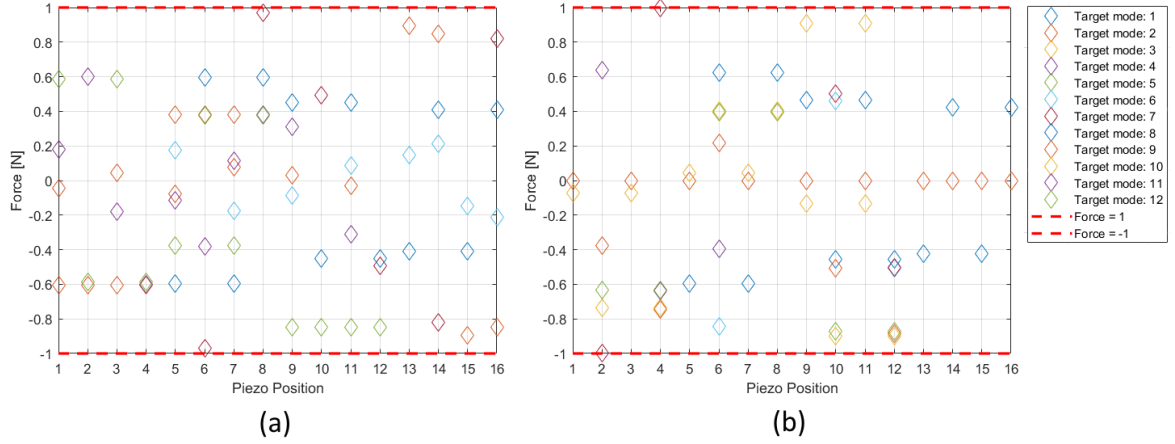


Figure 6.5: Forces, within a comparable range with respect to the excitation force, needed to suppress all modes with a force acting in 2 DOFs in a model with 2 DOFs per blade. (a) Tuned system. (b) Mistuned system.

Some conclusions can be extracted from these plots. First, locating the piezos linking the disks elements require a huge amount of force, in a tuned system, as it can be seen in the right hand side sector of plot (a) in figure 6.4. For example, 16 orders higher than the excitation force for $f_{14,6_t}$. Nonetheless, for the case of mistuning explored in this chapter some of these forces decrease considerably with respect to the tuned case, even some of them in a range comparable with the excitation force, as deduced from figure 6.5. Not only that, some of them are less than 1% of the excitation force and nearly zero, for example $f_{13-16,2/6/9_m}$ are 13 orders less than the excitation force, corresponding to the mistuned modes: 1F-1ND, 2F-1ND and 3F-0ND respectively. Noticeable, this occurs for all positions between disks: 13,14,15 and 16. This is a remarkable result. It means that, assuming that the structure have a similar mistuning configuration, a vibrations engineer would just need to place 1 single piezoelectric patch in the disk disregarding a treatment on the blades.

Second, positions 9-12, which link the tips of the blade with the disks, do offer for some locations and mode a reasonable force. For example, $f_{9/11,6/10_m} = -0.1$. However, this is unpractical since the piezoelectric patch would have to go through the entire blade without interfering at all with the rest of the blade. Nonetheless, these results deliver some insight in case in the future such technology, capable of connecting the tip and the disks of a blade, is available.

Third, some of these optimum locations for a mistuned system are the same as for a

tuned system. This means that if the system is almost tuned and the mistuning during operation of the structure is predictable (both very optimistic assumptions), only the tuned system need to be considered in order to find the optimal position.

Finally, now that this procedure is understood, the effect of this form of suppressing force is tested on the tuned and mistuned modes 2F-2ND(8). The minimum forces found by the algorithm correspond to: $f_{15,8_t} = -0.4108$ and $f_{13,8_m} = -0.4207$. Their results in the FRF are displayed in figures 6.6 and 6.7, respectively.

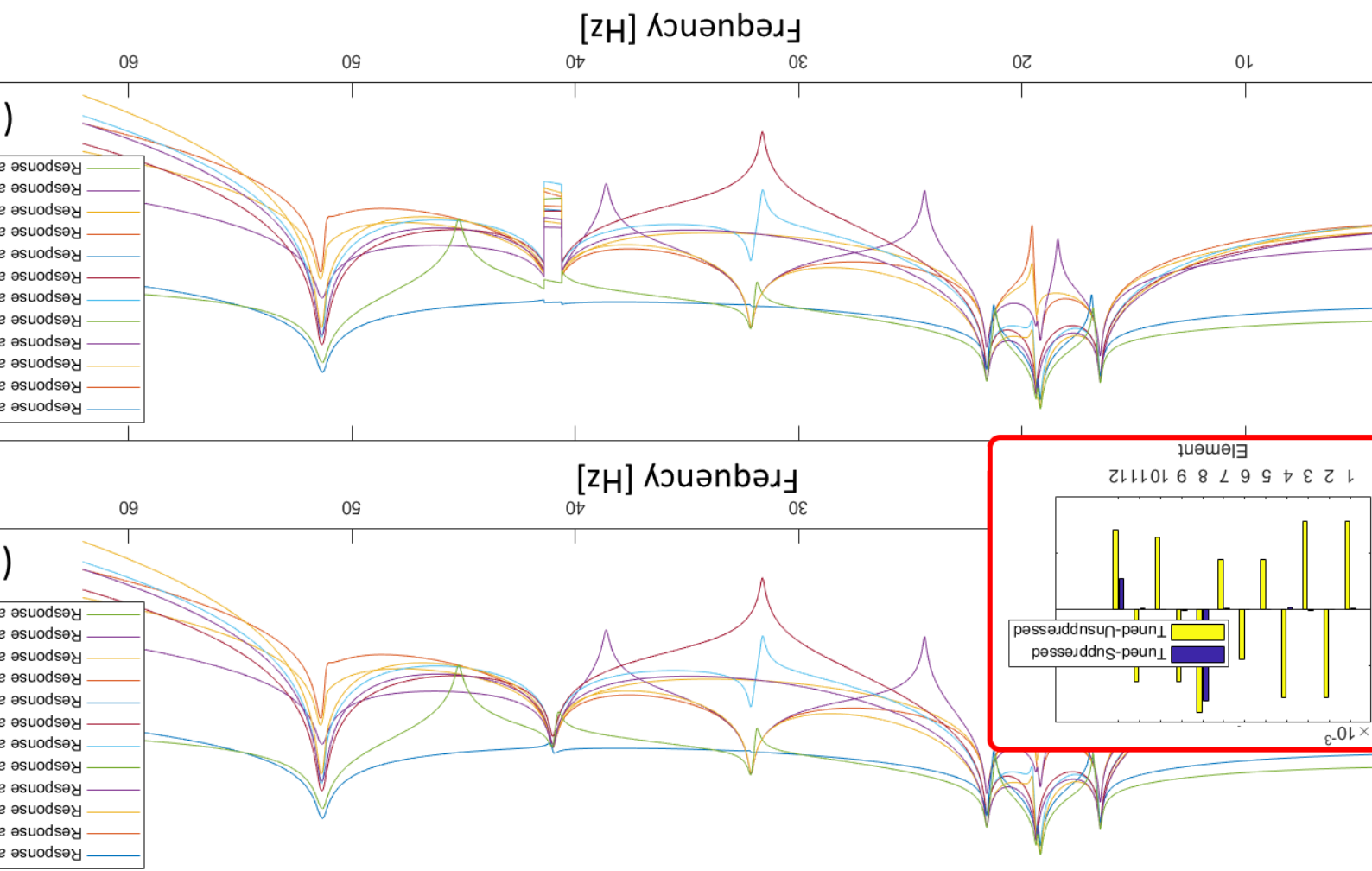
These plots, as for the type of force suggested in the previous chapter, offer a very successful suppression, sometimes making the displacement at certain DOFs nearly zero. However, their magnitudes are not realistic. Due to this restriction, the force is limited to a real value. 1% of the excitation force is chosen.

Up to this point, two relevant assumptions have been adopted to make the model more accurate and real. First, the model of the suppressing force is acting in 2 DOFs, which takes into account the contraction/tension of a real piezoelectric patch. Second, even though searching for a force capable to suppress totally a mode offers some extremely good results, it is better to set a real force magnitude to be executed by the piezo and then finding its optimal location.

In the next section, the effects of this force is considered in terms of the MSF.

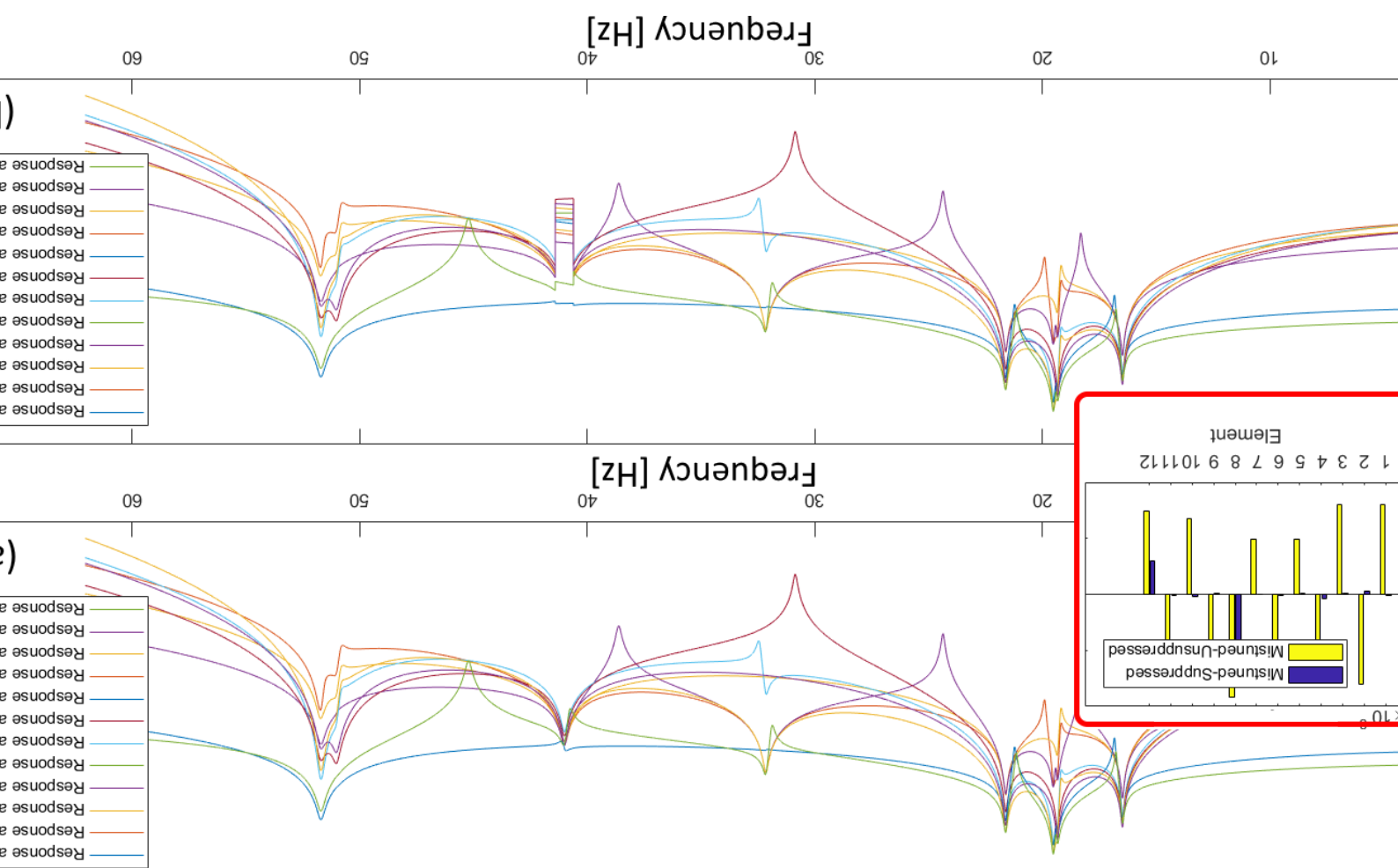
With a suppressing force acting in 2 DOFs.

Effect of a suppressing force $f_{15,8i} = -0.4108$ in a tuned system. (a) Unsuppressed displacement. (b) Suppressed displacement.



displacement. With a suppressing force acting in 2 DOFs.

7. Effect of a suppressing force $f_{13,8m} = -0.4207$ in a mistuned system. (a) Unsuppressed displacement. (b) Suppressed



6.2 Minimum MSF for a given force of 1% of the excitation force.

In this section a model of a piezoelectric force acting in 2 DOFs and with a magnitude of 1% (f^*) of the excitation force is explored. Here, the MSF is used in order to quantify the reduction in displacement in the ODS. The form of mistuning and the rest of structural properties remain the same as those described in the previous chapter.

The meta-algorithm followed in this section contains the next steps:

1. The model is checked to behaves as expected from the literature review.
2. A magnitude of 1% of the excitation force is imposed.
3. For 1 piezoelectric patch: $[2 \times 16]$ forces are generated. The 16 comes from the 16 possible positions, it is multiplied by 2 because they can be in-phase or out of phase with respect to the excitation force.

For 2 piezoelectric patches: $[2 \times 2 \times 16 \times 16]$ forces are generated. The first 16 comes from the 16 possible positions. The second 16 comes from every combination of an in-phase force with respect to the first group of 16. The first 2 comes from the fact that the second piezo can be out of phase with respect to the first one as well. The second 2 comes from the fact that those $[2 \times 16 \times 16]$ forces can be in phase or out of phase with the excitation force.

4. The unrealistic cases of piezos the piezo connecting the tip-blade and the disk are disregarded.
5. All the forces generated are applied in to target each mode.
6. The displacement are extracted from the FRFs for each case.
7. The MSF corresponding to every mode and force applied is calculated from the displacement at each DOF.
8. The minimum MSF is found for each mode. Along with this value, the position is found, and the magnitude is given from the 1% assumed in the first place.
9. The effect of this force on the FRF is tested.

6.2.1 Using 1 piezoelectric patch.

Suppression in one mode

Figure 6.9 illustrates the FRF and displacement comparison for every DOF in a tuned and mistuned system with f^* aiming to suppress mode 2F-2ND(8). Note that range of frequency has been focused in the area of interest. Before this the optimal force $f_{13,8_{t/m}}^*$ pattern is displayed in figure 6.8.

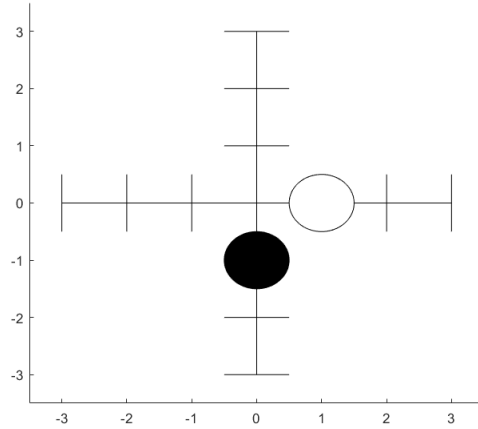


Figure 6.8: Scheme of force $f_{13,8_{t/m}}^*$

The unsuppressed and suppressed curves in 6.9 are apparently identical. This is due to fact that the suppressing force is little, at least 2 orders less than the forces explored in previous sections. However, images 6.9(a.2) and 6.9(b.2) reveal a jump around 40.6 [Hz] and 41.4 [Hz]. This window preserves the shape of the FRF, however it pulls the FRF down. This window is the predefined window of action of the suppressing force. From this FRF the displacement are extracted and displayed in 6.9(a.3) and 6.9(b.3). It can be notice that the displacement decrease for every DOF in the structure. This means that mode suppression is successful with force type f^* , it also means that the rest of the modes are not overexcited enough to offset this mode suppression. Note that this is may not be true for every mode under force f^* .

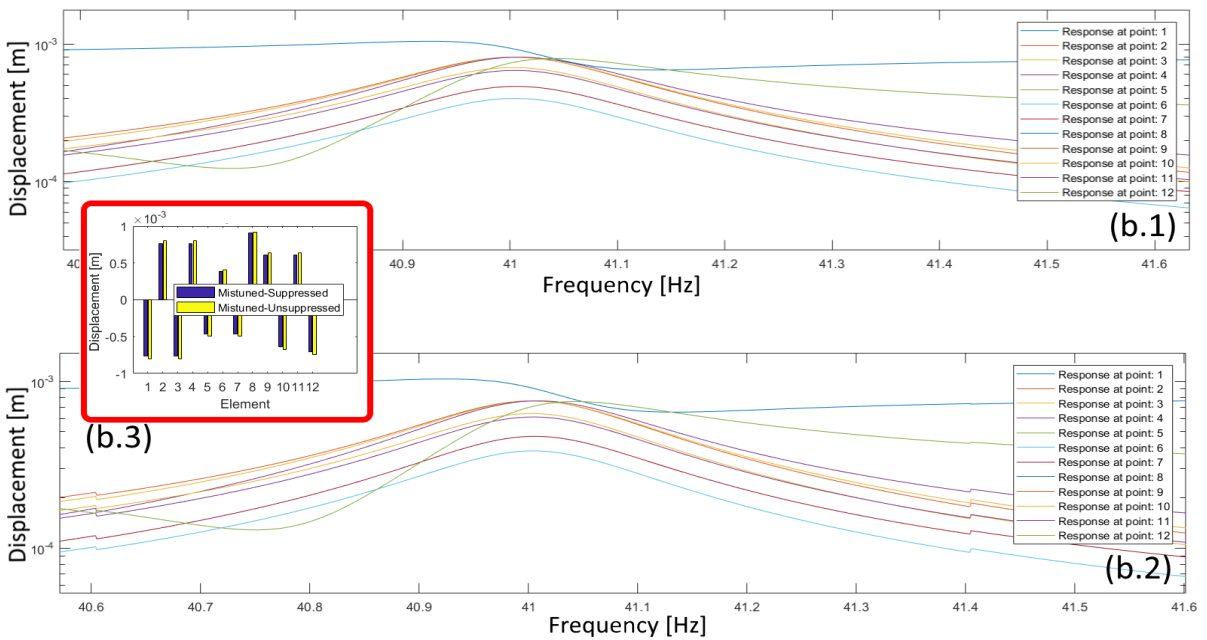
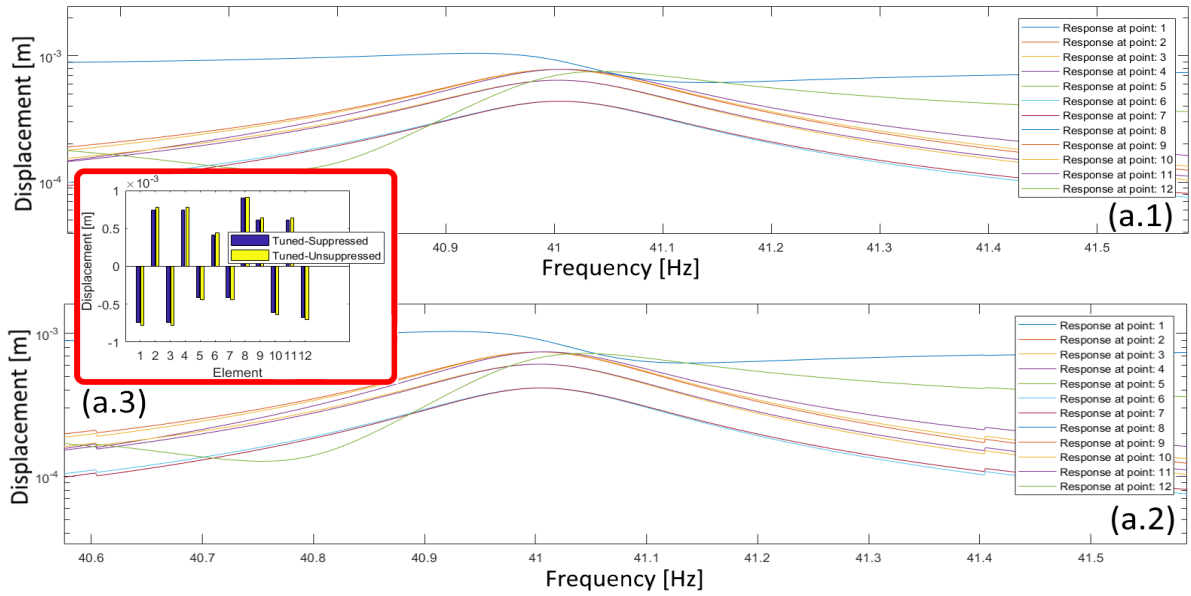


Figure 6.9: Effect of a suppressing force $f_{13,8t/m}^* = -0.01$ in a tuned and mistuned systems. (a.1) Tuned-unsuppressed. (a.2) Tuned-suppressed.(a.3) Tuned Displacements suppressed/unsuppressed. (b.1) Mistuned-unsuppressed. (b.2) Mistuned-suppressed. (b.3) Mistuned Displacements suppressed/unsuppressed.

A good approach to concentrate all this information is to visualise the ratios of the suppressed and unsuppressed displacements. Figure 6.10 shows the ratio of suppressed to unsuppressed displacement for mode 2F-2ND(8).

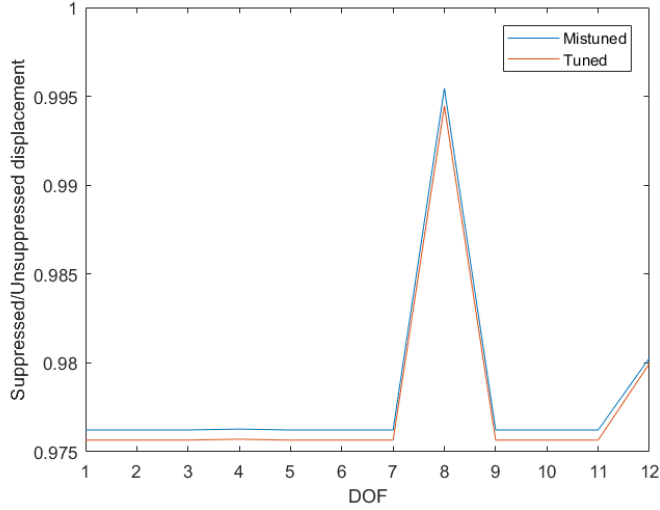


Figure 6.10: Ratio suppressed/unsuppressed displacement for every DOF at the frequency of mode 2F-2ND.

Three important things are to be noticed from this figure. First, the magnitude of the ratios is close to 1, it means that the reduction is not considerable, however, in real fans this reduction of around 2% can play an important role in a blade. This is due to the exponential increase in the lifetime when the stresses are reduced.

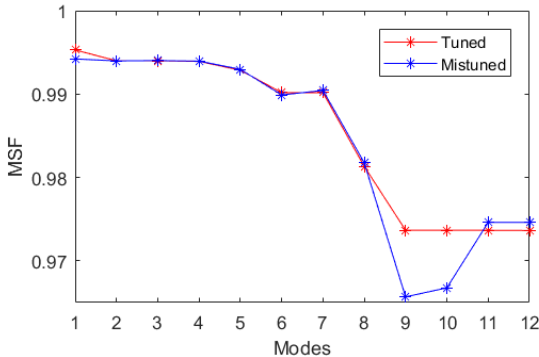
Second, DOFs 12, 8 and 4 (slightly) are reduced less than the rest. Recall that this is a forced response under an excitation force acting in the 12th DOF. The 12th DOF corresponds to the tip of the blade in the 4th sector. Elements 8 and 4 correspond to the base-blade and disk elements of that sector. Therefore, this behaviour is due to the excitation force as it is clearly seen in section chap:verifications. Finally, the ratio of the suppressed to the unsuppressed displacement also follows that tendency because the excitation caused by $f_{13,8}^*$ perform better in other DOFs. From all these, it can be argued that from a free response, meaning no excitation, a suppressing force should perform evenly for every DOF.

Third, it can be seen that the tuned and mistuned system behaves similarly. This is because the actual force pattern does not change from the tuned to the 5% m -mistuned system. In fact, both are located in position 13.

Finally, all this information can be grouped in the MSF. Thus, the MSF obtained in the suppression of tuned and mistuned mode 2F-2ND(8) is: $MSF_{8_t} = 0.9813$ and $MSF_{8_m} = 0.9818$.

Suppression in each mode

By means of the MSF, now the behaviour of each mode can be explored. Note that this parameter hides the information of the ratio of the suppressed to the unsuppressed displacement and the information of the exact displacement at each DOF whether it is suppress or not. Figure 6.11 displays $MSF_{x_{t/m}}$ for every ‘x’. Table 6.1 show the optimal position to achieve those MSFs.



MODES	t	m	MODES	t	m	MODES	t	m
1F-0ND(1)	4	3	2F-0ND(5)	4	4	3F-0ND(9)	8	5
1F-1ND(2)	4	4	2F-1ND(6)	8	8	3F-1ND(10)	8	5
1F-1ND(3)	4	4	2F-1ND(7)	8	4	3F-1ND(11)	8	8
1F-2ND(4)	4	4	2F-1ND(8)	13	13	3F-2ND(12)	8	8

Table 6.1: Positions of optimal forces f^* .

Figure 6.11: MSF for every mode under optimal suppressing force f^* .

From this image, some interesting conclusions can be derived. First, the suppression is more efficient as the frequency of vibration increases. Indeed, for the same amount of force and only modifying the location of a piezo the MSF can be reduced from 0.5% for mode 1F-0ND(1) to almost 3.5% for a mistuned mode 3F-0ND(12).

Second, the mistuned and tuned curves are very similar. This is due to the low level of mistuning introduced in the system, as explained previously for mode 2F-2ND. Not only the curves, but also the positions of the piezos are the same. This is also true for various modes, for example 1F-1ND(2-3), 1F-2ND(4), 2F-1ND(6), among others, as it can be seen from table 6.1.

Third, every mistuned mode is suppressed more than its tuned version, except for mode 2F-1ND(7). This is a good result, it means that some time introducing mistuning can be beneficial for suppression.

Fourth, every mode is indeed suppressed. This is a remarkable result, it means that even though some modes can be overexcited after suppression, the general ODS at the frequency of the targeted mode is globally reduced. Note that this results is not at all direct from the mathematical formulation of the suppressing force explored in chap:theory.

Finally, the optimum location for any force $f_{l,m_{t/m}}^*$ is not necessary unique. This con-

clusion, more than offering a practical solution, opens a new question. What would happen if both of those optimal positions are implemented simultaneously? This is explored in the next section.

6.2.2 Using 2 piezoelectric patches.

Controlling the vibration of the model with 2 piezos¹ arises two main questions. Are a couple of piezos capable of suppressing a mode? And secondly: Is this pair of piezos better at suppression than a single piezo?

Mistuning and structural properties remain the same as those in the previous sections.

Suppression in one mode

The same mode as for the previous section: 2F-2ND(8) is here studied. Figure 6.13 displays the effect of the optimum force of 2 piezoelectric patches of a magnitude of 1% of the excitation force (: f^{**}) acting in positions 13 and 14 ($l = 13 - 14$) aiming to suppress a tuned and mistuned mode 2F-2ND(8): $f_{13-14,8t/m}^{**}$. This pattern is shown before in figure 6.12.

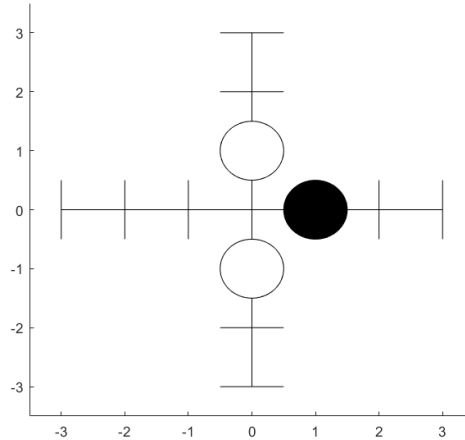


Figure 6.12: Scheme of force $f_{13-14,8t/m}^{**}$.

As expected, similar for the FRF under forces f^* , there is not an evident change in the curves in the suppressed FRFs: 6.12(a.2) and 6.12(b.2). However, there is indeed a small suppression, slightly more evident in the suppressed to unsuppressed displacements displayed in figures 6.12(a.3) and 6.12(b.3). Clearly, since the range of frequency where

¹It is now redundant to explore the case of the minimum magnitude of the force extracted from equation 3.11.

$f_{13-14,8t/m}^{**}$ is acting is the same as for $f_{13,8t/m}^*$ the small jump occurs in the same locations: around 40.6 [Hz] and 41.4 [Hz].

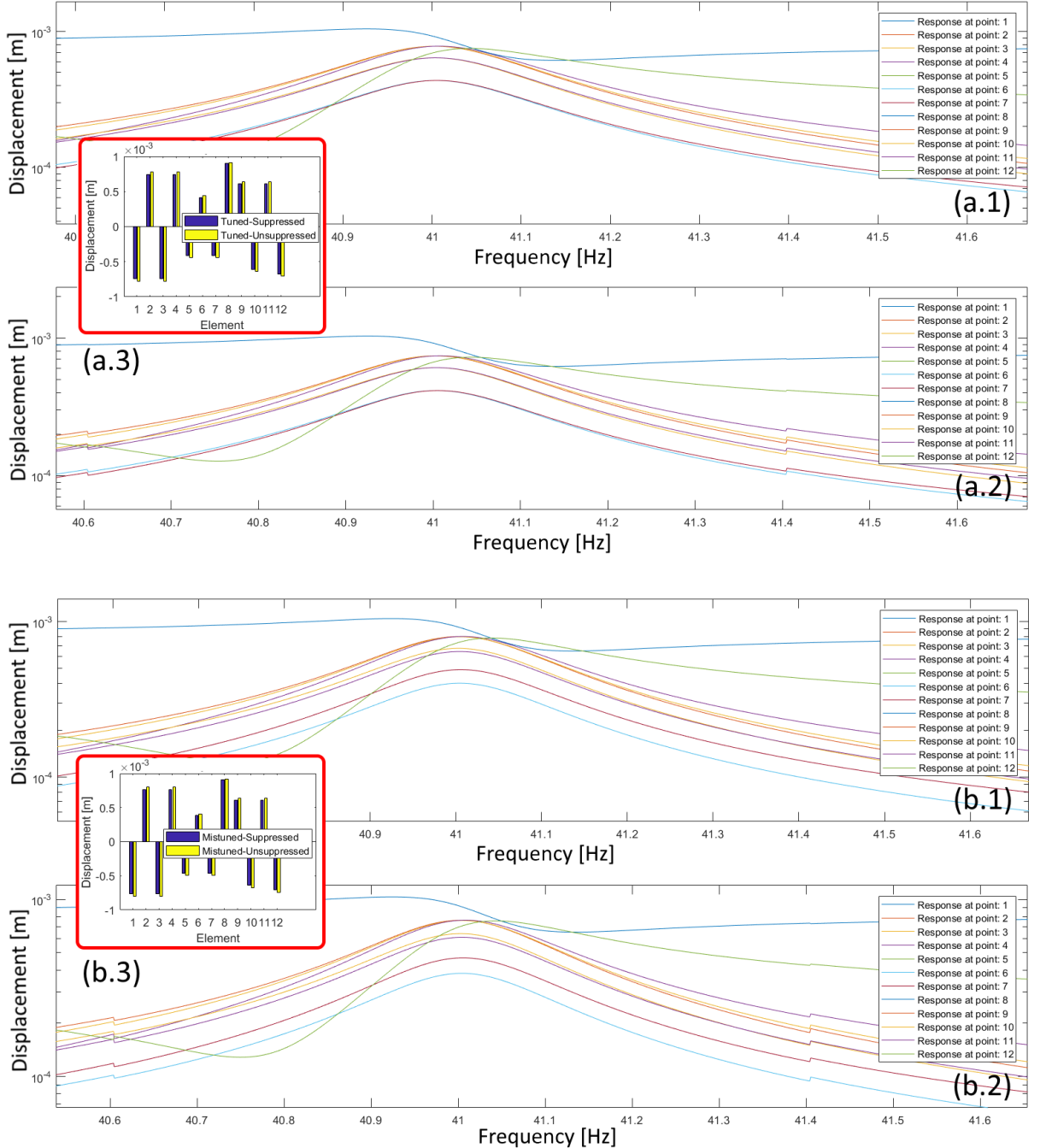


Figure 6.13: Effect of a suppressing force $f_{13-14,8t/m}^{**} = -0.01$ in a tuned and mistuned systems. (a.1) Tuned-unsuppressed. (a.2) Tuned-suppressed.(a.3) Tuned Displacements suppressed/unsuppressed. (b.1) Mistuned-unsuppressed. (b.2) Mistuned-suppressed. (b.3) Mistuned Displacements suppressed/unsuppressed.

Figure 6.14 compares the results of the suppression ratios: suppress/unsuppressed displacement, with 1 and 2 piezos for every DOF, for a tuned and mistuned model.

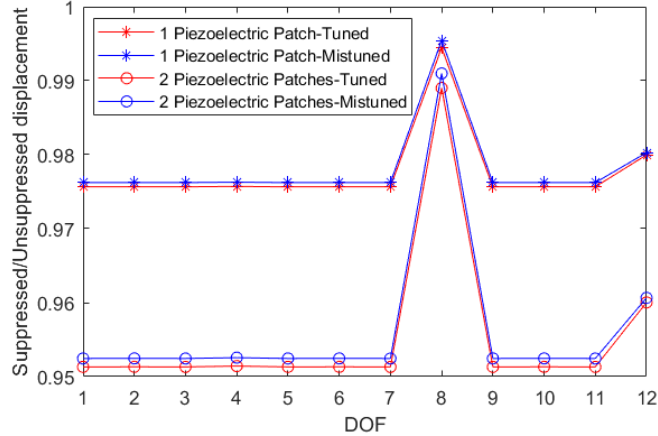


Figure 6.14: Comparison of ratios suppressed/unsuppressed displacement for every DOF at frequency of mode 2F-2ND, with 1 and 2 piezos.

Some conclusions can be extracted from these figures. First, note that for mode 2F-2ND the optimal positions for two piezos are 13 and 14 whereas for 1 piezo; it was position 13. This is an interesting result, this means that, in order to reduce more the amplitude of an ODS another piezo need to be added in position 14, without replacing the already set piezo at position 13.

Second, there is an improvement in the suppression of the ODS in every DOF of about 2.5%. Since the system is linear, this reduction is constant for every DOF, except for those excited by the single force in the tip-blade element of sector 4 (DOFs: 12, 8 and 4). This is a remarkable result, even though it may be intuitive to think that adding more piezos would suppress better, adding these forces into the system also collaborates in exciting other modes, which could offset the gain of the suppressing force targeting one mode only.

Finally, the MSFs for these four cases are summarised in the following table. These clearly show in one factor how 2 piezos are better than only one.

	t	m
MSF with 1 Piezo	0.9813	0.9818
MSF with 2 Piezos	0.9627	0.9636

Table 6.2: MSF for a tuned and mistuned mode 2F-2ND with 1 and 2 piezos.

Suppression in each mode

Figure 6.15 illustrates, using the MSF, how adding a second piezo is beneficial for each mode. Table 6.3 summarises all possible optimal location for every tuned and mistuned mode.

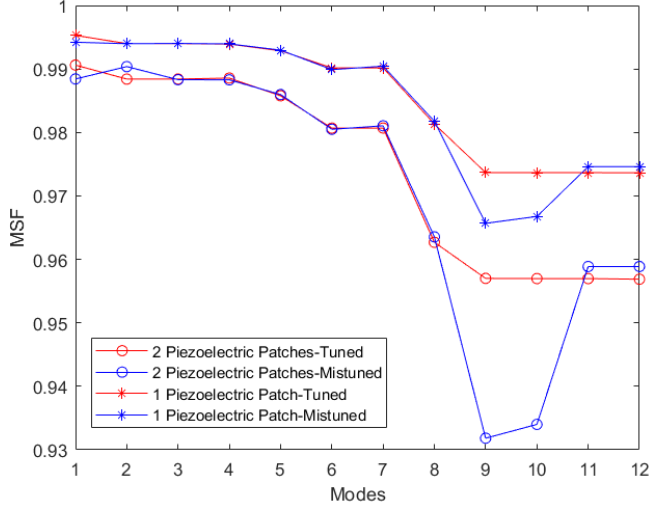


Figure 6.15: Comparison of MSFs for every mode under optimal suppressing forces type: f^* and f^{**} .

MODES	1 Piezo		2 Piezos		MODES	1 Piezo		2 Piezos		MODES	1 Piezo		2 Piezos	
	t	m	t	m		t	m	t	m		t	m	t	m
1F-0ND(1)	4	3	4-3	3-1	2F-0ND(5)	4	4	4-2	4-2	3F-0ND(9)	8	5	8-4	5-7
1F-1ND(2)	4	4	4-2	4-8	2F-1ND(6)	8	8	8-4	8-6	3F-1ND(10)	8	5	8-4	5-7
1F-1ND(3)	4	4	4-2	4-3	2F-1ND(7)	8	4	8-4	4-8	3F-1ND(11)	8	8	8-4	8-4
1F-2ND(4)	4	4	4-1	4-2	2F-2ND(8)	13	13	13-14	13-14	3F-2ND(12)	8	8	8-4	8-4

Table 6.3: Comparison of optimal locations of the piezos for f^* and f^{**} for every mode.

From figure 6.15 and table 6.3 some conclusions can be derived. First, as showed previously for mode 2F-2ND, the MSF after adding a second piezo reduces the ODS for all the modes. This is a good result, it means that regardless of the mode that is more harmful during operation having 2 piezos is better than 1.

Second, the reduction is almost linear for each mode. This means that, if with 1 piezo the reduction from a $\text{MSF} = 1$ (no reduction) is $p\%$, with 2 piezos is $2 \times p\%$. This result is remarkable, this means that there is a form of predicting how much an ODS will be reduced by means of a second piezo, assuming p is known. Therefore, an overall estimation of the

increase in the lifetime of a structure can be performed. This is not obvious, as stated previously, the mathematical model derived here aims to reduce a single mode, without considering the collateral effects on other modes, therefore, this linearity in the result is not immediate. Table 6.4 provides the percentage error between the linear extrapolation from 1 to 2 piezos for completeness. Also, note that this linearity occurs in the MSF and not in each DOF's displacement ratio for a tuned and mistuned system, which as explained before is dependent of the excitation force. In other words, the linearity in the reduction with respect to the amount of piezos incorporated in the system is independent of the excitation force, for a tuned and mistuned system.

	t	m
1F-0ND(1)	0,00058%	0,00054%
1F-1ND(2)	0,00006%	0,00006%
1F-1ND(3)	0,00060%	0,00056%
1F-2ND(4)	0,00016%	0,00015%
2F-0ND(5)	0,00058%	0,00054%
2F-1ND(6)	0,00006%	0,00006%
2F-1ND(7)	0,00060%	0,00056%
2F-2ND(8)	0,01077%	0,00902%
3F-0ND(9)	0,00058%	0,00054%
3F-1ND(10)	0,00006%	0,00006%
3F-1ND(11)	0,00060%	0,00056%
3F-2ND(12)	0,00921%	0,00850%

Table 6.4: Percentage error
between the linear projection of
the MSF with 1 piezoelectric piezo
to 2 piezoelectric piezos for all
tuned and mistuned modes.

Fourth, for some cases, the pair of location of the optimal piezos is the same for the tuned and mistuned cases. This, as mentioned in previous chapters, is beneficial because it allows to operate the control under perfectly tuned conditions.

Finally, so far suppressing a mode with 2 piezoelectric patches is the best form to reduce the ODS. In the next section, this configuration will be tested for different forms of mistuning, the suppressing forces patterns will be studied and the effect of an optimal pattern for one mode applied to another mode will be analysed.

Chapter 7

Active control: optimal suppressing patterns and their effect on secondary modes.

From this point onwards the model used contains 2 piezos acting in 2 DOFs each and a system with 2 DOFs per blade. In this chapter it is aimed to answer two important questions. The first question to answer is: Where are the optimal locations for suppression for different cases of mistuning and excitation forces? And more importantly: Why do the patterns lay there?. Secondly, now from a practical point of view: given that the optimal location for the 2 piezos is chosen for one selected mode: What would be the effect of these already set patches in the suppression of other secondary modes?

Before proceeding to show the results, it is important to clarify which type of mistuning is being implemented in the system. In this section, k -mistuning and m -mistuning are explored in an alternating pattern as shown in figure 7.1. This alternating pattern means that the same percentage of increase in the tip-blade mass or stiffness is substracted from the next sector, then added and substracted again in the last sector. A range of mistuning is explored to check for a change in the localisation of the optimal forces patterns.

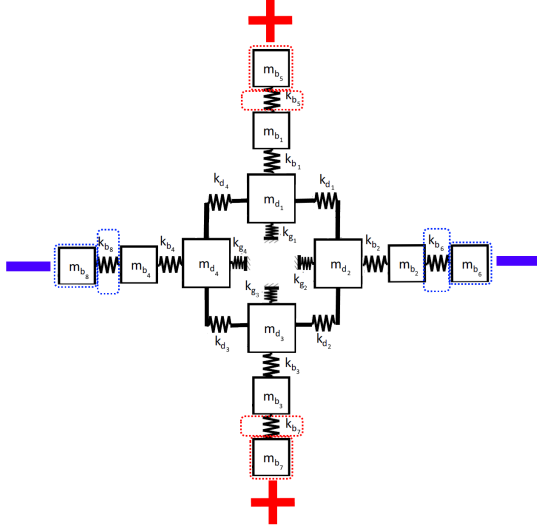


Figure 7.1: Alternating mistuning pattern in a 2 DOF per blade model.

In this section various restrictions are applied to make the model more realistic. First, the exploration of the mistuning, where the suppressing optimal force pattern changes, is searched in a range from 0-10%, more than this appears to be unrealistic. Also, since the focus of the research lies in the blades of a fan, the MSF explored for this analysis taking into account only the DOFs representing the blades, in other words, the DOFs representing the disks are disregarded in the calculation of the MSF.

7.1 Study of the different suppressing patterns.

Figures 7.2 and 7.3 show the mistuning threshold for a k -mistuning and m -mistuning for each mode. Also, they show the effect of implementing a MSF in the blades only compared with the entire vector of displacement ¹.

The values for every mode and mistuning form oscillate from 0 to 1. A magnitude of 0 means there is no change in the optimal force with respect to the perfectly tuned system. On the other hand, a value of 1 means that there is a change in the optimal force found by the optimisation. Note that this does not imply that the mistuned optimal patterns are all the same.

For example, observe the first mode (1F-0ND in a tuned system) for a k -mistuning considering disks and blades in the MSF (first plot at the top left of figure 7.2). There is a change between 0% and 1% of alternating mistuning. In other words, for that mode, a slight mistuning level between 0-1% is needed to change the optimal force found with respect to a perfectly tuned structure.

¹The formula for both MSFs can be found in equations 3.13 and 3.14

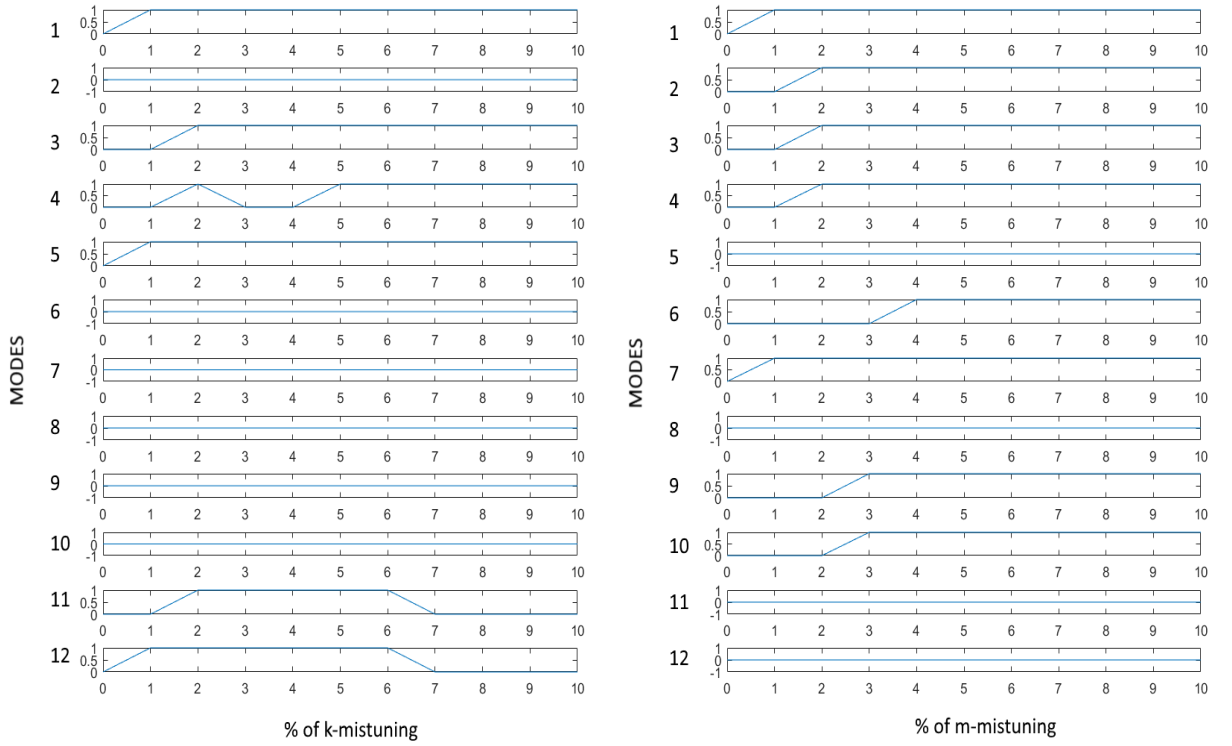


Figure 7.2: Comparison of the optimal forces found for k -mistuning and m -mistuning for a MSF considering disks and blades elements.

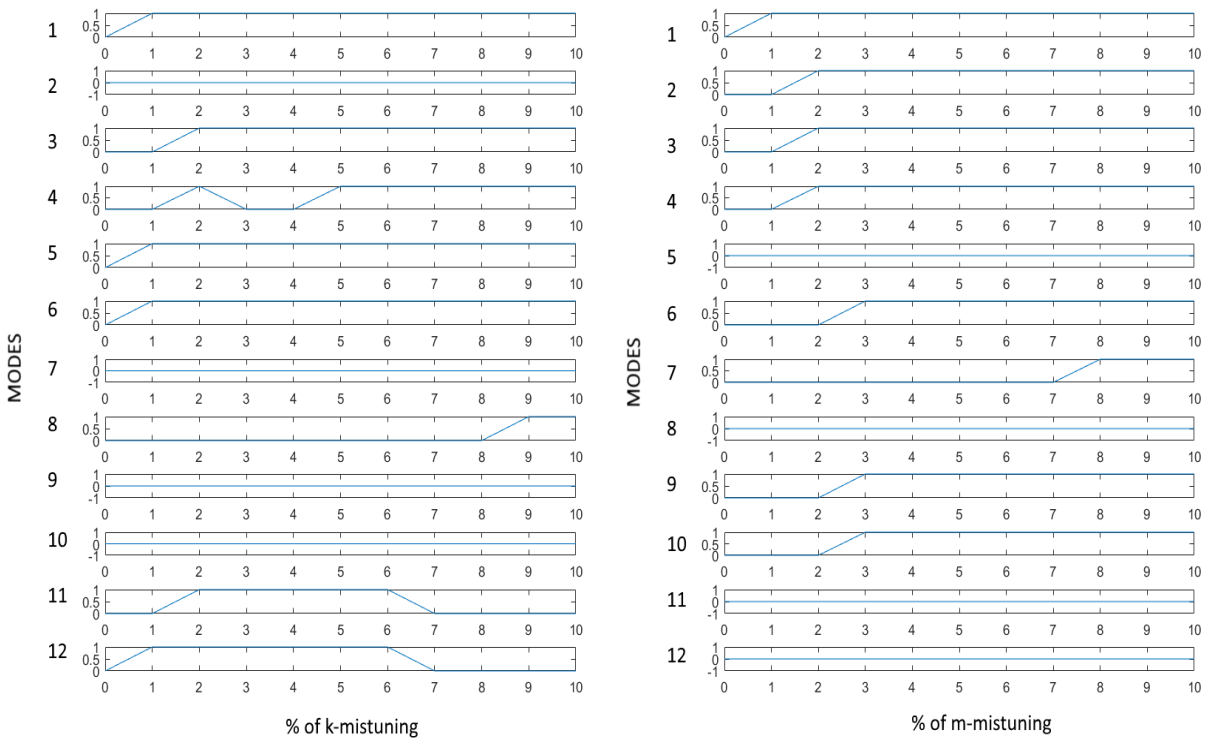


Figure 7.3: Comparison of the optimal forces found for k -mistuning and m -mistuning for a MSF considering blades elements only.

These results expose some interesting conclusions. First, for some modes more than 10% of mistuning is required to change the optimal force found at a perfectly tuned system. This is a remarkable result, it means that, for a control strategy, the optimal force to be used for a mistuned structure is the same that the force for a tuned system, which would mean that there is not necessity to actively measure the level of mistuning to feedback to the piezoelectric patches. This is, of course, under the assumptions of the alternating form of mistuned proposed above and the complete confidence that the mistuning level is less than 10%, or any confidence threshold level for that matter. This can be observed in figure 7.2 at modes 2,6,7,8,9 and 10 for k -mistuning (corresponding to the tuned modes: 1F-1ND, 2F-1ND, 2F-1ND, 2F-2ND, 3F-0ND and 3F-1ND) and modes 5,8,11 and 12 for m -mistuning (corresponding to the tuned modes: 2F-0ND, 2F-2ND, 3F-1ND and 3F-2ND).

Second, interestingly, the optimal force required for suppression can change from the optimal tuned force at certain level of mistuning and after adding some more mistuning this optimal mistuned force returns to be the same as the tuned system. This effect is depicted in the images as a curve going back to 0 from 1, after changing from 0 to 1. This, from a practical point of view, means there could be a window of mistuning where the control for suppression can operate executing a force predicted to alleviate the vibrations in the tuned system. This effect can be seen for k -mistuning in modes 4 (2-3%), 11 (6-7%) and 12 (6-7%) in figure 7.2 (corresponding to the tuned modes: 1F-2ND, 3F-1ND and 3F-2ND).

Finally, it can be observed that the effect of the masses, representing the disks in the model, can affect the total MSF and therefore the optimal force for suppression in the mistuned model. This can be clearly appreciated when comparing the following four modes between figures 7.2 and 7.3, these are: modes 6 and 8 for k -mistuning and modes 6 and 7 for m -mistuning. Considering only the blade masses obeys to a practical approach: the blades are the subject of analysis in this thesis and in most of the current research worldwide due to the reasons explained at the introduction of this work. Considering the disks masses in the MSF can affect the threshold at which the optimal force changes in 2 different ways. This consideration can increase or decrease the threshold. Increasing the threshold means that the disk elements are overexcited, meaning that the mistuned displacement is higher than the tuned displacement. Decreasing the threshold means the opposite: the disk elements are less excited when they are mistuned. An increasing effect can be seen at modes 6 and 8, where the thresholds move from 0-1% and 8-9%,

respectively, to more than 10% for k -mistuning when the disk elements are incorporated. Also, a decreasing effect is found at modes 6 and 7 for m -mistuning where the thresholds moves from 3-4% to 2-3% and 7-8% to 0-1%. With this under consideration and the practical approach above mentioned, only the blades elements are taken into account in the MSF in the following analyses.

Now that the general effect of k -mistuning and m -mistuning have been explained, the specific positions of the piezos at the threshold can be analysed. Note that the graphs displayed previously can be improved to check whether after the threshold the optimal force's patterns remain the same as in the threshold or vary for each level of mistuning. Figure 7.4 displays the positions of the pair of optimal piezos for every mode and level of k -mistuning. Figure 7.5 illustrates the same for m -mistuning.

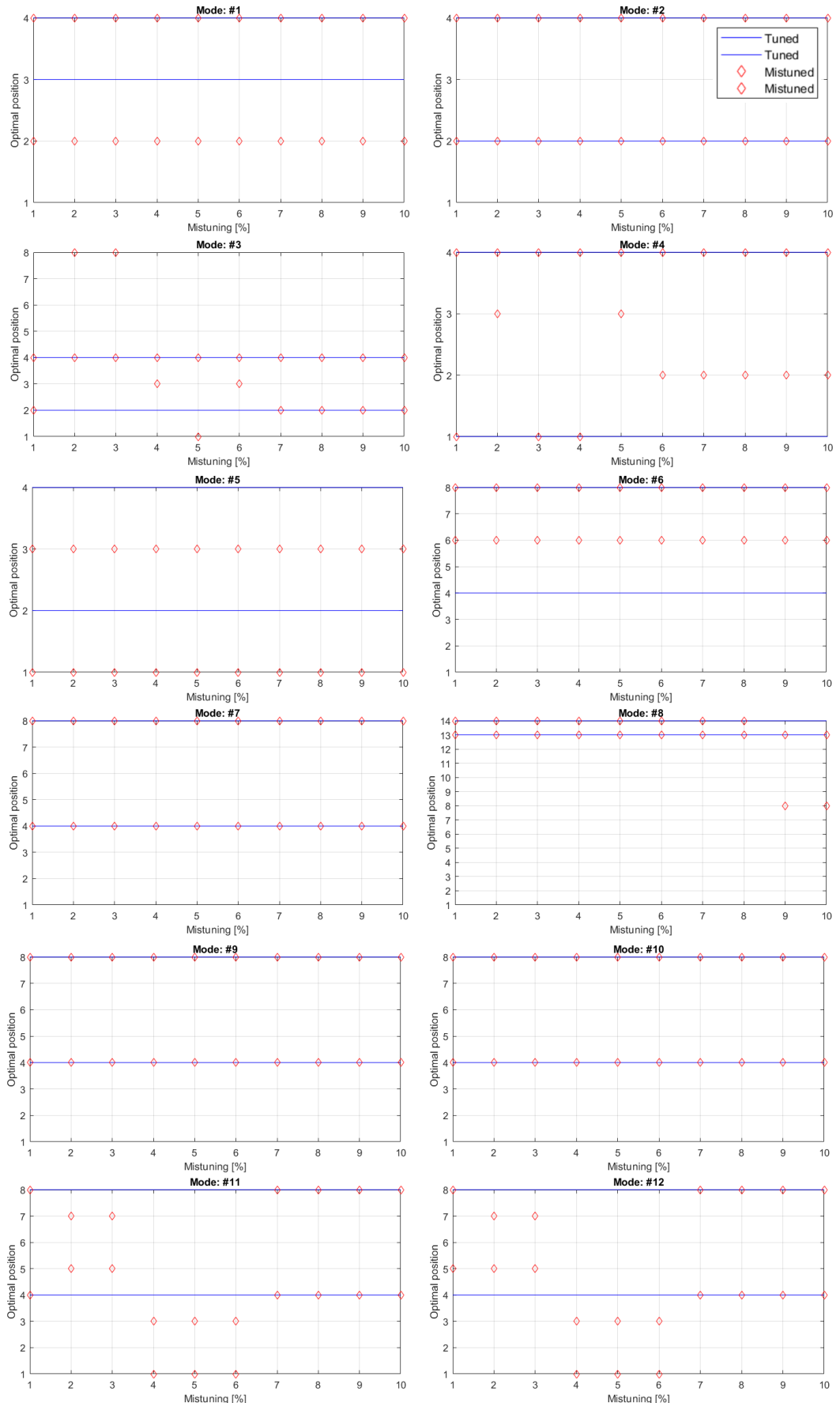


Figure 7.4: k -mistuning. Optimal positions of both piezos for various level of mistuning.

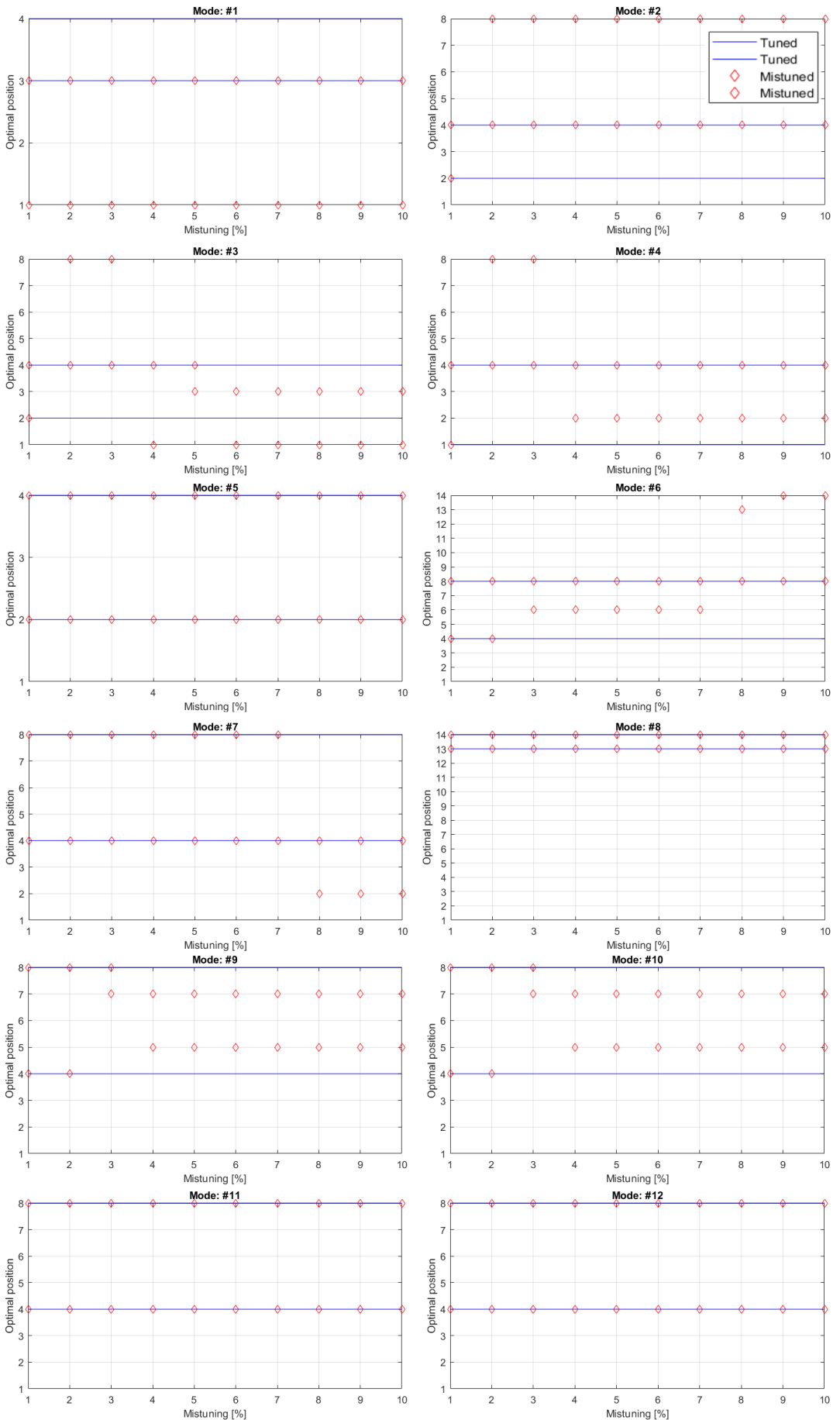


Figure 7.5: m -mistuning. Optimal positions of both piezos for various level of mistuning.

Figures 7.6 and 7.7 display the optimal forces for a tuned and mistuned system for each mode. Where there is no change in the optimal force pattern, in the range of exploration (0% to 10%), only one force is shown. Also, if there are 2 or more changes in the optimal mistuned force only the first one is displayed.

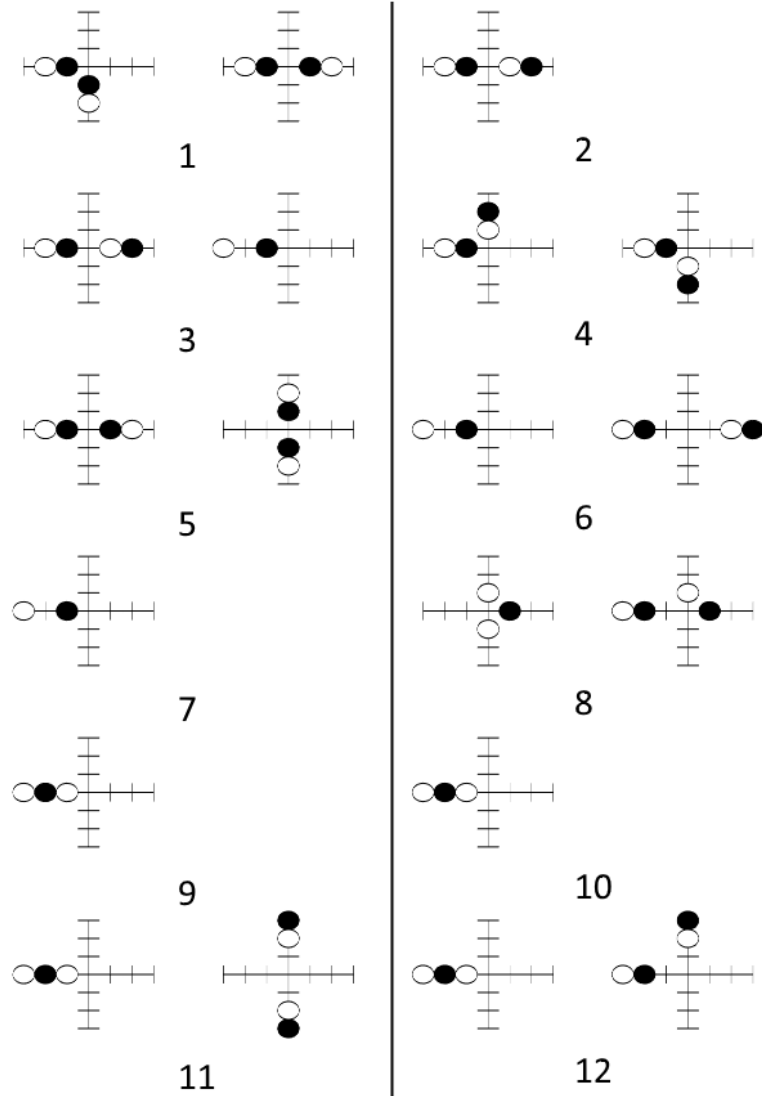


Figure 7.6: k -mistuning. Optimal force for each mode for the tuned and mistuned cases.

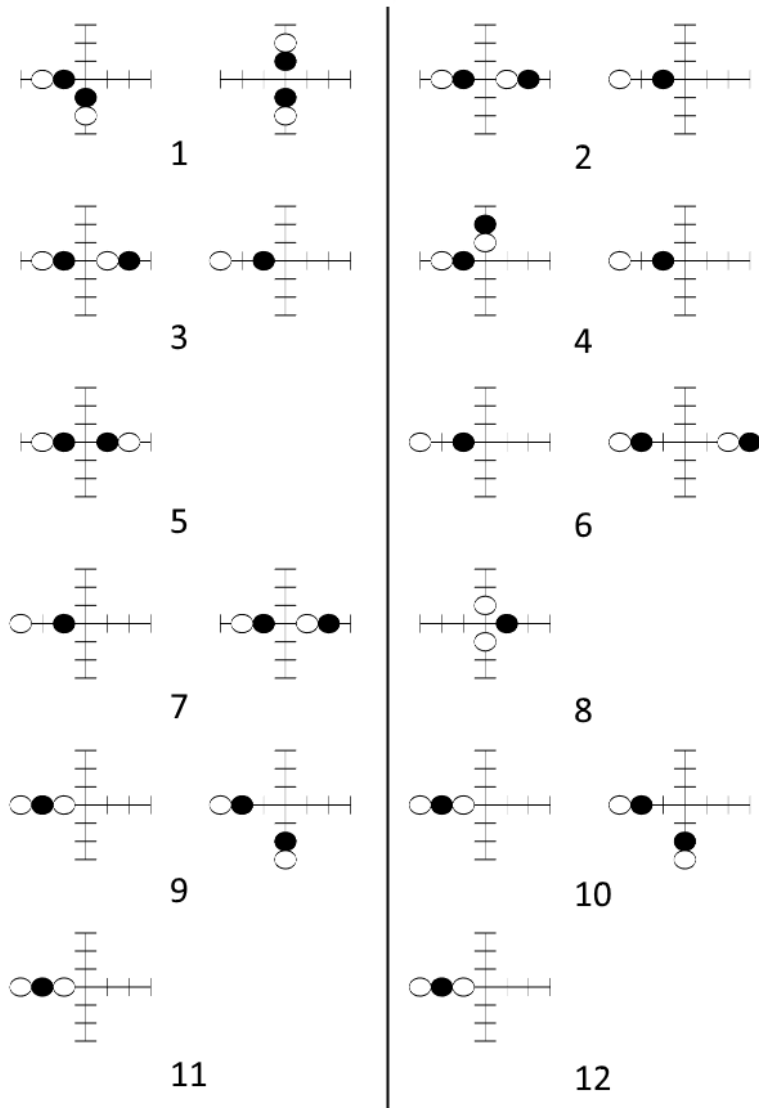


Figure 7.7: m -mistuning. Optimal force for each mode for the tuned and mistuned cases.

There are some remarks to mention from these patterns. First, note that for both types of mistuning and for almost every mode (except modes 5 and 11 of k -mistuning type), the change of the pattern after the threshold involves moving one piezo only. This is very interesting, recall from the previous chapter that adding a second piezo for suppression requires to keep the first piezo in its optimal location (i.e. not moving it) and that one remaining patch is the same as for the tuned case. This means that, under these mistuning and structural conditions, installing one piezo which is aimed to be the optimal force $f^*(\text{tuned})$ does not have any bad impact when changing the suppressing strategy to $f^{**}(\text{adding a second piezo in a mistuned case})$. Also, note that the piezo that remains in its original position continues to exert the same pattern of force: tension/contraction (relative to the excitation force) as the 2nd piezo is moved to another position after the

mistuning threshold is passed. This makes the control strategy even simpler.

Second, there is a tendency in the optimum patterns to have both or at least one of the pair of piezos in sectors 2 and 4 (horizontal sectors), regardless whether it is k -mistuning or m -mistuning. There are 2 main variables operating in those sectors that may cause this tendency: (1) The mistuning that softens the springs or reduces the mass of the tip elements in those sectors and: (2) The excitation force that is present in the tip of sector 4. If it was (1) the main factor, then the tuned optimal locations would not follow the same tendency necessarily, however, they do, therefore it is most likely not the cause of the tendency. To check if (2) is the main cause another excitation pattern is tried. This time a SBE excitation force in the tip blade element of sector 1 is applied. The m -mistuning pattern is the same and fixed at 5%. The results are displayed in figure 7.8.

Clearly, the predominant cause to align the piezos in the horizontal sector is the excitation force. From figure 7.8 it can be seen that with this new excitation pattern both of the piezos are aligned vertically, in sectors 1 and 3. This is clear for tuned modes 2,3,4,6,7,9,10, 11 and 12 and mistuned modes: 2,3,4,6,7,9,10 and 11 . This is significant in this specific case of a static blisk model. This means that knowing the excitation would define mostly the blades where the piezos will be installed. The reason behind this is the displacement caused by the forced response at those in those sectors, as it will be shown in the third point of this discussion. Note that this loses meaning in a rotating fan where that SBE would rarely occur.

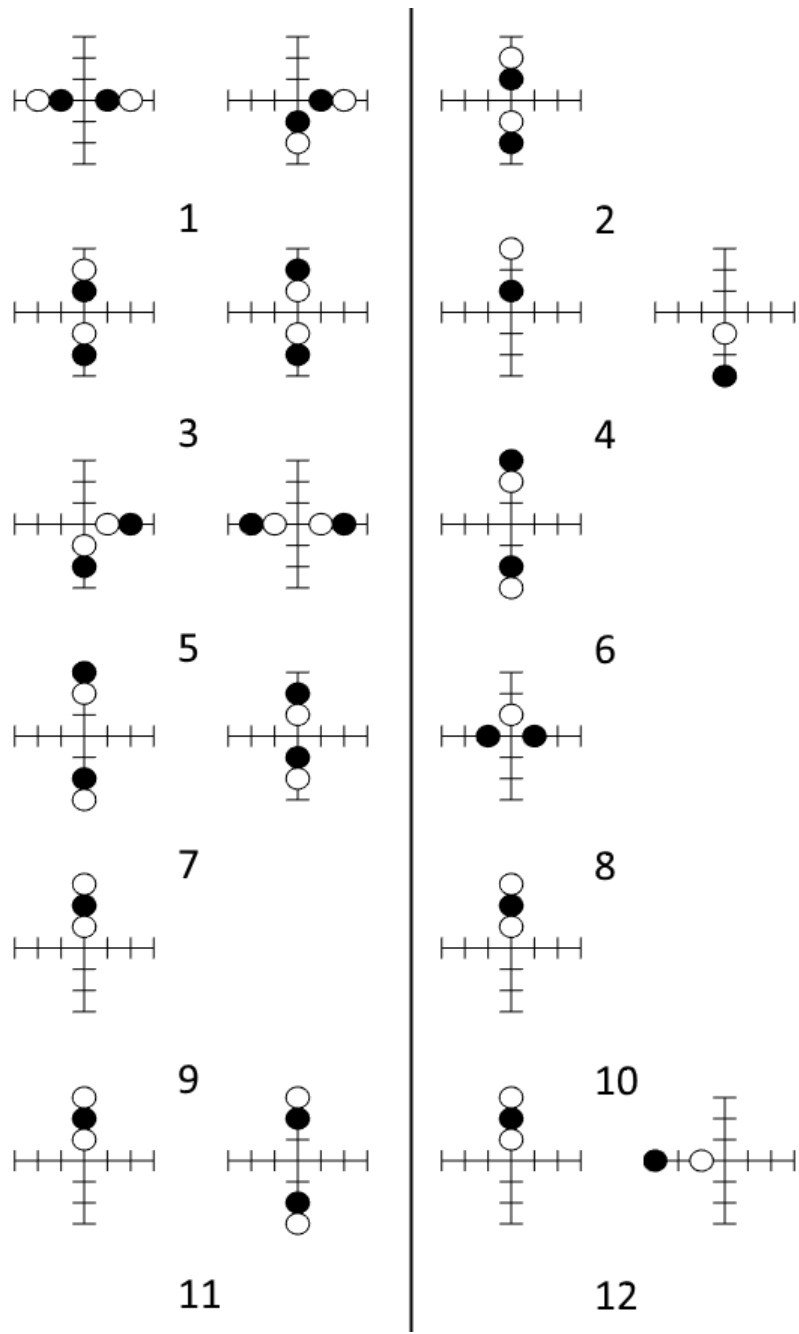


Figure 7.8: m -mistuning. Optimal force for each mode for the tuned and mistuned cases with an excitation force in the tip-blade element of the 1st sector.

Third, there is a weak correlation between the positions of the pair of piezos and the resonant frequencies. As the frequencies increase, the pair of piezos tend to go to outer positions (tip of the blades). The displacement on those locations must be therefore governed by some factors.

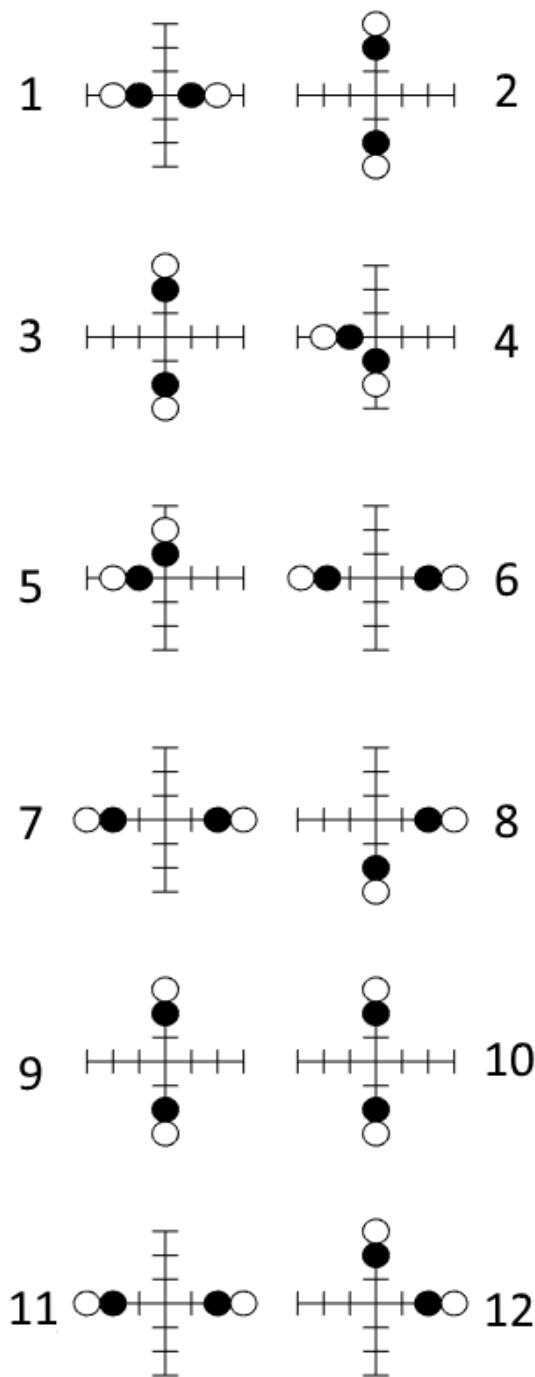


Figure 7.9: Suppressing force patterns for a tuned, symmetrically excited and low damped system.

The displacement at each location are governed by the (1) Mistuning pattern, (2) Asymmetric excitation force pattern and (3) Damping. In order to run a simplified test, these factors must be disregarded then: (1) Only a tuned model is tested, (2) The excitation pattern applied is totally symmetric: an equal force in the tips of the four sectors is applied and (3) Damping is extremely reduced so it has little effect: $\gamma=0.0005$ and $\beta=0.08$.

Figure 7.9 displays these results. An intuitive thought would be to consider that the optimal piezos would locate across a NC, in order to suppress the natural shape of that mode. However, these results show 2 important things. First, the optimal position can be in the link between the tip and base of the blade even though there is no NC in there, as it can be seen for double modes 1F-1ND(2-3). And second, even if there is a NC line, the optimal pattern tend to be in an outer position and not across the NC, as it is shown for modes 2F-1ND(6-7) and 2F-2ND(8), where the NC lays between the disk and the blade elements. However, if there are 2 NCs, the optimal pattern sits in the outer position always, as it is shown for modes 3F.

This correlates strictly with the difference in displacement between DOFs. This means that, where there is the biggest difference in displacement, between 2 DOFs, the optimal locations choose their positions in there, regardless whether it is across a NC or not. Indeed, this difference between one DOF and the next one is a measure of the strain between them, therefore it is a wise position to locate the piezos, as demonstrated experimentally by Duffy et al. (2013). Figure 7.10 shows the unsuppressed displacement for each DOF, for modes: 1F-0ND (1), 1F-1ND (2), 3F-0ND (9) and 3F-1ND (10), also it is indicated where and how the optimal piezoelectric patches are acting. The triangles represent the direction of the suppressing force displayed with circles in the patterns at the top right in 7.10(a), (b), (c) and (d).

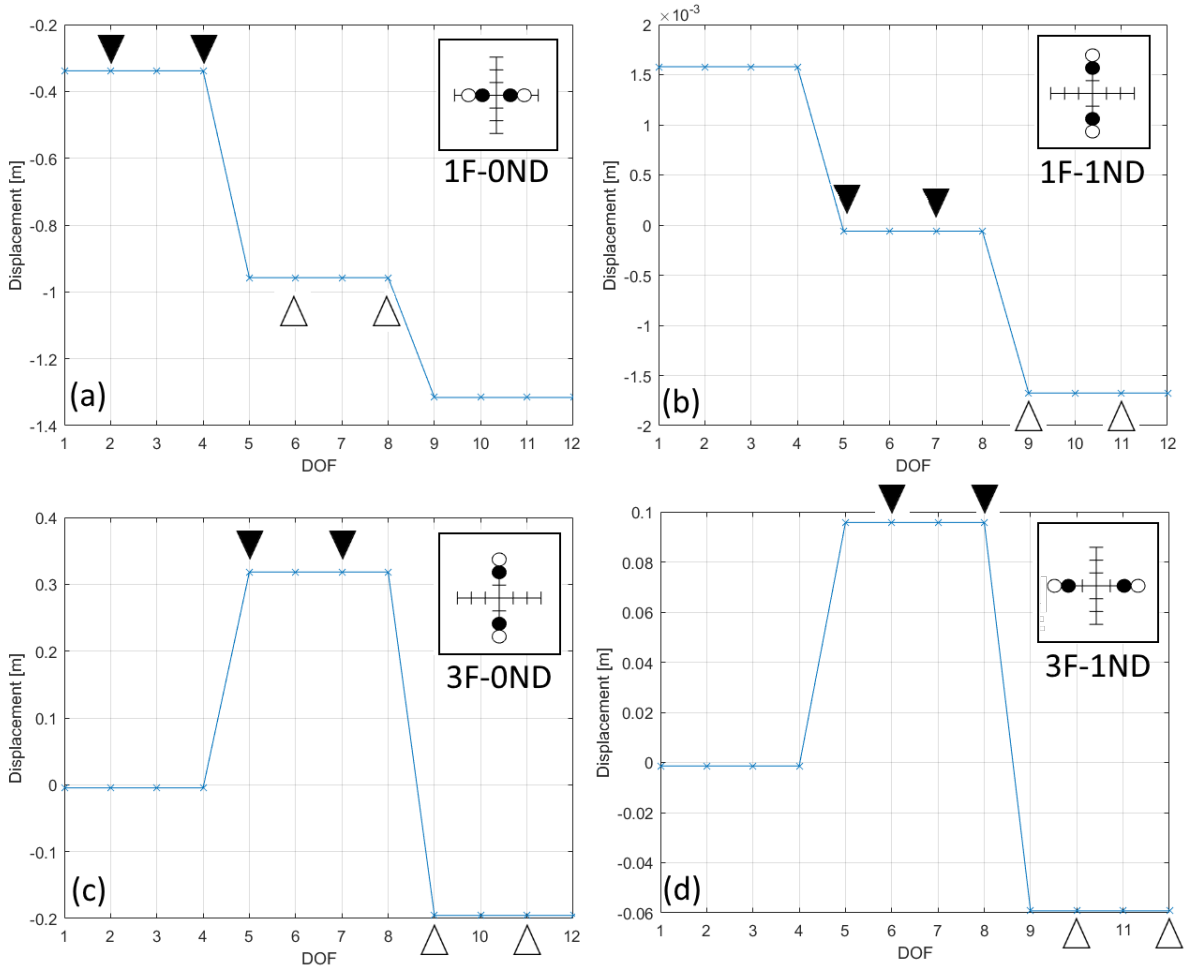


Figure 7.10: Displacement difference and optimal piezo locations for 4 modes.

Hence, if the difference in displacement is divided by an arbitrary large of the blade, say $L = 1[m]$, to provide a strain measure. The results can be summarised as follows. For mode 1F-0ND, the strain between disks and base of the blades is ≈ 0.6 , whereas for

the tip to base of the blades it is ≈ 0.26 , therefore the optimal locations are between the disks and the base of the blades. Also, as shown by the direction of the pointing triangles, the piezo forces are trying to reduce that strain by compressing it. Similarly, the biggest strains for modes 1F-1ND, 3F-0ND and 3F-1ND are: 0.0017, 0.5 and 0.16, located in the joints of the tip and base of the blades.

Note that the presence of the NDs in groups 1F and 3F is suppressed by the symmetric excitation force acting in the four tips of the blades, thus, there is no oscillation in the displacement of the four elements in the group of disks, base of the blades and tip of the blades.

7.2 Effect of the optimal location for all the suppressing forces over the rest of the modes.

Once the engineer has decided which mode is the most important to suppress with these two piezoelectric patches, she may still be interested in the suppression of other modes. Suppose that mode ‘X’ is the most harmful during the operation of a certain aircraft engine and the vibrations team desire to control it. An optimal location for the two piezos is found producing an optimum MSF: MSF_x (due to force f_x^{**} , here the location ‘l’ is disregarded for simplicity in the nomenclature).

However, the team discovers that under certain operating conditions the fan vibrates in a mode ‘Y’ which is also detrimental for the fan. Sadly, the patches are already installed. Then, two fundamental questions arise in the vibration team: Do this pair of patches, fixed as they are, suppress the new mode Y? Also, if indeed the patches can suppress mode Y where they are: Is this level of suppression comparable with the level of suppression achievable by looking directly for the optimum location for mode Y under force f_y^{**} (as it was performed for mode X initially, with f_x^{**})? This suppression can be assessed by means of the new MSF achieved at mode Y, from the initial fixation of mode X: $MSF_{x,y}$. If the suppression level is satisfactory then the patches will remain in their position, but if the level is unacceptable they may need to be removed and set in other locations for this new mode Y.

This section targets these questions. First, the optimal locations for these two piezos are found for every single mode. This optimum, as established previously, is found in the locations and phases (compression/tension) where the exerting suppressing forces produce

the minimum MSF for the blade elements (tip and base, no disks involved). Then, the two patches are ‘installed’ in these locations in the structure. After this, for each of the rest of the modes, the four possible combination of opposite phases are tried, in order to seek for the minimum achievable MSF. The four possible combinations of these two patches, once they are installed are: contraction/tension, contraction/contraction, tension/contraction and tension/tension. Note that this means they are in 0° phase or 180° phase with respect to the excitation force, no other phases within this range have been implemented in this study.

In each of the 12 images in figures 7.11 and 7.12 two curves are depicted. In blue, the curve describing $MSF_{x,y}$, the above mentioned optimisation, is represented. Each figure corresponds to the suppression of each mode and their corresponding impact in the rest of the modes (displayed in the horizontal axis). In red, the optimum for each mode is drew ($:MSF_x$), therefore this curve is the same for each of the 12 images, because it is the best MSF achievable without considering a prefixed positions of the piezos.

This analysis is carried out for a perfectly tuned system, in figure 7.11. On the other hand a system with a 4% of alternating m -mistuning is considered and its results displayed in figure 7.12. This 4% is chosen because at this level of mistuning all the modes, except for the 7th mode, change their tuned optimal suppressing force to another pattern, see figure 7.3. The level of mistuning for the 7th mode is between 7-8% which seems unrealistic in actual blades.

Figure 7.11: Optimal MSF for each mode and the effect on the rest of the modes in a perfectly tuned system.

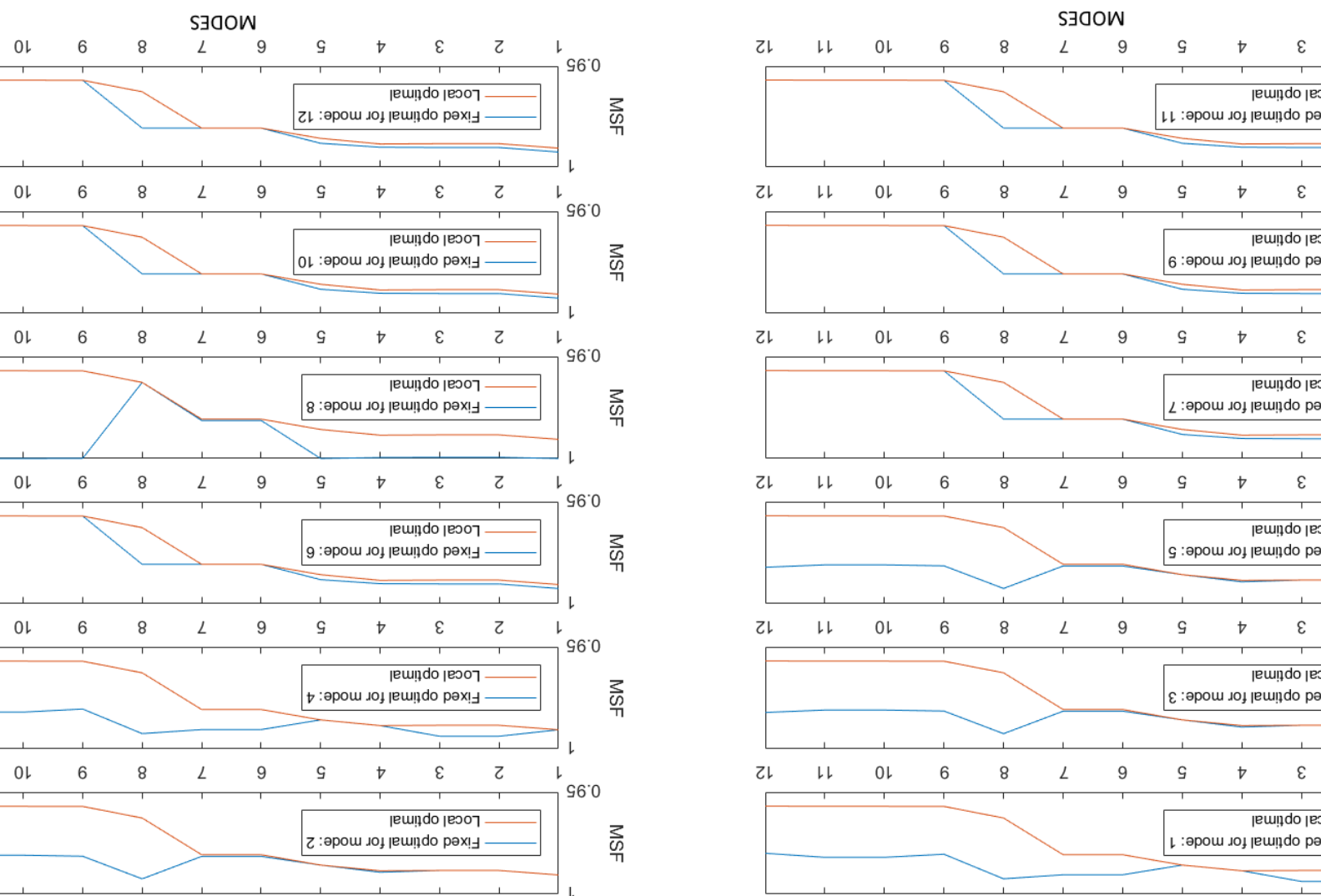
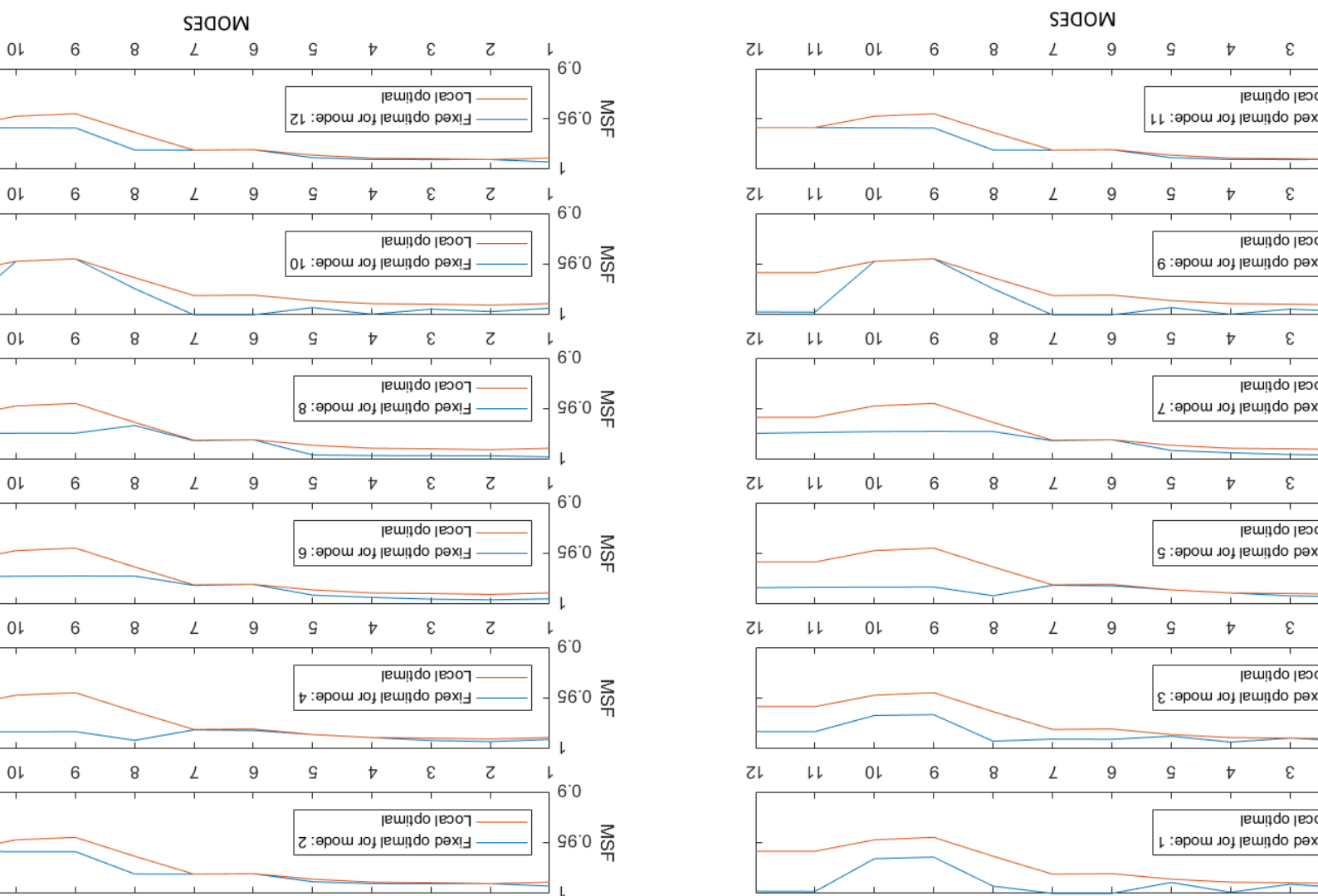


Figure 7.12: Optimal MSF for each mode and the effect on the rest of the modes in a mistuned system.



Before answering to the original questions, some general appreciations.

First, the maximum level of overall reduction accounted by the MSF is approximately 5% for the tuned and mistuned cases. Nonetheless, it is more than the 1% suppressing force assumed for the piezoelectric patches. It is hard to quantify in this model how improved the fatigue life is with this reduction in displacement, however, in real blades a reduction in the displacement lead to a reduction in stress and therefore an increase in the cycles it can handle.

Second, the achievable MSF_x for each mode (red curve) is less than one. This means that there actually are a couple of locations where a pair of patches can be connected to, such that the ODS is decreased. This is a remarkable result since no model in the literature has explored a contracting(tensing) model for the piezoelectric force capable of such effect in a structure.

Third, and now coming back to the original questions. It is observed that the curves $MSF_{x,y}$ are always less than unity. In other words, and answering to the first question in this chapter, it is indeed feasible to fix the location for a mode X and even in that case suppress a mode Y. This is true for every original fixed mode X and every secondary indirect mode Y. Also, this effect is applicable for a tuned and mistuned case (MSF_{x,y_t}, MSF_{x,y_m}). These are remarkable results since they demonstrate that, after a good optimisation (seeking for the good phase among the patches) a second mode can be targeted by the same initial distribution of suppressing forces. A long term derivative of this conclusion is that the costs of increasing the lifetime of blades in a fan do not necessarily depend on each blade in the group but it depends only on certain blades in the fan.

Fourth, now that it is possible to suppress secondary modes it is time to answer the next question. Sadly, even when $MSF_{x,y_{t/m}}$ is less than one, for every X and Y, it still bigger than $MSF_{x_{t/m}}$. This is a result to be expected, a second restriction on the optimisation of $MSF_{x_{t/m}}$ is added then it is predictable that the optimum MSF will be equal or higher than the original.

Fifth, in general, the difference between $MSF_{x,1-4_{t/m}}$ and MSF_{1-4} is less than when compared to the rest of the secondary modes. This is true even up to Y=7 for some Xs. This is an important result, it means that if the modes that are harmful for the fan are in the 1F-X ND group, there will a negligible reduction in the MSF if the patches are placed for the optimal locations of any of those modes. Which means that the strategy chosen by the engineer can be to suppress mode 1F-0ND or 1F-2ND and the effect on the

secondary effect in 1F-XND will not vary considerably.

These five conclusions are shared by the tuned and mistuned curves. Clearly, MSF_{x,y_t} are different from MSF_{x,y_m} , and MSF_{x_t} are different from MSF_{x_m} as well. Where and why they differ is explored here below.

Sixth, double modes present identical MSF_{x,y_t} . Double modes are numbered as 2-3, 6-7 and 10-11, corresponding to: 1F-1ND, 2F-1ND and 3F-1ND respectively. This duplicity is due to the fact that the displacement of each DOF used to compute the MSF is extracted from the FRF at resonance, which means that only one MSF is extracted for each pair of double modes. This does not occur with MSF_{x,y_m} because the modes are splitted.

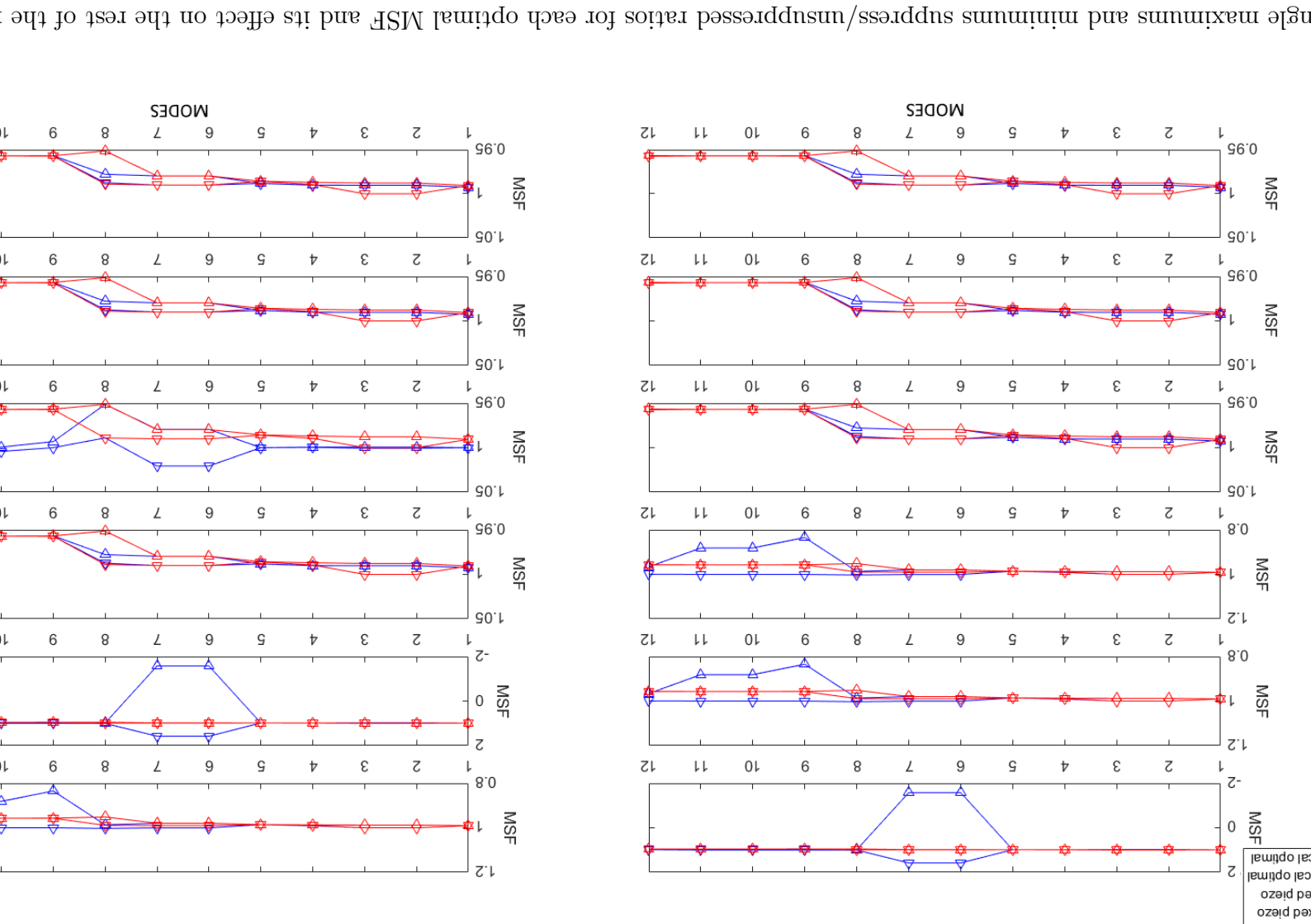
Seventh, note that even with mistuning some modes remain coupled, or at least not sufficiently separated. This is due to two reasons. First, the damping in the structure couples modes that are close together, this is more noticeable in the tuned $MSF_{x,y}$ where all four modes in the 3F-XND group are coupled. This can be observed easily from figure 4.7(a). Indeed the MSF_{9-12,y_t} are not the same but slightly different, unperceivable for the eye anyhow. Secondly, mistuning do separate some of these damping-coupled modes, however, it makes these splitted modes to couple with adjacent modes. For instance, in figure 7.12, MSF_{10-11,y_m} are decoupled, but MSF_{9,y_m} seem identical to MSF_{10,y_m} , likewise, MSF_{11,y_m} appears to be identical to MSF_{12,y_m} . Again, they are slightly different but apparently indistinguishable.

Eighth, the maximum and minimum values in the MSF_{x,y_m} are more scattered than the results for the MSF_{x,y_t} . This means that for some pairs of (X,Y) the mistuned MSF is really low but for others it is close to 1. This means, in practice, that if there is uncertainty in the piezoelectric patch's capabilities it may not be worthy to try to suppress that mode Y. These risky positions can be seen in figure 7.12 at $MSF_{10,(4/6/7/11/12)_m}$, among others.

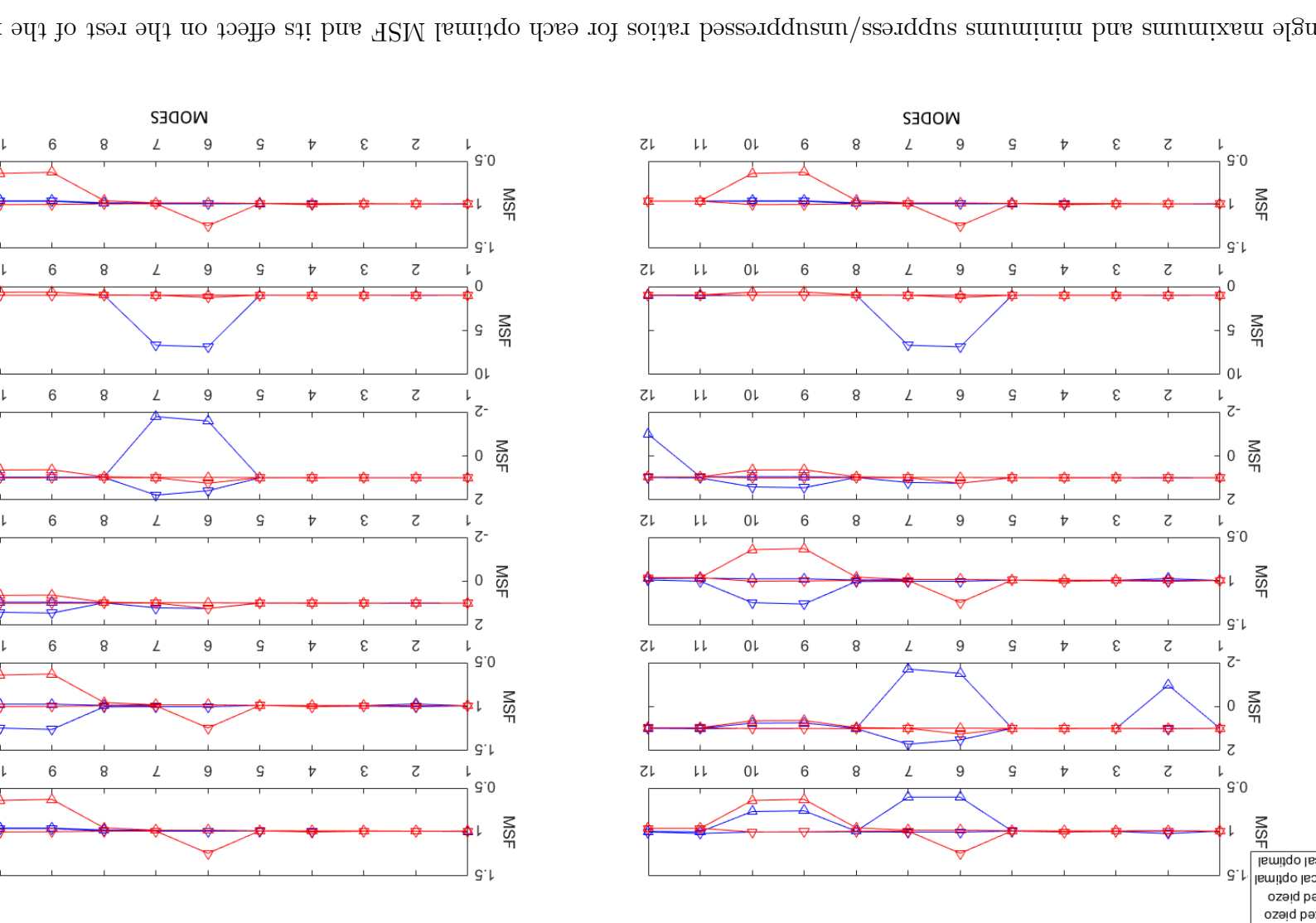
At this stage it is important to recall that the MSF is a global factor as deducted from equation 3.12. In other words, all the DOFs are mixed together to find a single factor. Thus, each $MSF_{x,y}$ and MSF_x is computed from 8 different DOFs. However, this hides information related to each specific tip-blade or base-blade element. Figures 7.13 and 7.14 offer some insight in this issue by providing the minimums and maximums local MSF. The minimum local MSF means the most suppressed tip/base blade element when a mode Y is targeted after previously aiming to suppress mode X: $\min_{x,y}$, and the maximum MSF means the less suppressed element: $\max_{x,y}$. Similarly, the same figures show the minimums and maximums for a single mode X suppression: \min_x and \max_x .

Note that the less suppressed element can have a ratio of suppressed to the unsuppressed displacements (ν_s/ν_{us}) bigger than one, meaning that indeed it is overexcited. Hence, as for the MSF, a value of 0 means absolute suppression, a value of 1 means no suppression at all, and everything above 1 means that the DOF is overexcited.

perfectly tuned system.



mistuned system.



Various conclusions can be elaborated from these figures. First, the locations of force f_x^{**} applied in mode Y ($:f_{x,y}^{**}$) is never totally beneficial. The most beneficial case would be that $\min_{x,y}$ and $\max_{x,y}$ are below \min_y and \max_x but that would mean that the $MSF_{x,y}$ is below MSF_x which, as discuss previously, cannot happen because they would be better than the local optimum. Nonetheless, a good result could be that $\max_{x,y} \leq \max_y$ and only $\min_{x,y} \geq \min_y$. This occurs for the tuned pairs (7/9/10/11/12,8) and mistuned pairs (11/12,9/10). In other words, the application of force f_x^{**} instead of f_y^{**} over mode Y will still decrease the overall ODS ($MSF_{x,y} < 1$), however it would decrease the lifetime of some fan blades ($\min_{x,y} > \min_y$).

Second, the most detrimental case is when $\max_{x,y} > \max_y$ and $\min_{x,y} > \max_y$. This only occurs for the pair of tuned modes (8,9/10/11/12). This would indicate a high $MSF_{x,y}$ as depicted in figure 7.11 where $MSF_{x,y} \approx 1$.

Third, in general there is a trade-off and some blades are improved while others are worsened. The most evident case is when $\max_{x,y} > \max_y$ and $\min_{x,y} < \min_y$. This occurs for the pairs: (1,6/7), (2/3,9/10/11/12), among others.

Fourth and most importantly, sometimes the trade off may not be worthy enough. For example, $\max_{9/10,6/7}$ is more than 5 times bigger than $\max_{6/7}$ for the mistuned case. In other words, applying the optimal forces patterns of modes 9/10 over 6/7 extremely rises the displacement of some DOFs. This presumes that the optimal pair of piezos capable of suppressing modes 9 and 10 are fixed, therefore the alternative is not changing the piezos to positions 6 or 7. The alternative then is not to suppress modes 6 or 7 at all. In this case, assuming $f_{9/10}^{**}$ is fixed, it may be worthy not to suppress the mode even though the $MSF_{x,y} < 1$, because it would advance the maintenance just for some blades, rather than doing the maintenance in a later stage, over more components.

Chapter 8

Conclusions

The main objectives of this research were twofold: to find the optimal location for the representation of the action of a piezoelectric patch in a semi-analytic model and to find the effect on secondary modes after the patches are installed.

Before answering any of those questions the models explored in chap:1DOF and chap:2DOF were successfully validated, according to the response to changes in damping, mistuning, and excitation forces. The model with 2 DOFs per blade captures more features of a real blisk, therefore, this model is mainly used.

In order to achieve the first main objective a model of the piezoelectric force is derived. This model acts in 2 DOFs to account for the tension/compression effect of real patches. After this, the force model shows to successfully suppress each targeted mode, quantified by means of the MSF. Some general tendencies of the locations of the patches are observed, under certain conditions. Piezos tend to locate in outer positions, close to the tip, even when the NC (2F group) is closer to the disk. In addition, the piezos, when there are 2 of them, tend to align in 2 sectors: the sector where the excitation force is applied and the opposite sector, this is: sectors 1&3 and 2&4. These tendencies are dominated by the differences in displacement between DOFs, or strain. In other words, optimal locations of the piezos lay in the locations where the strain is the biggest, for each mode.

Secondly, a practical case is studied. Initially, a mode is targeted and the optimal locations to suppress it are found, then the effects of the piezos in those optimal locations, when the target is changed, are explored. The models demonstrated how when there is a

new targeted mode the capability in the reduction of the ODS is decreased. Nonetheless, it can still develop a beneficial suppression. Even though this is a good result, care must be taken for the specific reactions at every single DOF, and not only to the overall MSF. The research showed that, even when the MSF is less than one the optimal pattern can over excite some of the DOFs.

Chapter 9

Future work

In this chapter, recommendations are divided into two levels. The first level is for the continuation of the semi-analytic model explored in this thesis. Secondly, recommendations are listed leading to a more experimental approach.

This model can be improved by working out the restrictions listed in chap:theory. Among the most important are:

1. To add more DOFs per blade in order to validate the tendencies of the location of the optimal positions for the piezos.
2. To incorporate rotation into the system, along with this EOE may be considered.
Hence, looking into the stiffening consequences of rotation.
3. To look for an optimum number of piezos to suppress a mode. It is not clear that the more piezos the better the suppression is.
4. To couple the electro-mechanical effects of the piezo. Thus the input signal would be voltage and not a simple SBE force.
5. To consider a piezo acting with its own phase therefore considering the effect of the suppression in the time domain.
6. To define a suppression factor that takes into account: local overexcited DOFs, the lifetime increase as a consequence of the suppression, etc.

Some steps can be followed in order to advance towards a more experimental approach:

1. To extensively study the capabilities and practical considerations of using a piezoelectric patch. This means, to understand its physical formulation as well as its technical considerations.
2. To elaborate a realistic FE model that consider various of the constrains explored in this report and also those mentioned above for future modelling work.
3. To add modern techniques of analysis capable to group tendencies in the model results faster than a singular person, such as unsupervised Machine Learning algorithms.
4. To experimentally validate the the results (or some of them) in an experimental rig.

Bibliography

Agulhon, T. (2015), Active Vibration Control of Turbine Engine Blades via Optimal Placement of Piezoelectric Plates: an Experimental Investigation, Masters dissertation, Imperial College London.

Bachmann, F., de Oliveira, R., Sigg, A., Schnyder, V., Delpero, T., Jaehne, R., Bergamini, A., Michaud, V. and Ermanni, P. (2012), ‘Passive damping of composite blades using embedded piezoelectric modules or shape memory alloy wires: a comparative study’, *Smart Materials and Structures* **21**(7), 075027.

URL: <http://stacks.iop.org/0964-1726/21/i=7/a=075027>

Ballas, R. G. (2007), *Piezoelectric multilayer beam bending actuators: static and dynamic behavior and aspects of sensor integration*, Springer Science & Business Media.

Biglar, M., Gromada, M., Stachowicz, F. and Trzepieciński, T. (2015), ‘Optimal configuration of piezoelectric sensors and actuators for active vibration control of a plate using a genetic algorithm’, *Acta Mechanica* **226**(10), 3451–3462.

URL: <https://doi.org/10.1007/s00707-015-1388-1>

Bladh, R., Castanier, M. and Pierre, C. (2001), ‘Component-mode-based reduced order modeling techniques for mistuned bladed disks—part i: Theoretical models’, *Journal of Engineering for Gas turbines and Power* **123**(1), 89–99.

Botta, F., Dini, D., Schwingshakl, C., di Mare, L. and Cerri, G. (2013), ‘Optimal placement of piezoelectric plates to control multimode vibrations of a beam’, *Advances in Acoustics and Vibration* **2013**.

Botta, F., Scorza, A. and Rossi, A. (2018), ‘Optimal piezoelectric potential distribution for controlling multimode vibrations’, *Applied Sciences* **8**(4), 551.

- Chandrasekhar, A., Adhikari, S. and Friswell, M. (2016), ‘Quantification of vibration localization in periodic structures’, *Journal of Vibration and Acoustics* **138**(2), 021002.
- Crawley, E. and Mokadam, D. (1984), ‘Stagger angle dependence of inertial and elastic coupling in bladed disks’, *Journal of vibration, acoustics, stress, and reliability in design* **106**(2), 181–188.
- Deng, P.-c., Li, L. and Li, C. (2017), ‘Study on vibration of mistuned bladed disk with bi-periodic piezoelectric network’, *Proceedings of the Institution of Mechanical Engineers, Part G: Journal of Aerospace Engineering* **231**(2), 350–363.
- Duffy, K. P., Choi, B. B., Provenza, A. J., Min, J. B. and Kray, N. (2013), ‘Active piezoelectric vibration control of subscale composite fan blades’, *Journal of Engineering for Gas Turbines and Power* **135**(1), 011601.
- EWINS, D. (1976), ‘Vibration modes of mistuned bladed disks’, *Journal of Engineering for power* **98**(3), 349–355.
- EWINS, D. and HAN, Z. (1984), ‘Resonant vibration levels of a mistuned bladed disk’, *Journal of vibration, acoustics, stress, and reliability in design* **106**(2), 211–217.
- EWINS, D. J. (2000), *Modal testing : theory, practice, and application*, 2nd ed edn, Baldock, Hertfordshire, England ; Philadelphia, PA : Research Studies Press. Previous ed.: 1995.
- Firrone, C. M. and Zucca, S. (2009), ‘Underplatform dampers for turbine blades: The effect of damper static balance on the blade dynamics’, *Mechanics Research Communications* **36**(4), 515 – 522.
- URL:** <http://www.sciencedirect.com/science/article/pii/S0093641309000111>
- Glasstone, M. (2016), Finite Element model for active vibration control of a turbine engine blades via optimal placement of piezoelectric plates., Maters dissertation, Imperial College London.
- Griffin, J. (1988), ‘On predicting the resonant response of bladed disk assemblies’, *Journal of Engineering for Gas Turbines and Power* **110**(1), 45–50.
- Han, J.-H. and Lee, I. (1999), ‘Optimal placement of piezoelectric sensors and actuators for vibration control of a composite plate using genetic algorithms’, *Smart Materials and Structures* **8**(2), 257.
- URL:** <http://stacks.iop.org/0964-1726/8/i=2/a=012>

Jalili, N. (2009), *Piezoelectric-based vibration control: from macro to micro/nano scale systems*, Springer Science & Business Media.

Jung, C., Saito, A. and Epureanu, B. I. (2012), ‘Detection of cracks in mistuned bladed disks using reduced-order models and vibration data’, *Journal of Vibration and Acoustics* **134**(6), 061010.

Lin, C.-C. and Mignolet, M. P. (1993), Effects of damping and damping mistuning on the forced vibration response of bladed disks, in ‘ASME 1993 International Gas Turbine and Aeroengine Congress and Exposition’, American Society of Mechanical Engineers, pp. V03AT15A045–V03AT15A045.

Maia, N. M. M. and e Silva, J. M. M. (1997), *Theoretical and experimental modal analysis*, Research Studies Press.

Menq, C.-H., Chidamparam, P. and Griffin, J. (1991), ‘Friction damping of two-dimensional motion and its application in vibration control’, *Journal of sound and vibration* **144**(3), 427–447.

Mokrani, B., Bastaits, R., Viguié, R. and Preumont, A. (2012), Vibration damping of turbomachinery components with piezoelectric transducers: Theory and experiment, in ‘International Conference of Noise and Vibration Engineering (ISMA 2012)’, Leuven, Belgium’.

Muszyńska, A. and Jones, D. (1983), ‘On tuned bladed disk dynamics: Some aspects of friction related mistuning’, *Journal of Sound and Vibration* **86**(1), 107–128.

Pesaresi, L., Stender, M., Ruffini, V. and Schwingshakl, C. (2017), Dic measurement of the kinematics of a friction damper for turbine applications, in ‘Dynamics of Coupled Structures, Volume 4’, Springer, pp. 93–101.

Petrov, E. and Ewins, D. (2004), Method for analysis of nonlinear multiharmonic vibrations of mistuned bladed discs with scatter of contact interface characteristics, in ‘ASME Turbo Expo 2004: Power for Land, Sea, and Air’, American Society of Mechanical Engineers, pp. 385–395.

Petrov, E. and Ewins, D. (2006), ‘Effects of damping and varying contact area at blade-disk joints in forced response analysis of bladed disk assemblies’, *Journal of turbomachinery* **128**(2), 403–410.

Platzer, M. F. and Carta, F. O. (1988), Agard manual on aeroelasticity in axial-flow turbomachines. volume 2. structural dynamics and aeroelasticity, Technical report, ADVISORY GROUP FOR AEROSPACE RESEARCH AND DEVELOPMENT NEUILLY-SUR-SEINE (FRANCE).

Poon, J. (2016), Experimental Investigation on Measurement System of Rotating Turbine Disc for Piezoelectric Active Vibration Control., Bachelors dissertation, Imperial College London.

Rolls-Royce (2016), ‘Trent 1000 poster’. [Online; accessed March 26, 2018].

URL: https://www.rolls-royce.com/_/media/Files/R/Rolls-Royce/documents/civil-aerospace-downloads/High-Res-posters/High-Res-poster-trent-1000.pdf

Rotea, M. and D’Amato, F. (2002), New tools for analysis and optimization of mistuned bladed disks, in ‘38th AIAA/ASME/SAE/ASEE Joint Propulsion Conference & Exhibit’, p. 4081.

Sanliturk, K. and Ewins, D. (1996), ‘Modelling two-dimensional friction contact and its application using harmonic balance method’, *Journal of sound and vibration* **193**(2), 511–523.

Schwingshackl, C., Petrov, E. and Ewins, D. (2012), ‘Effects of contact interface parameters on vibration of turbine bladed disks with underplatform dampers’, *Journal of Engineering for Gas Turbines and Power* **134**(3), 032507.

Sever, I. A. (2004), Experimental Validation of Turbomachinery Blade Vibration Predictions, PhD dissertation, Imperial College London.

Sever, I. A., Petrov, E. P. and Ewins, D. J. (2008), ‘Experimental and numerical investigation of rotating bladed disk forced response using underplatform friction dampers’, *Journal of Engineering for Gas Turbines and Power* **130**(4), 042503.

Skingle, G. W. (1989), Structural dynamic modification using experimental data., PhD thesis, Imperial College London (University of London).

Wang, P. and Li, L. (2014), Vibration of bi-periodic bladed disk, in ‘ASME. Turbo Expo: Power for Land, Sea, and Air, Volume 7B: Structures and Dynamics’.

Wei, S.-T. and Pierre, C. (1988), ‘Localization phenomena in mistuned assemblies with cyclic symmetry part i: free vibrations’, *Journal of Vibration, Acoustics, Stress, and Reliability in Design* **110**(4), 429–438.

Whitehead, D. S. (1996), The maximum factor by which forced vibration of blades can increase due to mistuning, in ‘ASME 1996 International Gas Turbine and Aeroengine Congress and Exhibition’, American Society of Mechanical Engineers, pp. V005T14A020–V005T14A020.

Wilkie, W. K., Bryant, R. G., Fox, R. L., Hellbaum, R. F., High, J. W., Little, B. D., Mirick, P. H., Jalink Jr, A. et al. (2007), ‘Method of fabricating a composite apparatus’. US Patent 7,197,798.

Yang, B., Chu, M. and Menq, C. (1998), ‘Stick-slip-separation analysis and non-linear stiffness and damping characterization of friction contacts having variable normal load’, *Journal of Sound and vibration* **210**(4), 461–481.

Yu, H. and Wang, K. (2007), ‘Piezoelectric networks for vibration suppression of mistuned bladed disks’, *Journal of Vibration and Acoustics* **129**(5), 559–566.

Appendix A

Constitutive matrices for a model with 1 DOF per blade.

$$[K]_{8 \times 8} = \begin{bmatrix} [H]_{4 \times 4} & -\text{diag}(k_{b_1}, \dots, k_{b_4}) \\ -\text{diag}(k_{b_1}, \dots, k_{b_4}) & \text{diag}(k_{b_1}, \dots, k_{b_4}) \end{bmatrix} \quad (\text{A.1})$$

where:

$$[H] = \begin{bmatrix} k_{d_1} + k_{d_4} + k_{g_1} + k_{b_1} & -k_{d_1} & 0 & -k_{d_4} \\ -k_{d_1} & k_{d_2} + k_{d_1} + k_{g_2} + k_{b_2} & -k_{d_2} & 0 \\ 0 & -k_{d_2} & k_{d_3} + k_{d_2} + k_{g_3} + k_{b_3} & -k_{d_3} \\ -k_{d_4} & 0 & -k_{d_3} & k_{d_4} + k_{d_3} + k_{g_4} + k_{b_4} \end{bmatrix} \quad (\text{A.2})$$

$$[M]_{8 \times 8} = \begin{bmatrix} \text{diag}(m_{d_1}, \dots, m_{d_4}) & [0]_{4 \times 4} \\ [0]_{4 \times 4} & \text{diag}(m_{b_1}, \dots, m_{b_4}) \end{bmatrix} \quad (\text{A.3})$$

Note: $\text{diag}(x_1, \dots, x_n)$ indicates a diagonal Matrix of dimensions $n \times n$.

Appendix B

Constitutive matrices for a model with 2 DOFs per blade.

$$[K]_{8 \times 8} = \begin{bmatrix} [H]_{4 \times 4} & -\text{diag}(k_{b_1}, \dots, k_{b_4}) & [0]_{4 \times 4} \\ -\text{diag}(k_{b_1}, \dots, k_{b_4}) & [H]_{4 \times 4} + \text{diag}(k_{b_5}, \dots, k_{b_8}) & -\text{diag}(k_{b_5}, \dots, k_{b_8}) \\ [0]_{4 \times 4} & -\text{diag}(k_{b_5}, \dots, k_{b_8}) & [H]_{4 \times 4} \end{bmatrix} \quad (\text{B.1})$$

where:

$$[H] = \begin{bmatrix} k_{d_1} + k_{d_4} + k_{g_1} + k_{b_1} & -k_{d_1} & 0 & -k_{d_4} \\ -k_{d_1} & k_{d_2} + k_{d_1} + k_{g_2} + k_{b_2} & -k_{d_2} & 0 \\ 0 & -k_{d_2} & k_{d_3} + k_{d_2} + k_{g_3} + k_{b_3} & -k_{d_3} \\ -k_{d_4} & 0 & -k_{d_3} & k_{d_4} + k_{d_3} + k_{g_4} + k_{b_4} \end{bmatrix} \quad (\text{B.2})$$

$$[M]_{8 \times 8} = \begin{bmatrix} \text{diag}(m_{d_1}, \dots, m_{d_4}) & [0]_{4 \times 8} \\ [0]_{8 \times 4} & \text{diag}(m_{b_1}, \dots, m_{b_8}) \end{bmatrix} \quad (\text{B.3})$$

Note: $\text{diag}(x_1, \dots, x_n)$ indicates a diagonal Matrix of dimensions $n \times n$.

Appendix C

Optimum forces $f_{l,m_{t/m}}$ for a suppressing force acting in 2 DOFs for a model with 2 DOFs per blade.

POS.	MODES							
	1F-0ND(1)		1F-1ND(3)		1F-1ND(3)		1F-2ND(4)	
t	m	t	m	t	m	t	m	
1	2,1	1,7	-5,E-02	-7,5E-15	60,4	-1,5	-1,6	-4,5,E+13
2	2,1	2,2	-1,7	-2,3	-1,7	1,7	1,6	-1,7
3	2,1	1,7	5,E-02	7,5E-15	-60,4	-1,5	-1,6	-3,7,E+13
4	2,1	2,2	1,7	1,6	1,7	1,7	1,6	1,7
5	3,7	2,9	-7,E-02	-1,2E-14	98,6	-2,3	-2,7	-7,0,E+13
6	3,7	3,9	-2,7	-3,3	-2,7	2,8	2,7	-2,8
7	3,7	2,9	7,E-02	1,2E-14	-98,6	-2,3	-2,7	-6,0,E+13
8	3,7	3,9	2,7	3,1	2,7	2,8	2,7	2,8
9	-1,3	-1,1	3,E-02	4,6E-15	-37,5	0,9	1,0	2,7,E+13
10	-1,3	-1,4	1,0	1,4	1,0	-1,0	-1,0	1,0
11	-1,3	-1,1	-3,E-02	-4,6E-15	37,5	0,9	1,0	2,3,E+13
12	-1,3	-1,4	-1,0	-1,1	-1,0	-1,0	-1,0	-1,0
13	-9,6,E+15	-343,2	9,E-01	1,45E-13	-30,7	30,5	31,8	-30,7
14	-1,9,E+16	343,2	8,E-01	1,45E-13	32,5	-30,5	-31,8	30,7
15	-6,4,E+15	-343,2	-9,E-01	-1,45E-13	30,7	30,5	31,8	30,7
16	3,2,E+15	343,2	-8,E-01	-1,45E-13	-32,5	-30,5	-31,8	-30,7

Table C.1: $f_{l,1-4_{t/m}}$ for a force acting in 2 DOFs in a tuned model of 2 DOFs per blade.

POS.	MODES							
	2F-0ND(5)		2F-1ND(6)		2F-1ND(7)		2F-2ND(8)	
t	m	t	m	t	m	t	m	
1	1,4	2,0	0,2	9,0E-15	-5,6	-1,3,E+14	-1,9	-2,2
2	1,4	1,4	-1,0	-1,0	-1,0	-1,0	1,9	1,7
3	1,4	2,0	-0,2	-9,0E-15	5,6	1,2,E+14	-1,9	-2,2
4	1,4	1,4	1,0	1,0	1,0	1,0	1,9	1,7
5	2,1	2,9	0,2	8,3E-15	-5,4	-1,3,E+14	-0,6	-0,6
6	2,1	2,3	-1,0	-0,8	-1,0	-1,0	0,6	0,6
7	2,1	2,9	-0,2	-8,3E-15	5,4	1,2,E+14	-0,6	-0,6
8	2,1	2,3	1,0	1,0	1,0	1,0	0,6	0,6
9	-0,8	-1,2	-0,1	-4,3E-15	2,7	6,6,E+13	0,5	0,5
10	-0,8	-0,9	0,5	0,5	0,5	0,5	-0,5	-0,5
11	-0,8	-1,2	0,1	4,3E-15	-2,7	-5,9,E+13	0,5	0,5
12	-0,8	-0,9	-0,5	-0,5	-0,5	-0,5	-0,5	-0,5
13	-4,0,E+15	184,7	0,1	8,33E-15	1,2	1,0	-0,4	-0,4
14	-9,6,E+15	-184,7	0,2	8,33E-15	-0,8	-1,0	0,4	0,4
15	6,9,E+15	184,7	-0,1	-8,33E-15	-1,2	-1,0	-0,4	-0,4
16	4,8,E+15	-184,7	-0,2	-8,33E-15	0,8	1,0	0,4	0,4

Table C.2: $f_{l,5-8_{t/m}}$ for a force acting in 2 DOFs in a tuned model of 2 DOFs per blade.

POS.	MODES							
	3F-0ND(9)		3F-1ND(10)		3F-1ND(11)		3F-2ND(12)	
t	m	t	m	t	m	t	m	
1	-0,6	8,0,E-15	-2,0	-0,1	0,2	4,0,E+13	0,6	5,7
2	-0,6	-0,4	0,6	-0,7	0,6	0,6	-0,6	-0,6
3	-0,6	-8,0,E-15	2,0	-0,1	-0,2	1,4,E+14	0,6	5,7
4	-0,6	-0,7	-0,6	-0,7	-0,6	-0,6	-0,6	-0,6
5	0,4	-5,2,E-15	1,3	4,6,E-02	-0,1	-2,8,E+13	-0,4	-4,1
6	0,4	0,2	-0,4	0,4	-0,4	-0,4	0,4	0,4
7	0,4	5,2,E-15	-1,3	4,6,E-02	0,1	-1,2,E+14	-0,4	-4,1
8	0,4	0,4	0,4	0,4	0,4	0,4	0,4	0,4
9	-1,0	1,5,E-14	-3,5	-0,1	0,3	9,3,E+13	1,1	14,8
10	-1,0	-0,5	1,0	-0,9	1,0	1,0	-1,1	-1,0
11	-1,0	-0,0	3,5	-0,1	-0,3	6,6,E+14	1,1	14,8
12	-1,0	-0,9	-1,0	-0,9	-1,0	-1,0	-1,1	-1,0
13	2,4,E+14	0,0	-22,6	-2,2	12,5	-32,0	8,6	17,2
14	1,5,E+14	0,0	41,9	2,2	6,8	32,0	-8,6	-17,2
15	-3,3,E+14	-0,0	22,6	-2,2	-12,5	32,0	8,6	17,2
16	-1,3,E+14	-0,0	-41,9	2,2	-6,8	-32,0	-8,6	-17,2

Table C.3: $f_{l,9-12_{t/m}}$ for a force acting in 2 DOFs in a tuned model of 2 DOFs per blade.